JAERI-M
83-199

ANNUAL REPORT OF THE OSAKA LABORATORY FOR RADIATION CHEMISTRY JAPAN ATOMIC ENERGY RESEARCH INSTITUTE

(NO. 16)

April 1, 1982 - March 31, 1983

November 1983

Osaka Laboratory for Radiation Chemistry

日本原子力研究所
Japan Atomic Energy Research Institute

JAERI-Mレポートは，日本原子力研究所が不定期に公刊している研究報告書です。
入手の問合わせは，日本原子力研究所技術情報部情報資料課（〒319-11茨城県那珂郡東海村）あて，お申しこしください。なお，このほかに財団法人原子力弘済会資料センター（〒319-11 茨城県那珂郡東海村日本原子力研究所内）で複写による実費頒布をおこなっております。

JAERI-M reports are issued irregularly.
Inquiries about availability of the reports should be addressed to Information Section, Division of Technical Information, Japan Atomic Energy Research Institute, Tokai-mura, Naka-gun, Ibaraki-ken 319-11, Japan.

編集兼発行　日本原子力研究所
印　　刷　いばらき印刷㈱

Osaka Laboratory for Radiation Chemistry
Japan Atomic Energy Research Institute
25-1 Mii-minami machi, Neyagawa
Osaka, Japan

JAERI-M 83-199

ANNUAL REPORT OF THE OSAKA LABORATORY FOR RADIATION CHEMISTRY JAPAN ATOMIC ENERGY RESEARCH INSTITUTE

(No. 16)

April 1, 1982 - March 31, 1983

(Received October 28 , 1983)

This report describes research activities of Osaka Laboratory for Radiation Chemistry, JAERI during one year period from April 1, 1982 through March 31, 1983. The latest report, for 1982, is JAERI-M 82-192.

Detailed descriptions of the activities are presented in the following subjects: studies on reactions of carbon monoxide, water and methane; polymerization under the irradiation of high dose rate electron beams; modification of polymers, degradation, cross-linking, and grafting.

Previous reports in this series are:

Annual Report,	JARRP,	Vol. 1	1958/1959*
Annual Report,	JARRP,	Vol. 2	1960
Annual Report,	JARRP,	Vol. 3	1961
Annual Report,	JARRP,	Vol. 4	1962
Annual Report,	JARRP,	Vol. 5	1963
Annual Report,	JARRP,	Vol. 6	1964
Annual Report,	JARRP,	Vol. 7	1965
Annual Report,	JARRP,	Vol. 8	1966
Annual Report,	No. 1,	JAERI 5018	1967
Annual Report,	No. 2,	JAERI 5022	1968
Annual Report,	No. 3,	JAERI 5026	1969
Annual Report,	No. 4,	JAERI 5027	1970
Annual Report,	No. 5,	JAERI 5028	1971
Annual Report,	No. 6,	JAERI 5029	1972
Annual Report,	No. 7,	JAERI 5030	1973
Annual Report,	No. 8,	JAERI-M 6260	1974
Annual Report,	No. 9,	JAERI-M 6702	1975
Annual Report,	No.10,	JAERI-M 7355	1976
Annual Report,	No.11,	JAERI-M 7949	1977
Annual Report,	No.12,	JAERI-M 8569	1978
Annual Report,	No.13,	JAERI-M 9214	1979
Annual Report,	No.14,	JAERI-M 9856	1980
Annual Report,	No.15,	JAERI-M 82-192	1981

* Year of the activities

Keywords: Electron Beam Irradiation, γ-Irradiation, Carbon Monoxide-Water Reaction, Methane, Radiation-Induced Reaction, Polymerization, Emulsion Polymerization, Grafting, Polymer Modification, Cross-Linking, Vinyl Monomer, Dienes, Polystyrene, Polyvinyl Chloride Disc, Radiation Chemistry

JAERI－M 83-199

昭和57年度日本原子力研究所　大阪支所年報

日本原子力研究所・高崎研究所・大阪支所

（１９８３年１０月 28 日受理）

本報告は、大阪支所において昭和５７年度に行なわれた研究活動を述べたものである。主な研究題目は、一酸化炭素、水およびメタンの反応ならびにそれに関連した研究、高線量率電子線照射による重合反応の研究、ポリマーの改質および上記の研究と関連して重合反応、高分子分解、架橋ならびにグラフト重合に関する基礎的研究などである。

日本放射線高分子研究協会年報	Vol. 1		1958／1959
日本放射線高分子研究協会年報	Vol. 2		1960
日本放射線高分子研究協会年報	Vol. 3		1961
日本放射線高分子研究協会年報	Vol. 4		1962
日本放射線高分子研究協会年報	Vol. 5		1963
日本放射線高分子研究協会年報	Vol. 6		1964
日本放射線高分子研究協会年報	Vol. 7		1965
日本放射線高分子研究協会年報	Vol. 8		1966
日本原子力研究所大阪研における放射線化学の基礎研究№1	JAERI	5018	1967
日本原子力研究所大阪研における放射線化学の基礎研究№2	JAERI	5022	1968
日本原子力研究所大阪研における放射線化学の基礎研究№3	JAERI	5026	1969
日本原子力研究所大阪研における放射線化学の基礎研究№4	JAERI	5027	1970
日本原子力研究所大阪研における放射線化学の基礎研究№5	JAERI	5028	1971
日本原子力研究所大阪研における放射線化学の基礎研究№6	JAERI	5029	1972
日本原子力研究所大阪研における放射線化学の基礎研究№7	JAERI	5030	1973
Annual Report, Osaka Lab., JAERI, №8	JAERI－M	6260	1974
Annual Report, Osaka Lab., JAERI, №9	JAERI－M	6702	1975
Annual Report, Osaka Lab., JAERI, №10	JAERI－M	7355	1976
Annual Report, Osaka Lab., JAERI, №11	JAERI－M	7949	1977
Annual Report, Osaka Lab., JAERI, №12	JAERI－M	8569	1978
Annual Report, Osaka Lab., JAERI, №13	JAERI－M	9214	1979
Annual Report, Osaka Lab., JAERI, №14	JAERI－M	9856	1980
Annual Report, Osaka Lab., JAERI, №15	JAERI－M	82－192	1981

CONTENTS

III. LIST OF PUBLICATIONS

I. INTRODUCTION

Osaka Laboratory was founded in 1958 as a laboratory of the Japanese Association for Radiation Research on Polymers (JARRP), which was organized and sponsored by some fifty companies interested in radiation chemistry of polymers. The JARRP was merged with Japan Atomic Energy Research Institute (JAERI) on June 1, 1967, and the laboratory has been operated as Osaka Laboratory for Radiation Chemistry, Takasaki Radiation Chemistry Establishment, JAERI. The research activities of Osaka Laboratory have been oriented towards the fundamental research on applied radiation chemistry.

The results of the research activities of the Laboratory were published from 1958 until 1966 in the Annual Reports of JARRP which consisted essentially of original papers. During the period between 1967 and 1973, the publication had been continued as JAERI Report which also consisted mainly of original papers. From 1974, the Annual Report has been published as JAERI-M Report which contains no original papers, but presents outlines of the current research activities in some detail. Readers who wish to have more information are advised to contact with individuals whose names appear under subjects.

The present annual report covers the research activities of the Laboratory between April 1, 1982 and March 31, 1983.

Most of the studies carried out in the Laboratory are continuation from the previous year, emphasis being laid on two fields; one is "Effect of radiation on the reaction of carbon monoxide, methane and hydrogen" and the other, "Radiation research on polymers".

In an attempt to improve the selectivity of the reaction to form ethane in the radiation chemical reaction of methane, studies have been continued using flow system without circulation under electron beam irradiation in the presence of molecular sieves which have pores of uniform dimensions. In some experiments, methane was irradiated using γ-rays under

elevated pressures up to 5 x 10^6 Pa in a batch system. Ethane and hydrogen are the main products at the dose below 10,000 rad, whereas ethane is consumed by further irradiation producing liquid higher hydrocarbons. In order to elucidate the reaction scheme of the rise and decay of ethane by irradiation, studies have been carried out on the change of the product distribution from methane by the addition of small amounts of ethylene or ethane. The results indicate that ethane and other higher hydrocarbons are produced via ethylene, and ethane once produced is converted to higher hydrocarbons by repeated abstraction reaction of hydrogen and combination reaction of radicals.

The selectivity toward reactions producing olefins was improved with the simultaneous decrease of the amount of deposition of carbonaceous solid on the solid surface, when the flowing methane was irradiated with electron beams over silica gel or molecular sieves in the temperature range from 300 to 500°C.

Composition of carbonaceous solids produced from methane by radiation was examined by studying the material balance of the radiation induced reaction of methane-Ar mixtures in the presence of molecular sieve (MS) 5A and silica gel. The result obtained revealed that the number ratio of carbon to hydrogen in the carbonaceous solid was 2.8 for the solid obtained over silica gel and 7.7 for that obtained over MS 5A, indicating that the hydrogenolysis reaction occurs more favorably over silica gel surface than over MS 5A surface.

Water-gas shift reaction of CO-H_2O mixture under electron irradiation was markedly enhanced by the presence of silica gel. It was concluded that formic acid is an intermediate of the reaction from the experimental result that the irradiation of formic acid over silica gel gave the same product distribution to that obtained by the radiation-induced water gas shift reaction.

A combined surface analysis system of Auger electron and secondary ion mass spectrometers was installed in the laboratory at the end of the second quarter to investigate elemental reaction

over catalyst surface under irradiation. Using this system studies have been carried out on the structure change of silica gel surface induced by electron beam irradiation and the secondary ion emission from the surface by argon ion bombardment and it was found that electron irradiation resulted in reduction by the Si-O bond scission on the surface and simultaneous irradiation of electron and argon ion on the surface produced $SiOH^+$ and Si_2OH^+, the intensities of both ions being strongly dependent on the amount of water adsorbed on the surface.

The studies in an attempt to synthesize reactive oligomer having halogen atoms at its end by the telomerization reaction of styrene with telogen have been performed. The electron beam-induced telomerization reaction of styrene and chain transfer agent such as 3-chloro-1-butene was concluded to proceed by the cationic mechanism from the experimental results that the rate of reaction is proportional to the dose rate and the reaction is prohibited by the addition of cation scavenger such as triethylamine. The results of IR analysis and elemental analysis of the product proved that the products contain C=C bond at the initiation end and Cl atom at the termination end, confirming that the desired reactive oligomer was obtained.

In the studies on emulsion polymerization, polymer emulsion particles of high molecular weight and of average diameter of 50 nm were obtained in high yield in the presence of anionic emulsifier. The mechanisms of the emulsion polymerization in the presence of the emulsifier of the three types, anionic, cationic and nonionic, were also studied from the molecular weight distribution of the polymers obtained with each emulsifier.

Radiation-induced vapor phase graft copolymerization of fluorine containing vinyl compounds onto polyvinyl chloride (PVC) disc has continued. Optical microscopic examination revealed that polymer islands were formed on the disc surface at early stage of the reaction and the polymer was developed to cover the entire surface of the PVC disc as the reaction proceeded. The reaction was also followed by the contact angle

measurements and contact electric resistance of the grafted surface. The degree of grafting toward the direction perpendicular to the surface was evaluated by the abundance ratio of Cl and F atoms determined by ESCA analysis.

Studies on the radiation-induced grafting of styrene onto carbon black have been carried out in an attempt to improve the dispersion properties of carbon black powder in polymers. It was found that the degree of grafting can be evaluated from the change of wet property of the grafted powder to water, hexane, and n-decane.

The molecular weight of polymethylmethacrylate (PMMA) was found to decrease proportionally with dose resulting in coloration of the PMMA.

It is our most regret to announce that Dr. Kanae Hayashi died on Feb. 16th, 1983. He served as a research scientist since 1964 and as the leader of the polymer research group from 1979. His enthusiasm toward radiation research on polymers has been a great surprise for those who know him.

Dr. Isamu Kuriyama, Director
Osaka Laboratory for Radiation Chemistry
Japan Atomic Energy Research Institute

II. RECENT RESEARCH ACTIVITIES

1. Radiation Chemical Reaction of Methane-Ethylene and Methane-Ethane Mixtures by Electron Beam Irradiation Using Flow System

It was reported that ethane and hydrogen were the main products in the radiation chemical reaction of methane at the dose below 10^4 Mrads, but ethane was consumed and converted to higher liquid hydrocarbons when the irradiation continued further[1]. In an attempt to clarify the reaction scheme of the formation and the decay of ethane, the studies have been carried out on the amounts of radiolysis products from methane containing ethylene which is assumed to be a precursor of ethane, and from methane containing ethane.

Flowing methane containing ethylene or ethane was irradiated in a reaction vessel (463 ml in volume) with electron beam from an accelerator of rectifying transformer type. The flow rate of the gas was 160 ml/min which gave average residence time of 2.8 min. The dose rate determined from an N_2O dosimeter was 88.8 Mrad/sec. The concentration of the additives was from 0 to 2 mole%.

The irradiated gas was analyzed simultaneously by three gas chromatographs to minimize the time required for the analysis without sacrificing the resolution of the peaks; hydrogen on 3m MS-5A column with argon carrier, alkanes ($\leq C_2$) on 3m Porapak N column with helium, and alkanes ($\geq C_3$) on 3m Porapak Q column with helium. The gaschromatographic data were processed to convert into concentrations and G-values of the products by use of a Shimadzu CR2AX computing integrator.

In Table 1, G-values of the products from pure methane obtained in the present study are compared to those obtained in the previous study[1] where the irradiation vessel of smaller volume was used. The G-values of the main products agreed well in both experiments within experimental error, but the G(ethylene) was smaller than that reported previously. In Figs. 1 and 2,

Table 1 The G Values of Products from Methane

	This work	Arai, et al.[2]
H_2	6.18 ± 0.81	7.1
C_2H_4	0.0	0.16
C_2H_6	2.24 ± 0.42	2.25
C_3H_8	0.291 ± 0.037	0.34
$n\text{-}C_4H_{10}$	0.137 ± 0.026	0.092
$i\text{-}C_4H_{10}$	0.0558 ± 0.0249	0.037
$n\text{-}C_5H_{12}$	$(2.11 \pm 1.45) \times 10^{-3}$	0.004
$i\text{-}C_5H_{12}$	0.0364 ± 0.048	0.048
$neo\text{-}C_5H_{12}$	0.0184 ± 0.017	0.0061

the G-values of the main products were plotted as a function of concentration of ethylene and ethane, respectively. It is noted that $G(H_2)$ decreased to 60% of the original value (7.5) by the addition of 0.2 mole% of ethylene, and asymptoted to 3.5 by further addition of ethylene. The G(ethane) increased with increasing concentration of ethylene, reached a maximum value at 0.3 mole% ethylene, and then decreased with further addition of ethylene. The G-values of higher hydrocarbons increased with increasing concentration of ethylene. The G-value of ethylene consumption, $(G(-C_2H_4))$ calculated from the difference of ethylene concentration before and after irradiation was plotted in Fig. 3 as a function of ethylene concentration. The $G(-C_2H_4)$ increased with increasing ethylene concentration to reach a constant value, but the $G(-C_2H_4)$ increased markedly with the further addition of C_2H_4 above 1 mole%.

By the addition of C_2H_6, $G(H_2)$ value did not change. The G-values of C_3H_8 and higher hydrocarbons also increased with increasing concentration of ethane, but the effects of ethane on the amounts of the hydrocarbons were not as large as those observed in the experiment where ethylene was used as additive.

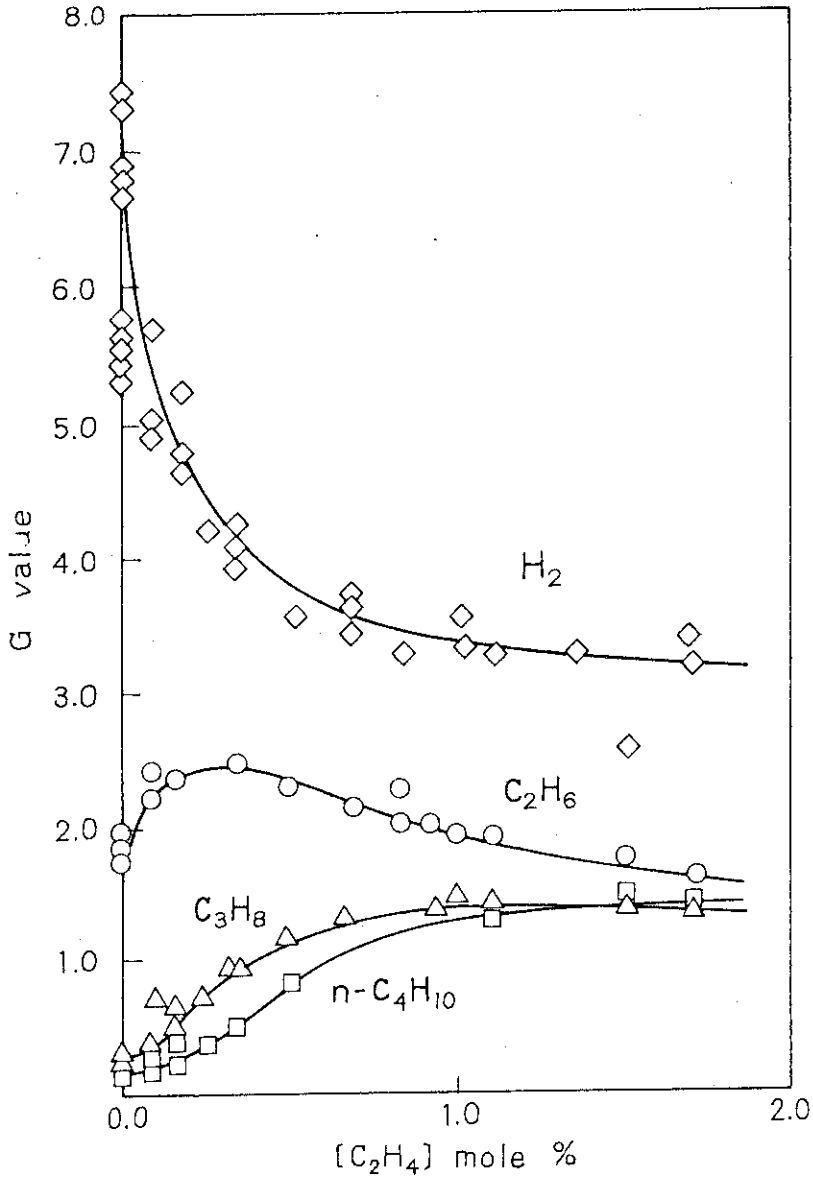

Fig. 1 G-values of main products as a function of ethylene content.

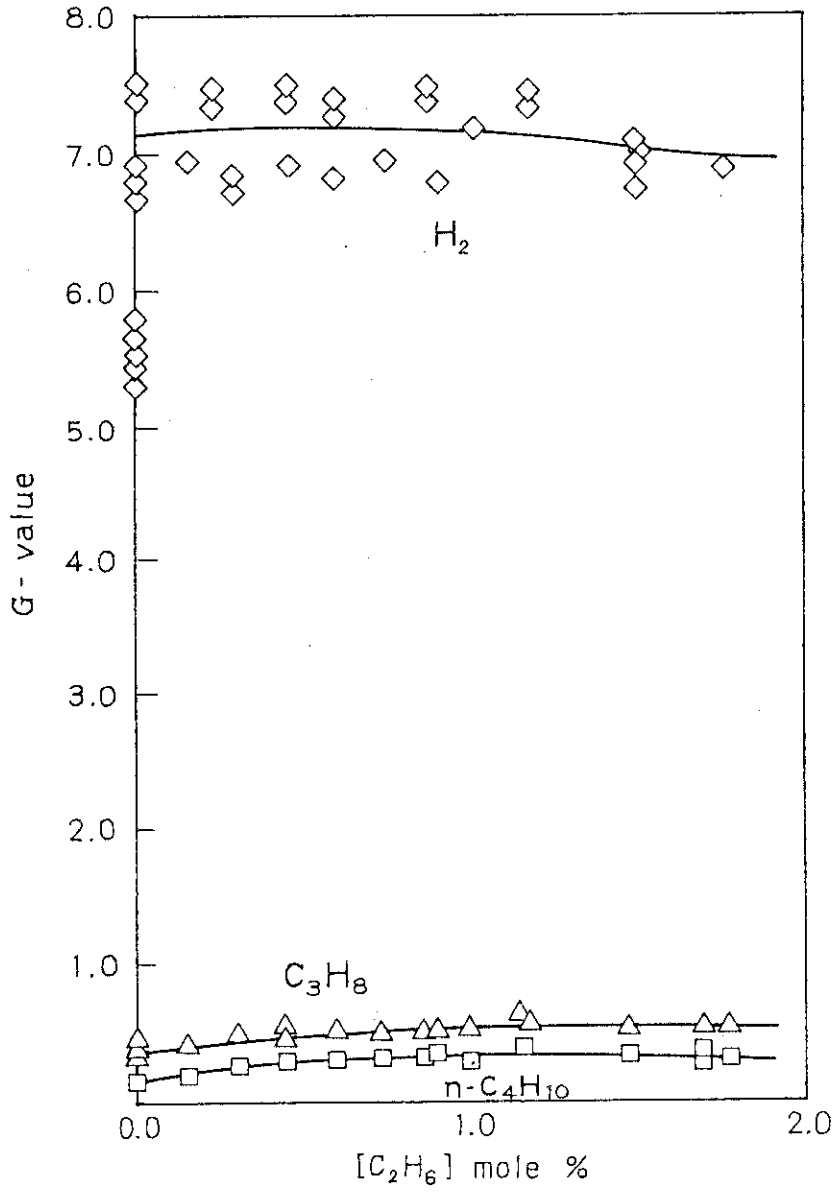

Fig. 2 G-values of main products as a function of ethane content.

The $G(C_2H_6)$ calculated from the difference between the concentrations of ethane added and found after irradiation was plotted in Fig. 3 as a function of ethane concentration. The G-value of ethane formation seems to decrease slightly with increasing amount of ethane added, indicating that a part of ethane converted to higher hydrocarbons.

The decrease of $G(H_2)$ observed by the addition of a small

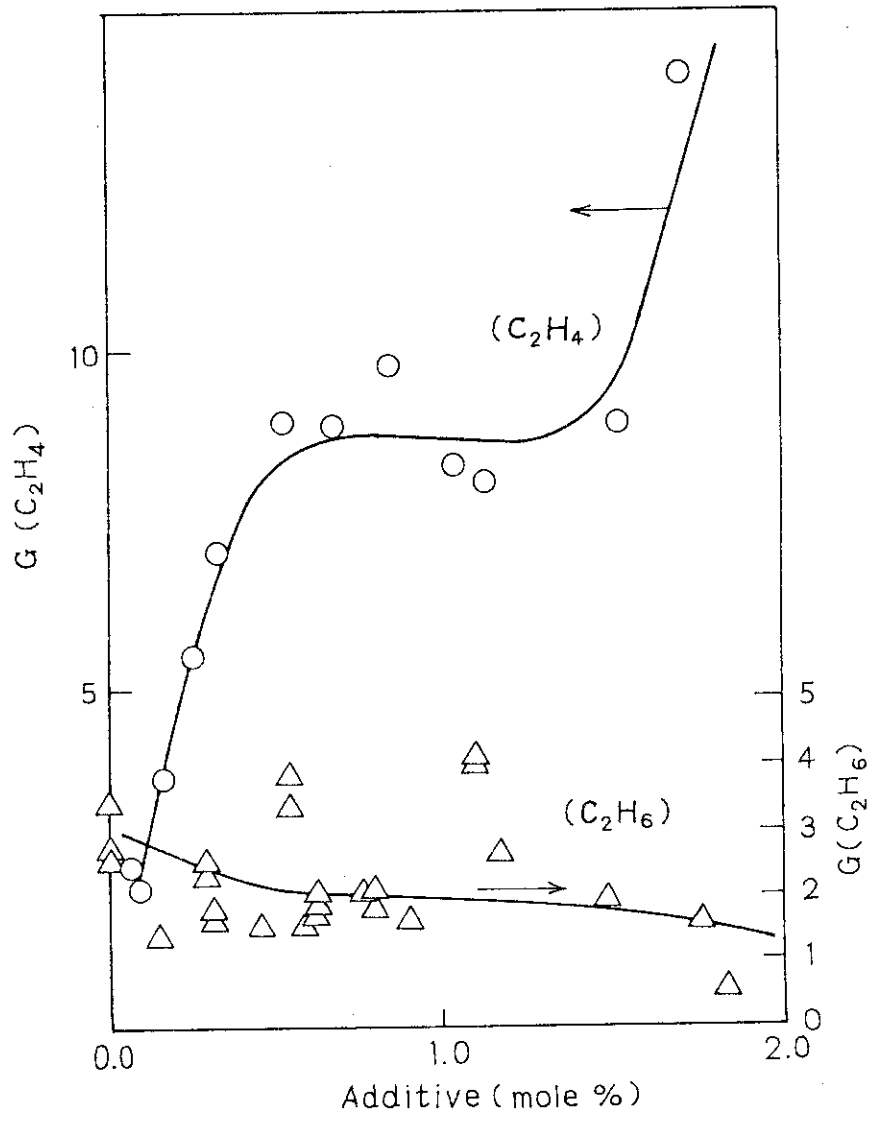

Fig. 3 The G-values of concentration change of additives as a function of the added amounts of the additives: (○) C_2H_4, (△) C_2H_6.

amount of ethylene is explained by a set of following reactions:

$$CH_4 \rightsquigarrow \cdot CH_3 + H \qquad (1)$$

$$H + CH_4 \dashrightarrow H_2 + \cdot CH_3 \qquad (2)$$

$$H + C_2H_4 \dashrightarrow \cdot C_2H_5 \qquad (3)$$

$$H + H + CH_4 \dashrightarrow H_2 + CH_4 \qquad (4)$$

Assuming steady state concentration of H atoms, the following equation was obtained:

$$\frac{G_H \cdot I \cdot (CH_4)}{N_A \times 100} - k_2(H)\cdot(CH_4) - k_3(H)\cdot(C_2H_4) - k_4(H)^2\cdot(CH_4) = 0 \qquad (5)$$

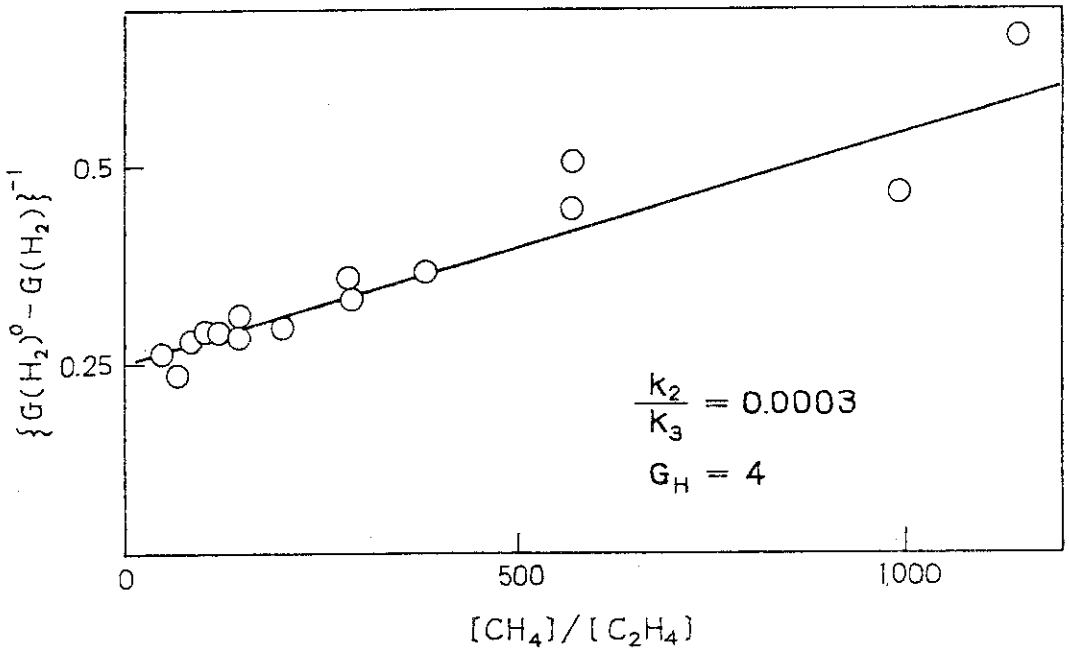

Fig. 4 $\{G(H_2)^0 - G(H_2)\}^{-1}$ as a function of $[CH_4]/[C_2H_4]$.

where G_H is the G-value of H atom formation, I denotes dose rate, and N_A Avogadro number. The G-value of hydrogen molecule formation is given by

$$G(H_2) = G_{H_2} + \frac{(d(H_2)/dt) \times N_A \times 100}{I \times (CH_4)} \qquad (6)$$

where G_{H_2} denotes the G-value of hydrogen molecules via a molecular process or a process involving hot hydrogen atoms, which are not suppressed by a scavenger. Combination of eqs. (5) and (6) with the relation: $G^0(H_2) = G_H + G_{H_2}$ leads to the following equation:

$$1/(G^0(H_2) - G(H_2)) = (1/G_H)(1+k_2(CH_4)/(k_3(C_2H_4))) \qquad (7)$$

where $G^0(H_2)$ is the G-value of hydrogen formation from pure methane, G_H is the G-value of H atom which is scavenged by ethylene. The plot of eq. (7) shown in Fig. 4 gives the G_H of 4 and k_2/k_3 ratio of 0.0003. The G_H value found in this study is higher than the estimated value 0.85 at 25°C in the previous study[2], and the k_2/k_3 ratio is higher than that calculated from the literature values (ca. 1.6×10^{-4})[3] for H atoms generated by discharge. These results suggest that radiation chemically produced hydrogen atoms contain "Hot" atoms which are not scavenged by ethylene.

The fact that $G(C_2H_6)$ increased with the addition of a small amount of ethylene up to 0.3 mole% and then decreased with further increase of ethylene may be qualitatively explained by the increase of C_2H_5 radical produced by reaction (3) and by decrease of CH_3 radical concentration caused by the decrease of steady state concentration of H atom by reaction (3). The limiting G values of propane and butane reached by the addition of 1 mole% ethylene were about 8 times as large as those found in the methane-ethane mixture indicating that these compounds are produced via ethylene.

Ethane thus produced reacts to be converted to higher hydrocarbons by further irradiation through radical formation and their combination reactions. (M. Hatada and S. Sugimoto)

1) H. Arai, S. Nagai, K. Matsuda, and M. Hatada, Radiat. Phys. Chem., 17, 217 (1981).
2) H. Arai, S. Nagai, K. Matsuda, and M. Hatada, Radiat. Phys. Chem., 17, 151 (1981).
3) P. Reed, "Radiation Chemistry of Gaseous Methane", Ph. D. Thesis, Purdue University (1971).

2. The γ-Ray Induced Radiolysis of Methane-Ethylene and Methane-Ethane Mixture at Elevated Pressures

In the previous study[1], in which pressurized methane was irradiated with γ-rays in a stainless steel autoclave, it was found that the G-values of hydrocarbon products having more than three carbon atoms in a molecule increased with increasing pressure while the G-values of ethane and hydrogen were independent of pressure. The results together with the effect of temperature on the G-values of these products indicate that propane and higher hydrocarbon products were produced by complex processes including combination, disproportionation and addition reactions of radicals produced either primarily or secondarily. The present study was carried out on the effects of pressure and composition of the reactants in the γ-ray radiolysis of pressurized mixtures of methane-ethylene, methane-ethane and methane-propane in an attempt to elucidate the reaction scheme of ethane formation and that of ethane disappearance by further irradiation as in the previous study[2] where the irradiations were carried out using electron beams of the same mixtures at atmospheric pressure.

The γ-irradiations were carried out at 323K and 4.9×10^6 Pa in an autoclave (78 ml in capacity) with a Bourdon type gauge in the composition range from 0 to 6 mole% of the additive to methane. The irradiations were also carried out at the same temperature on the mixture containing 2 mole% additive in the pressure range from 5×10^5 to 5×10^6 Pa. The dose rate was 0.06 Mrad/h and the dose was 6.7 Mrad.

The G-values of the products obtained at 4.9×10^6 Pa are

plotted in Figs. 1 and 2 as a function of C_2H_4 content in mole% along with the G-value of C_2H_4 consumption as estimated from the difference between the amounts of ethylene charged and found after irradiation. The plots were shown for the G-values obtained for ethylene content below 2 mole%, but the G-values obtained at 6 mole% came on the extentions of the curves.

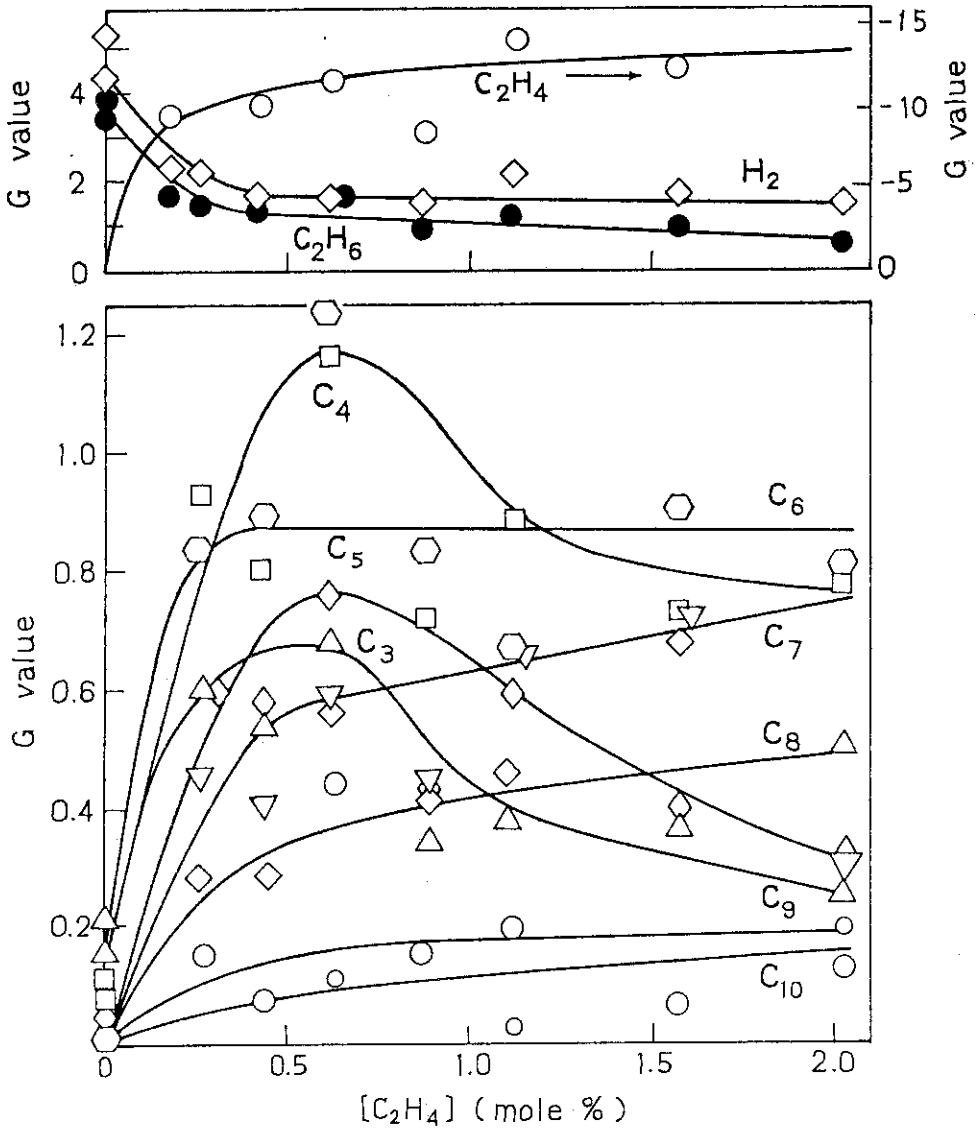

Fig. 1 G-values of products as a function of ethylene content: Top: hydrogen, ethane, and consumed ethylene; Bottom: hydrocarbons grouped by carbon number. Pressure, 4.9×10^6 Pa; temperature, 323K; and dose, 6.7 Mrad.

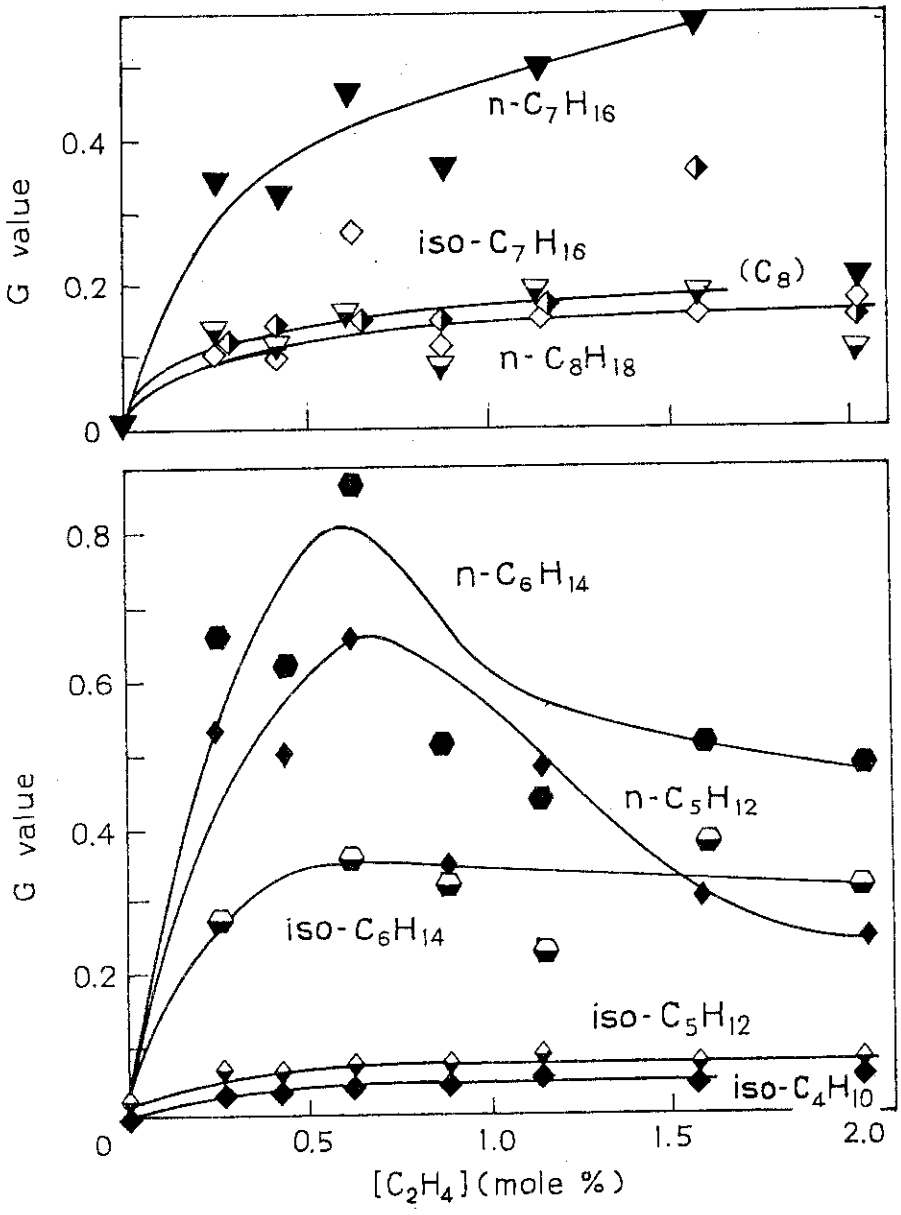

Fig. 2 G-values of higher hydrocarbons ($C_5 \sim C_8$) as a function of ethylene content. Irradiation conditions are given in the caption to Fig. 1.

The G-values of hydrogen and ethane decreased by the addition of small amounts of C_2H_4, but were almost independent of the ethylene concentration above 0.5 mole%. The dependence of $G(H_2)$ on ethylene content is similar to that observed previously[2] in the electron beam radiolysis of atmospheric methane, whereas the G-value of ethane formation changes with increasing ethylene content somewhat differently from that observed in the previous experiment[2] where $G(C_2H_6)$ increased to a maximum value and then decreased with increasing ethylene content.

The decrease of $G(H_2)$ can be explained as the result of competition reactions of H atom as described previously[2].

$$CH_4 \rightsquigarrow \dot{C}H_3 + H \qquad (1)$$

$$H + CH_4 \longrightarrow \dot{C}H_3 + H_2 \qquad (2)$$

$$H + C_2H_4 \longrightarrow \dot{C}_2H_5 \qquad (3)$$

The fact that no maximum $G(C_2H_6)$ appeared at 4.9×10^6 Pa may be resulted from another set of competition reactions (4) ∿ (6) where the reaction (5) producing C_3 or higher hydrocarbons at this pressure, favors over the reaction (4) which produces ethane.

$$\dot{C}_2H_5 + H \xrightarrow{CH_4} C_2H_6 \qquad (4)$$

$$\dot{C}_2H_5 + CH_3 \xrightarrow{CH_4} C_3H_8 \qquad (5)$$

$$\dot{C}_2H_5 + C_2H_4 \longrightarrow \dot{C}_4H_9 \qquad (6)$$

The amount of ethylene consumed increases and reaches asymptotically a limiting value of G = 13 as the ethylene content increases (Fig. 1) in a symmetrical way to the curves of $G(H_2)$ and $G(C_2H_6)$.

The G-values of hydrocarbons having 3 - 5 carbons in a molecule increase to maximum values and then decrease with increasing amount of ethylene added to methane as was observed

for $G(C_2H_6)$ in the electron beam radiolysis of methane at atmospheric pressure[2]. The sum of the G-values of C_6 hydrocarbons increases to a limiting value asymptotically with increasing ethylene content in a way in-between $C_3 \sim C_5$ and C_7 or higher hydrocarbons, the G-values of the latter being increased gradually with increasing ethylene content after sharp rise of the values at smaller contents of ethylene below 0.5 mole%. The maxima appeared on G(products) vs. ethylene content curves for $C_3 \sim C_5$ products may be explained as the

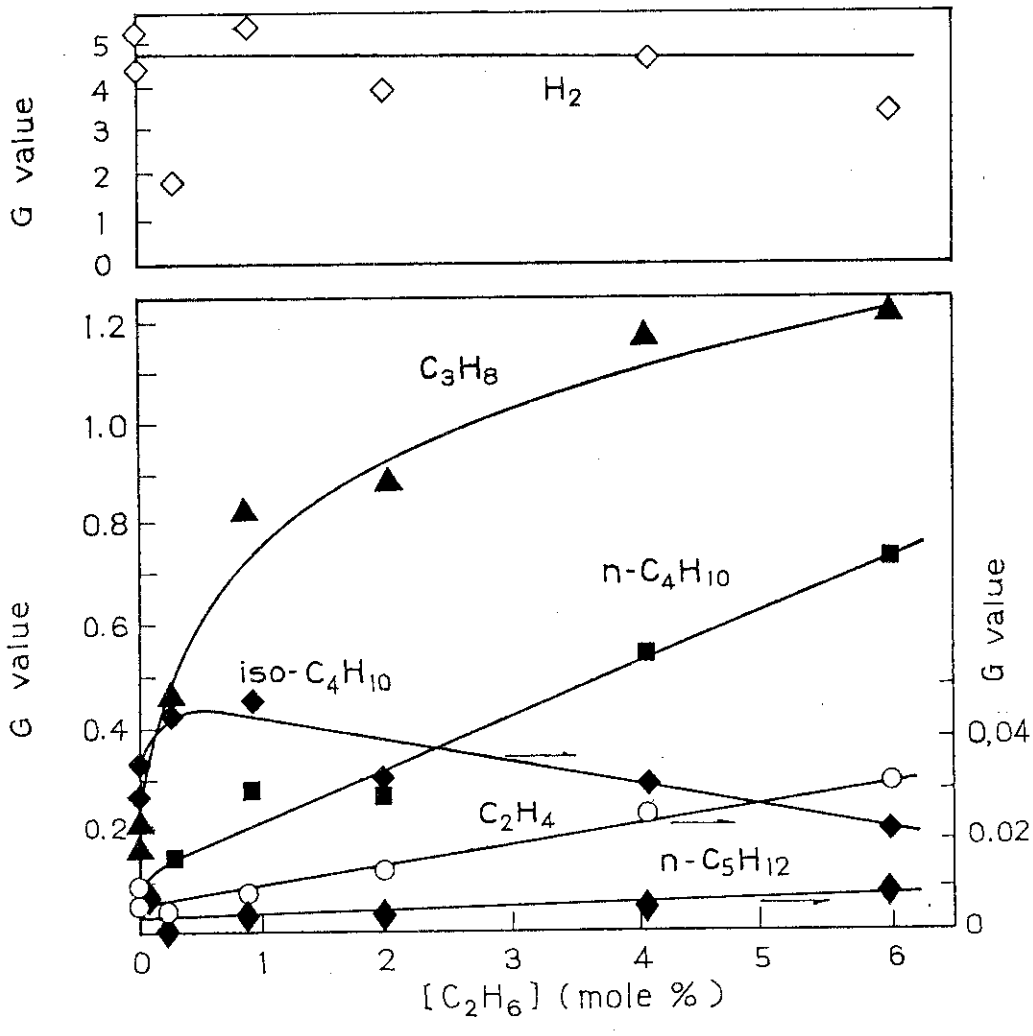

Fig. 3 G-values of hydrogen and hydrocarbons ($C_2 \sim C_5$) as a function of ethane content. Irradiation conditions are the same as those shown in the caption of Fig. 1.

results of two opposite reactions: one producing these hydrocarbons by the reactions involving ethylene and the other sacrificing the hydrocarbons to produce higher hydrocarbons by the addition of ethylene. The gradual increase of the higher hydrocarbons (> C_7) with increasing ethylene content above 0.5 mole% (Fig. 2) supports this explanation.

The dependence of G(products) on the amount of additive observed for ethane is different from that observed for ethylene: the addition of ethane does not affect $G(H_2)$ (Fig. 3), whereas G-values of most hydrocarbons increase with ethane content except those of iso-C_4H_{10} and neo-C_5H_{12} (Fig. 3 and Fig. 4) which gave maxima at ethane content of 0.3 mole%. The difference may be due to the fact that ethane does not scavenge hydrogen atom. The small increase of the G-values of higher

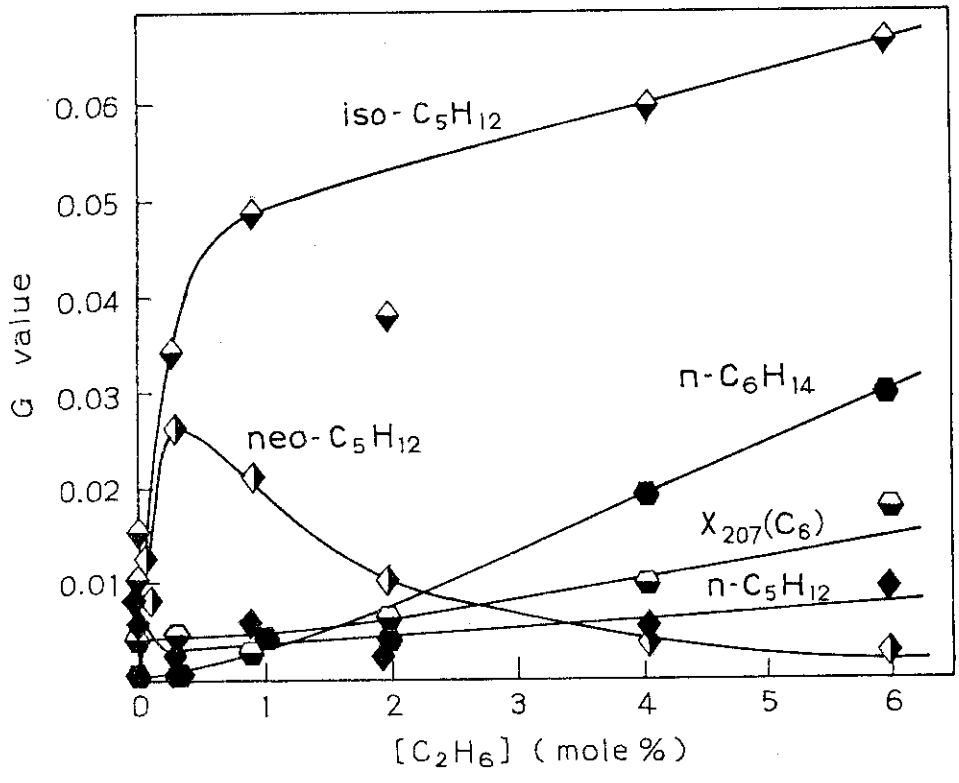

Fig. 4 G-values of hydrocarbons (C_5, C_6) as a function of ethane content. Irradiation conditions are the same as those shown in the caption of Fig. 1.

hydrocarbons is explained by the formation of alkyl radical from ethane by abstraction reaction of hydrogen followed by combination reactions with radicals to produce these hydrocarbons. The explanations for the increase and decrease of $G(iso\text{-}C_4H_{10})$ (Fig. 3) and $G(neo\text{-}C_5H_{12})$ (Fig. 4) with increasing ethane content are not known at present.

The G-values of hydrocarbons grouped by carbon number are plotted as a function of ethane content in Fig. 5, where the G-values decrease with increasing number of carbons in a molecule in the whole region of ethane content studied.

The G-values of hydrogen and hydrocarbon products are plotted as a function of propane content in Figs. 6, 7 and 8,

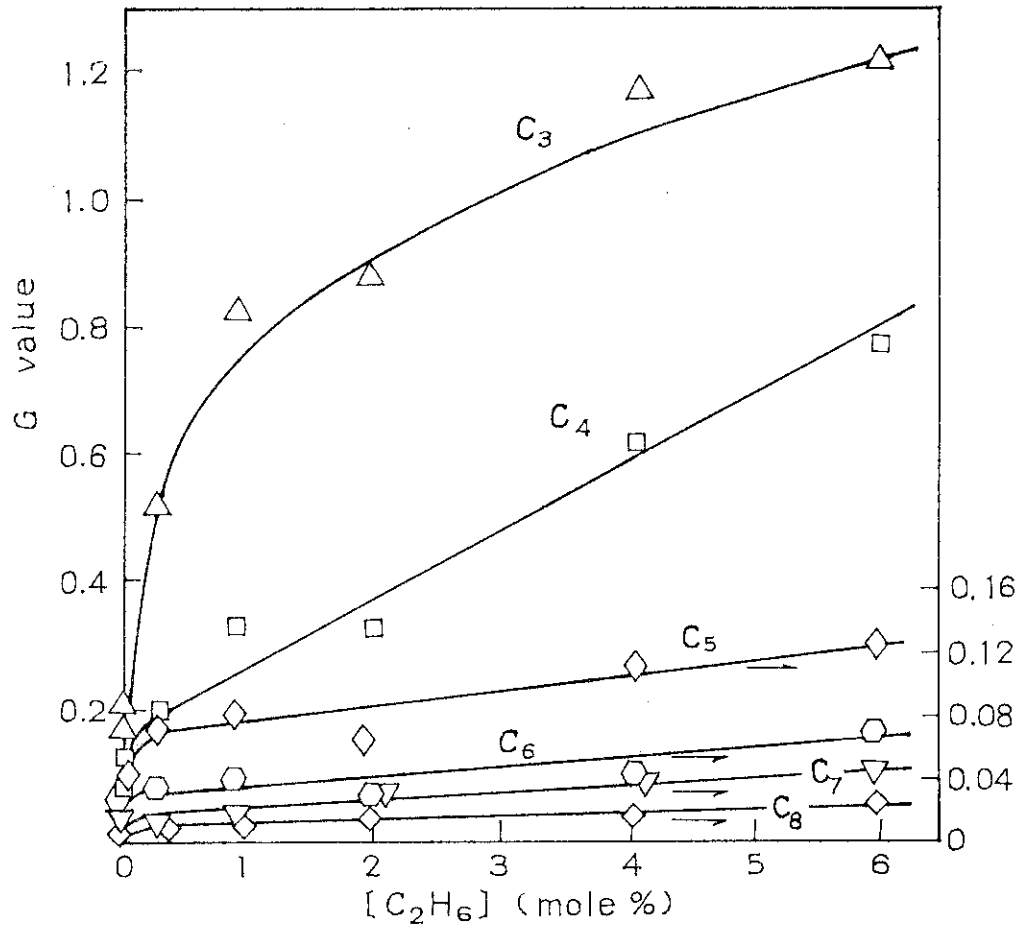

Fig. 5 G-values of hydrocarbons grouped by carbon number ($C_3 \sim C_8$) as a function of ethane content.

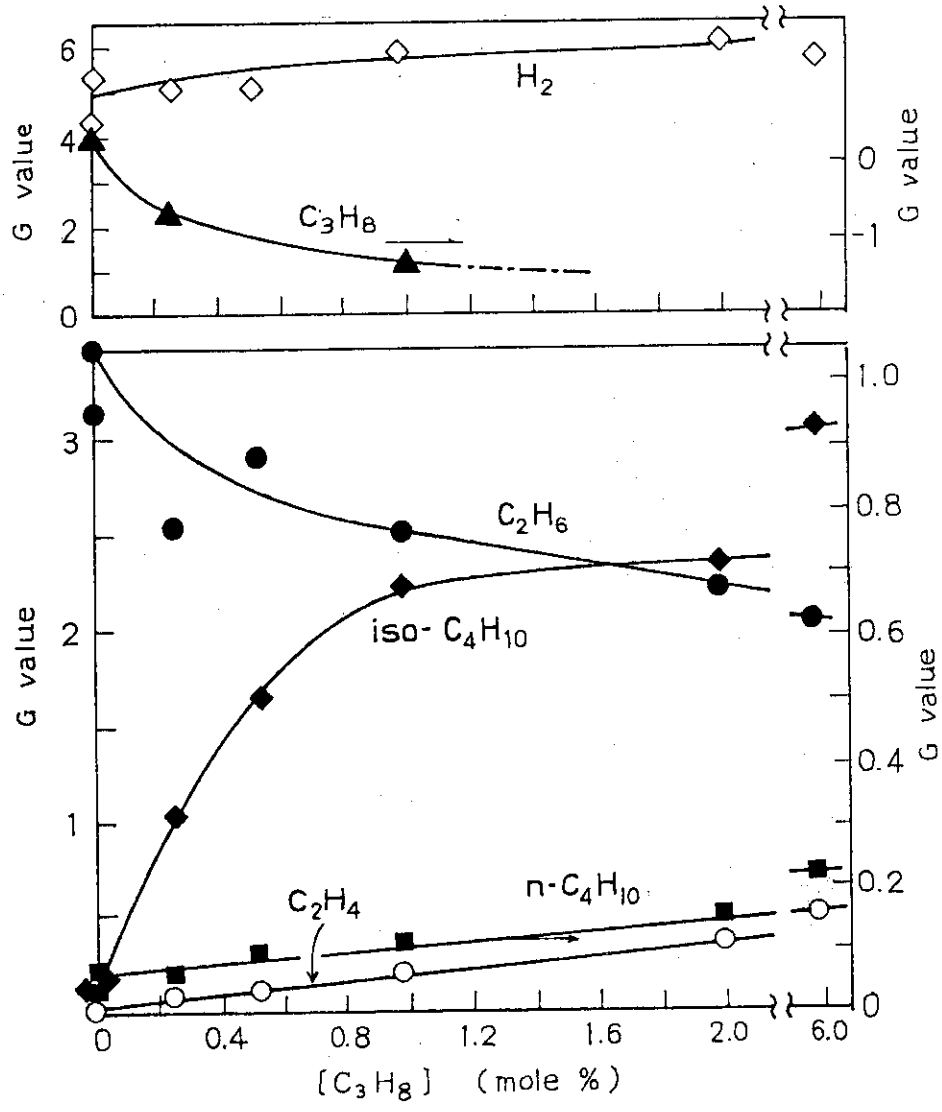

Fig. 6 G-values of hydrogen and hydrocarbons as a function of propane content: Top: hydrogen and consumed propane; Bottom: C_2 and C_4 hydrocarbons. Irradiation conditions are the same as those shown in the caption of Fig. 1.

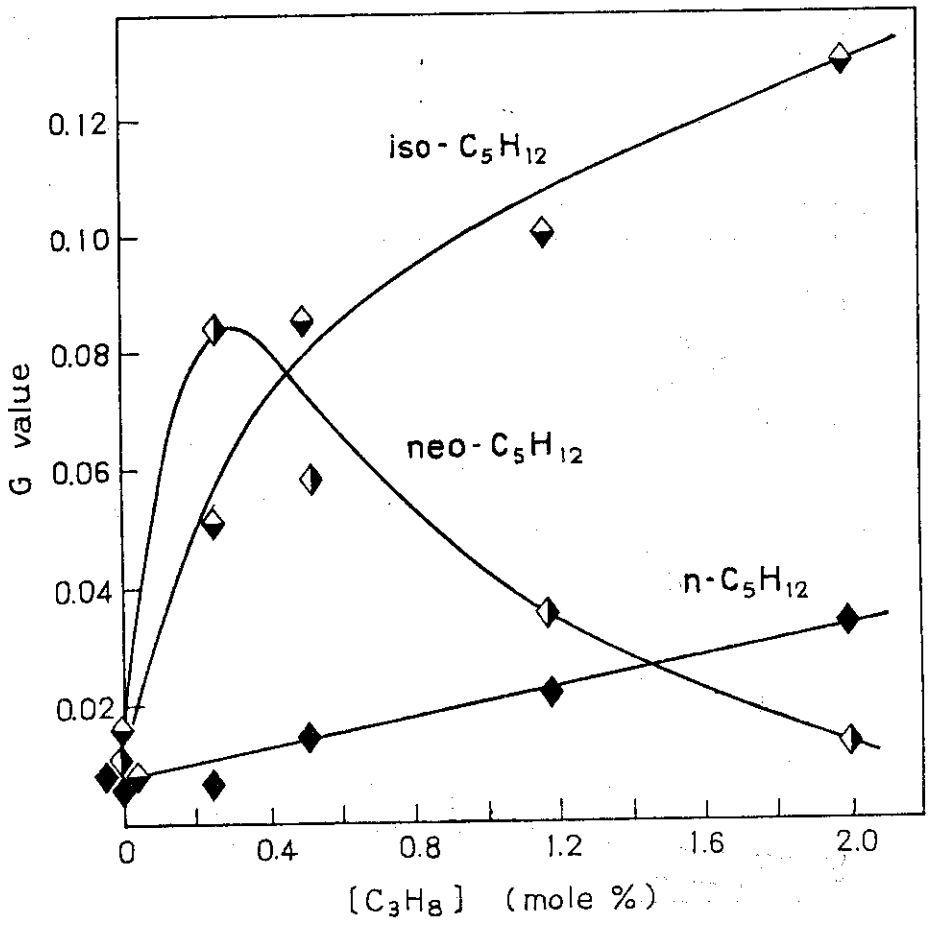

Fig. 7 G-values of pentanes as a function of propane content. Irradiation conditions are the same as those shown in the caption of Fig. 1.

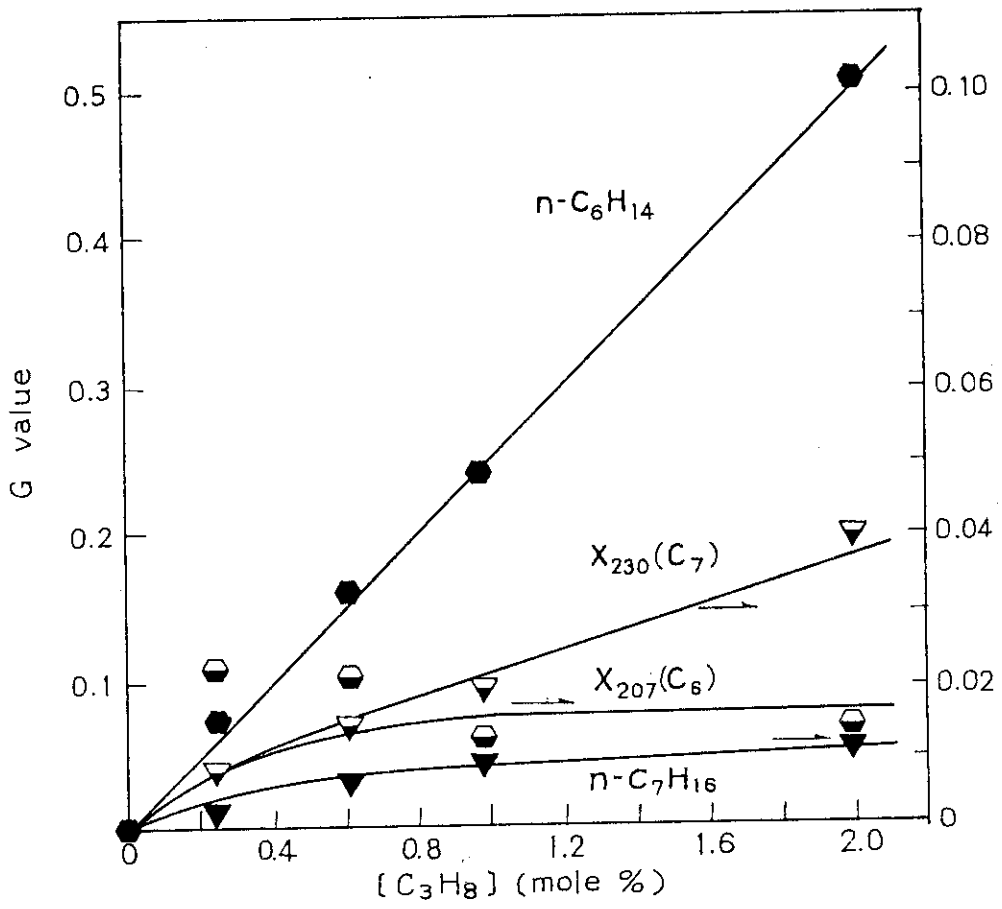

Fig. 8 G-values of hexanes and heptanes as a function of propane content. Irradiation conditions are the same as those shown in the caption of Fig. 1.

and those of hydrocarbon products grouped by carbon number in Fig. 9.

The G-value of hydrogen formation increases gradually while the G-value of ethane decreases with increasing propane content. The increase of $G(H_2)$ by the addition of 2 mole% propane is larger than that expected from simple additivity rule of $G(H_2)$ for each component ($G(H_2)$ from methane = 5.3; $G(H_2)$ from propane = 5.9), and therefore, energy transfer process from propane resulting in hydrogen formation may occur.

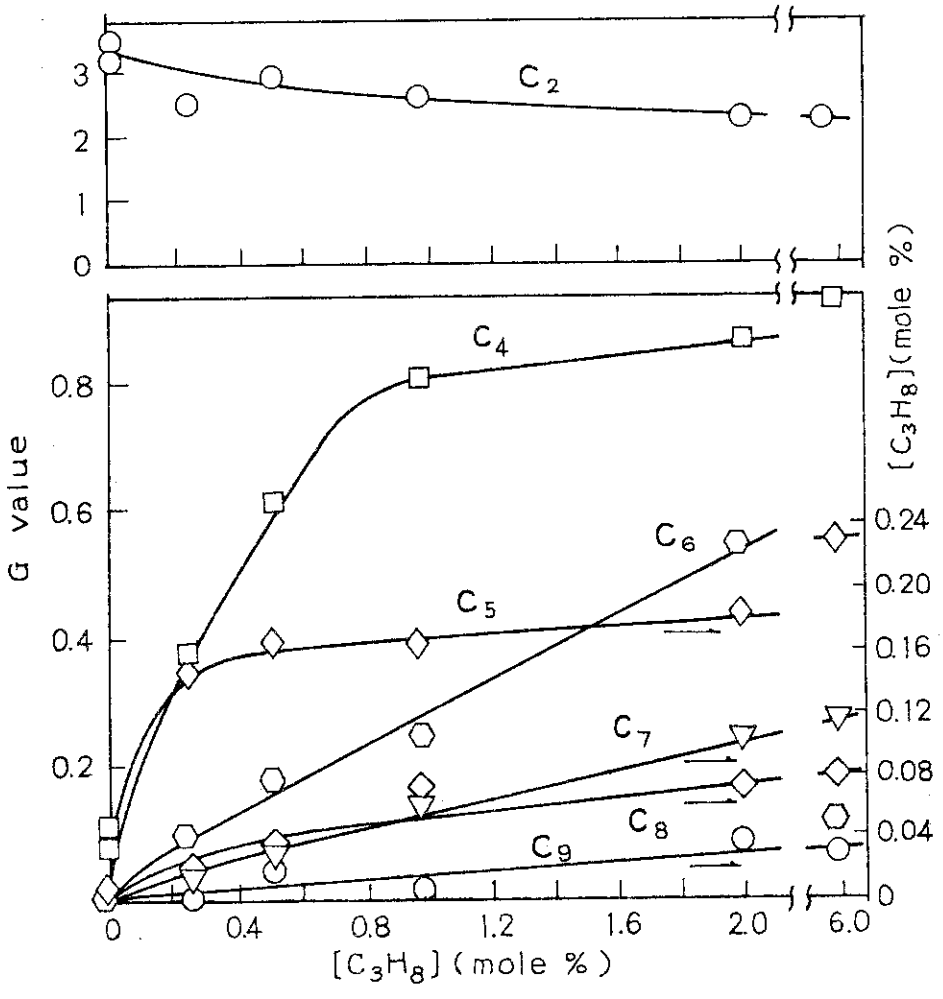

Fig. 9 G-values of hydrocarbons grouped by carbon number as a function of propane content.

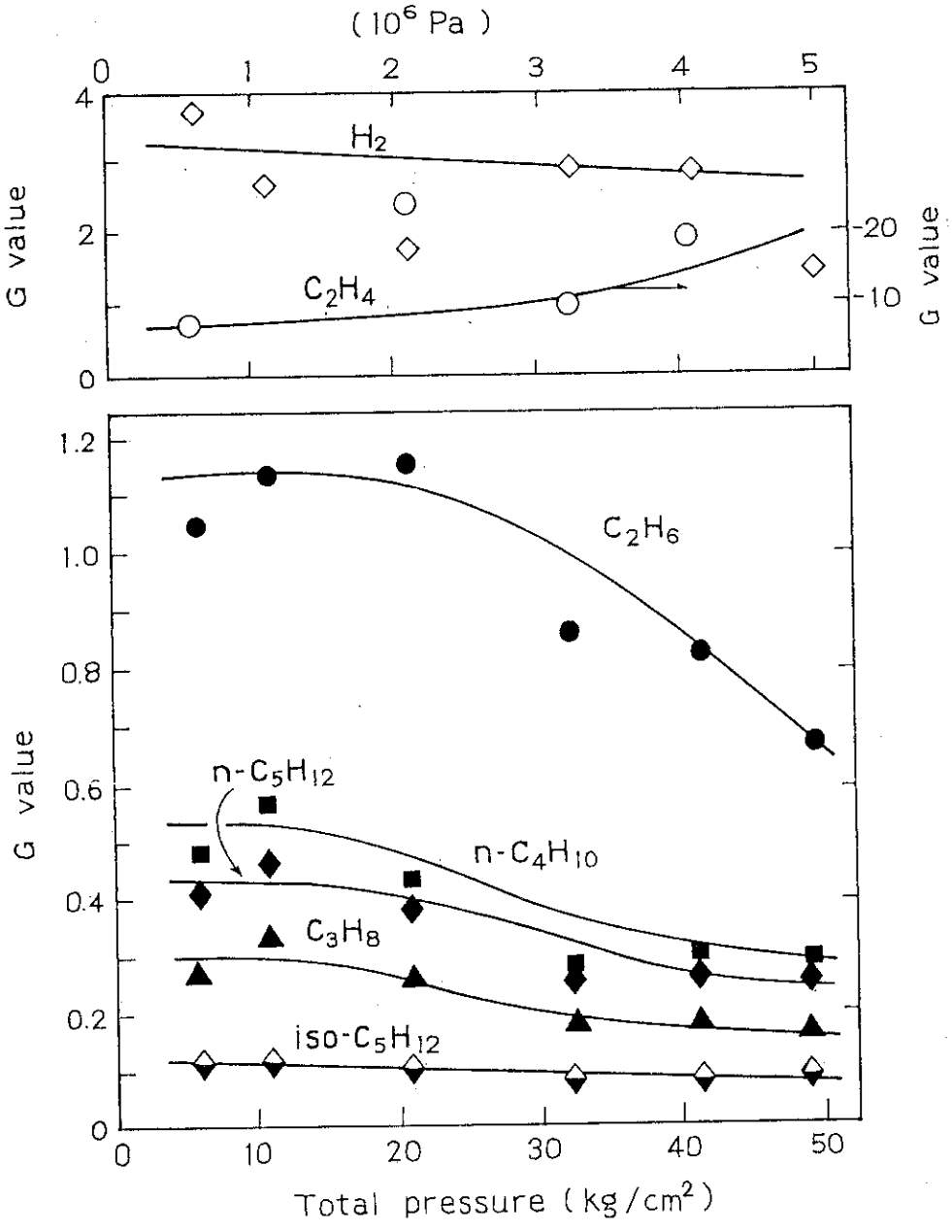

Fig. 10 G-values of products as a function of pressure: Top: hydrogen and consumed ethylene; Bottom: hydrocarbons ($C_2 \sim C_5$); ethylene content, 2 mole%; temperature, 323K.

The decrease of $G(C_2H_6)$ may be explained by a series of competition reactions (7) ∿ (9).

$$C_3H_8 + H \longrightarrow \dot{C}_3H_7 + H_2 \quad (7)$$

$$\cdot CH_3 + \cdot CH_3 \xrightarrow{CH_4} C_2H_6 \quad (8)$$

$$CH_3 + CH_3\dot{C}HCH_3 \text{ (or } \dot{C}H_2CH_2CH_3) \longrightarrow C_4H_{10} \quad (9)$$

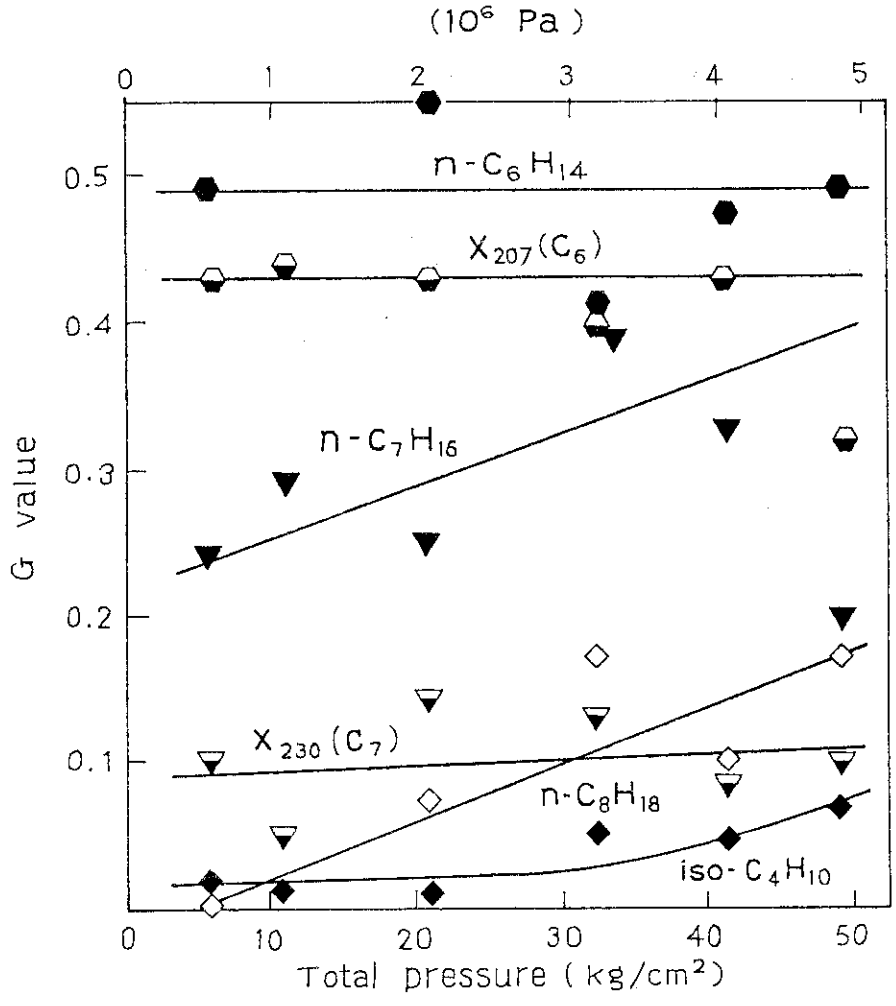

Fig. 11 G-values of hydrocarbon products (C_6 ∿ C_8) as a function of pressure. Irradiation conditions are the same as those shown in the caption of Fig. 10.

As observed for the radiolysis of methane-ethane mixture, the G-value of neo-C_5H_{12} gives a maximum at propane content of 0.3 mole% by unknown reason.

Effect of propane content on G-values of hydrocarbons grouped by carbon number (Fig. 9) is more complex than that observed for methane-ethane mixture; G-values of C_4, C_5, and C_8 asymptote to certain values with increasing propane content

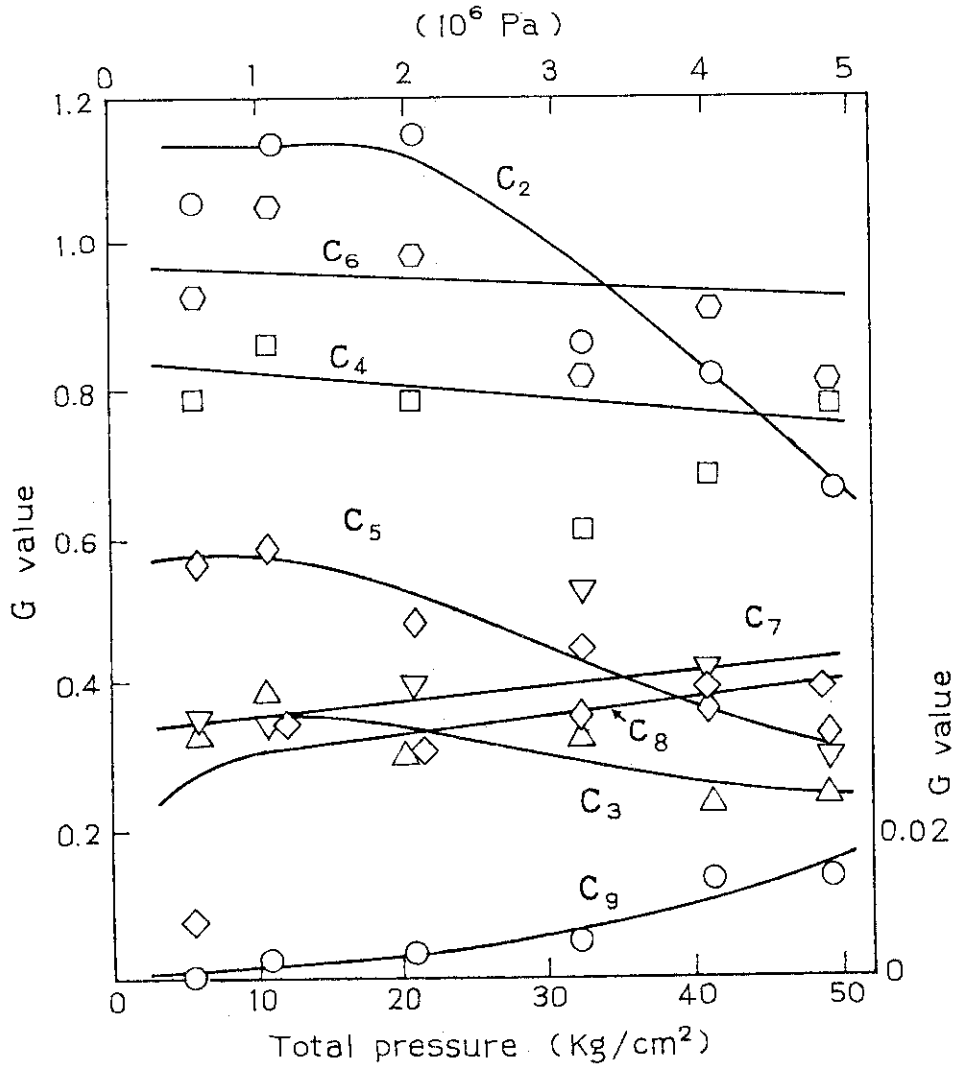

Fig. 12 G-values of hydrocarbons grouped by carbon number ($C_2 \sim C_9$) as a function of pressure. Irradiation conditions are the same as those shown in the caption of Fig. 10.

after sharp rise at small propane content, while those of C_6, C_7 and C_9 increase linearly with increasing propane content.

G-values of hydrogen and hydrocarbon products from methane -ethylene mixture are plotted in Figs. 10 and 11, as a function of pressure, and those of hydrocarbons grouped by carbon number in Fig. 12. The G-values of hydrocarbons of even carbon number are higher than those of odd carbon number up to C_7 at 1×10^6 Pa. This tendency is more clearly recognized at 5×10^6 Pa up to carbon number of 9, indicating that the hydrocarbon chain extends by ethylene unit more favorably at higher pressures.

(S. Sugimoto and M. Hatada)

1) S. Sugimoto and M. Hatada, JAERI-M 82-192, 4 (1982).
2) M. Hatada and S. Sugimoto, This report.

3. Composition of the Carbonaceous Solids Produced by Irradiation of Methane over Molecular Sieve 5A and Silica Gel

In the last annual report[1], it was reported that deposition of carbonaceous solid on the surface of molecular sieve (MS) 5A during irradiation is responsible for the loss in activity for the selective formation of C_2 and C_3 hydrocarbons from radiation chemical reaction of methane. Carbonaceous solid was found to deposit also on the surface of silica gel, but the solid showed little effect on the formation of low molecular weight hydrocarbons. The present study was carried out in an attempt to determine the amount and composition of the carbonaceous solids deposited on MS 5A and silica gel. For this purpose, Ar containing 2 mole% methane was irradiated in the presence of MS 5A and silica gel, and the amount of methane lost was determined from the difference in peak areas on the gaschromatograms of the effluent gas, recorded both before and after irradiation. The concentrations of the products in the effluent gas were monitored by gaschromatography in the same manner as described already[2].

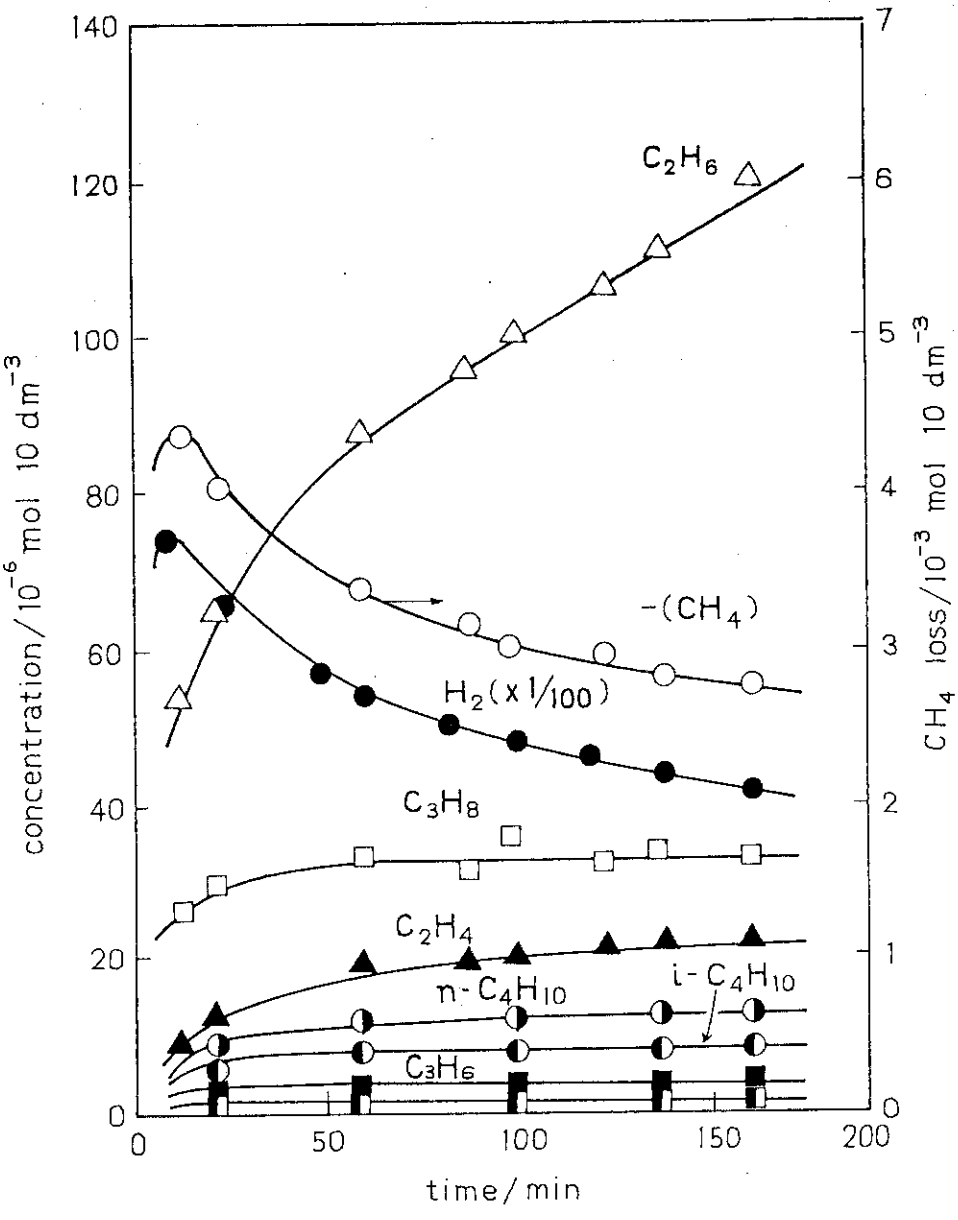

Fig. 1 Concentration of methane consumed and concentrations of products over MS 5A as a function of time after initiating irradiation.

The concentration of methane consumed and the concentrations of hydrogen and low molecular weight hydrocarbons formed by irradiation of Ar containing 2 mole% methane over MS 5A at 300°C are shown in Fig. 1 as a function of irradiation time. The curve for methane loss indicates that the rate of consumption of methane reaches a maximum within 20 min of irradiation and then decreases gradually with time. The curve for evolved H_2 closely resembles that for methane loss, showing that H_2 is produced in proportion to the amount of methane consumed. On the other hand, the concentrations of most hydrocarbons tend to increase gradually with time.

From the data in Fig. 1, one may estimate the material balance of the reaction. Fig. 2 shows, in addition to the

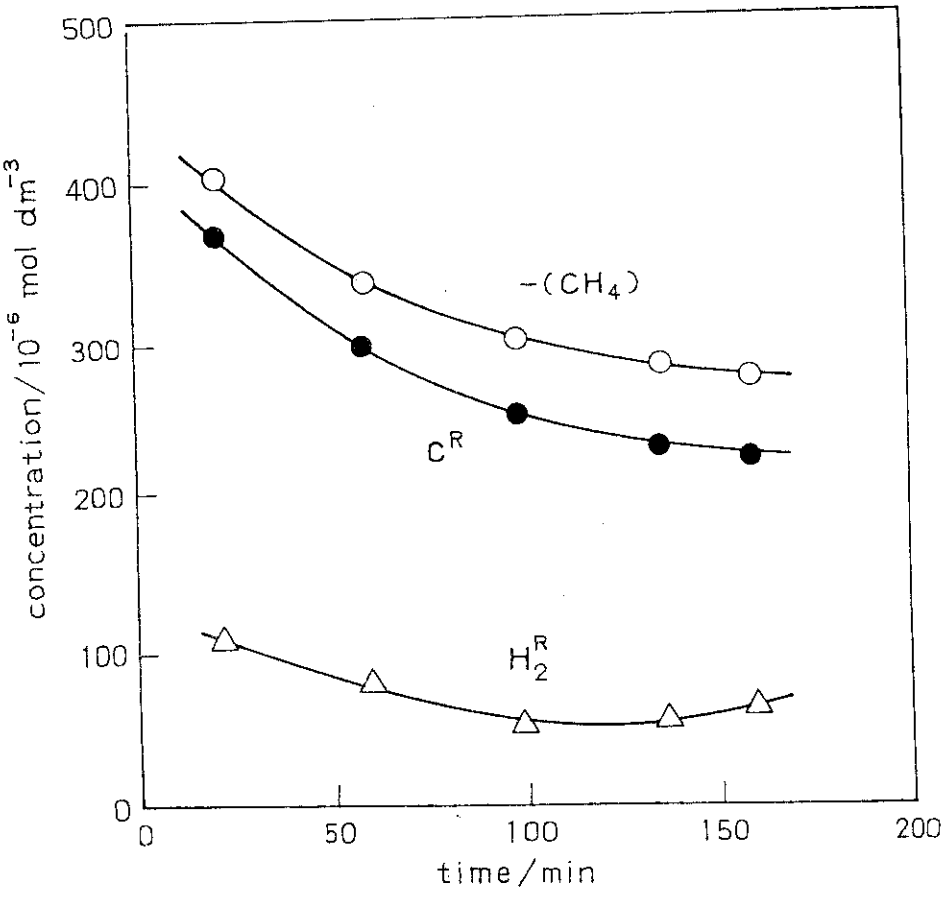

Fig. 2 A plot of material balance over MS 5A.
For notations, see text.

concentration of methane loss, the concentrations of C^R and $H_2{}^R$. C^R denotes the residual carbon, i.e. the difference between the concentration of carbon in the consumed methane and that of carbon contained in all the hydrocarbons detected. Similarly, $H_2{}^R$ denotes the residual H_2, obtained by subtracting the sum of concentrations of H_2 observed and H_2 contained in all the hydrocarbons produced from the concentration of hydrogen in the consumed methane. Fig. 2 shows that most of the carbon in the methane consumed is left on the surface of MS 5A as C^R, the remaining 10 ∿ 20% being incorporated in the low molecular weight hydrocarbons. On the other hand, most of the hydrogen in the methane consumed is incorporated in H_2 and low molecular weight hydrocarbons. The ratio $[C^R]/\frac{1}{2}[H_2{}^R]$, which is thought to be a measure of the composition of the carbonaceous solid remaining on the surface of MS 5A, lies in the range 7.0 ∿ 9.8, showing that the carbonaceous solid produced from methane over MS 5A is highly abundant in carbon atoms.

The result obtained over silica gel is shown in Fig. 3. The curve for methane loss indicates that the rate of consumption of methane, which is much greater than that over MS 5A, decreases rapidly in the initial stage followed by a gradual decrease after 20 min of irradiation. On the other hand, the concentration of H_2 decreases gradually with time. Thus, the curve for evolved H_2 resembles that for methane loss except for the initial stage. It is noted, however, that the concentration of H_2 is not much different from that over MS 5A (Fig. 1) although the conversion of methane over silica gel is much greater than the value over MS 5A. The concentrations of most hydrocarbons formed over silica gel are greater than twice that over MS 5A and increase with time. In particular, the concentrations of C_2H_6 and C_2H_4 increase rapidly in the initial stage of irradiation.

Fig. 4 shows the material balance of the reaction over silica gel obtained by the same way as in the case of MS 5A. The curves for methane loss and C^R in Fig. 4 indicate that 70 ∿ 80% carbon in the methane consumed is left in the carbonaceous solid and the remaining 20 ∿ 30% carbon is incorporated in low

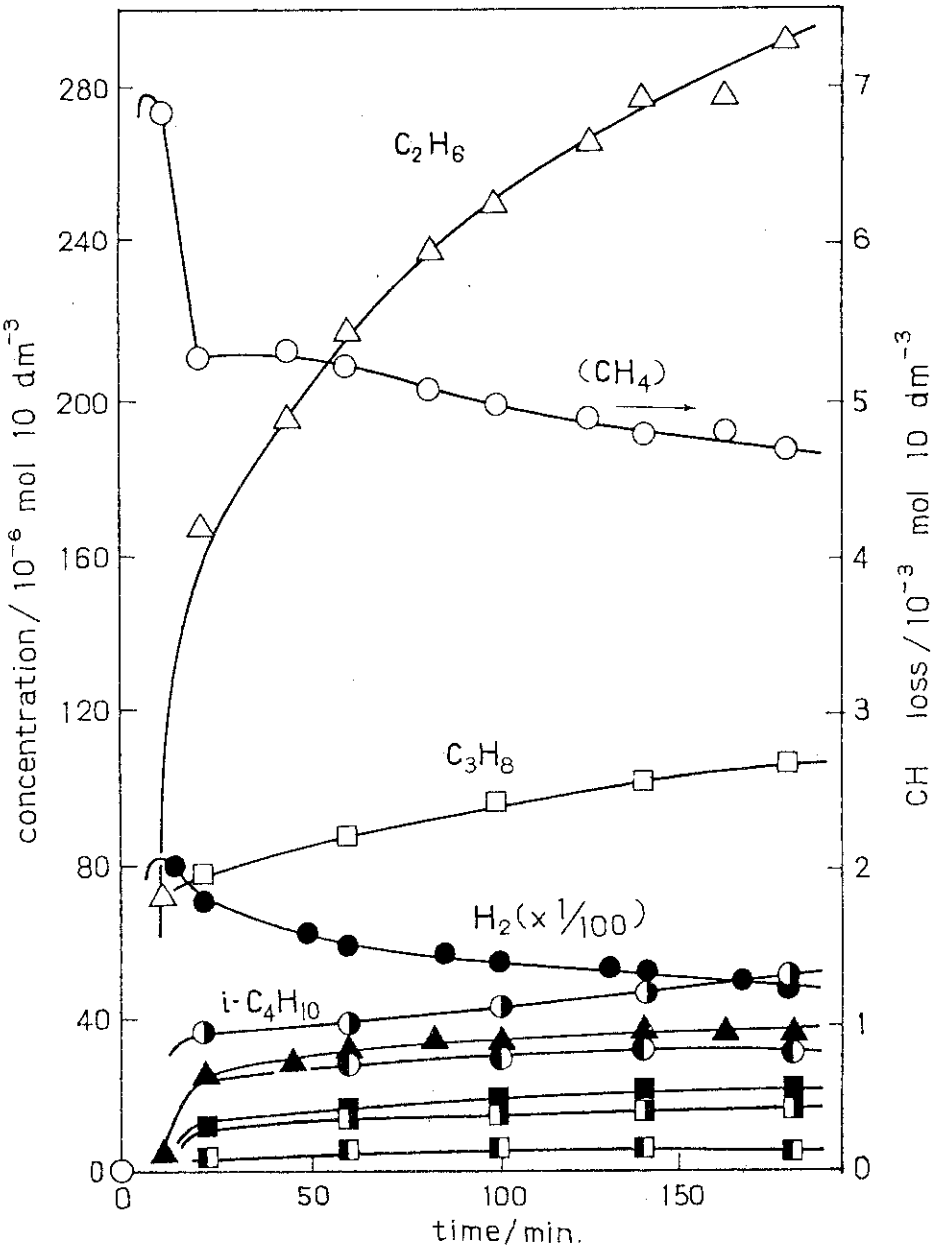

Fig. 3 Concentration of methane consumed and concentrations of products over silica gel as a function of time after initiating irradiation.

molecular weight hydrocarbons. The $[C^R]/\frac{1}{2}[H_2{}^R]$ ratio obtained from Fig. 4 lies in the range 4.2 ∿ 2.6 with a maximum value in the initial stage of irradiation, showing that the carbon content in the carbonaceous solid produced from methane over silica gel is much lower than that over MS 5A.

As described already, although both the conversion of methane and the concentrations of low molecular weight hydrocarbons are much greater over silica gel than over MS 5A, the concentration of H_2 evolved over silica gel is close to that over MS 5A. This fact suggests that some of the H_2 once

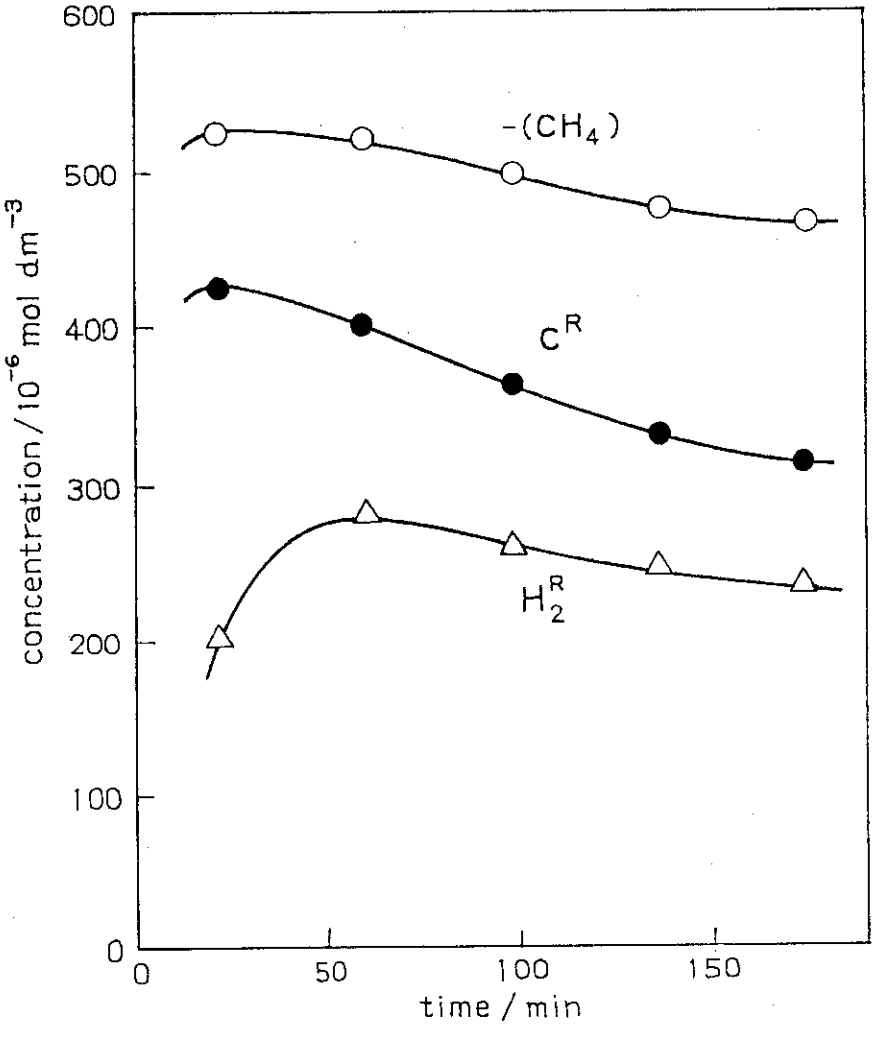

Fig. 4 A plot of material balance over silica gel. For notations, see text.

produced over silica gel would be consumed in the reaction with the carbonaceous solid to produce low molecular weight hydrocarbons, by taking into account the previous finding[1] that the carbonaceous solid produced over silica gel is efficiently decomposed by irradiation under flowing hydrogen.

Although the present experiments provide no information on the mechanism for the formation of the carbonaceous solids on the surface of MS 5A and silica gel, they may be produced by successive cycles of dehydrogenation of the hydrocarbons formed from methane and a combination of the radicals thus formed. Since MS 5A and silica gel adsorb alkenes strongly, the radiation-induced polymerization of alkenes on the surfaces of MS 5A and silica gel may be responsible to some extent for the formation of the carbonaceous solids.

(Y. Shimizu, S. Nagai and M. Hatada)

1) S. Nagai, Y. Shimizu, and M. Hatada, JAERI-M 82-192, 29 (1982).
2) S. Nagai, Y. Shimizu, and M. Hatada, JAERI-M 9856, 72 (1981).

4. The Water-Gas Shift Reaction Induced by Electron Beam Irradiation

The water-gas shift reaction (1) finds extensive use in

$$CO + H_2O \rightarrow CO_2 + H_2 \qquad (1)$$

industry to produce hydrogen and is currently carried out using an iron oxide based catalyst or a copper-zinc oxide catalyst[1]. In spite of the importance from both fundamental and practical points of view, however, the reaction (1) has not been studied radiation chemically yet. Previous studies on the radiation induced reaction of CO and H_2O adsorbed on silica gel[2], alumina and MgO[3] indicate that such insulators which show no activity for the reaction without radiation exhibit under

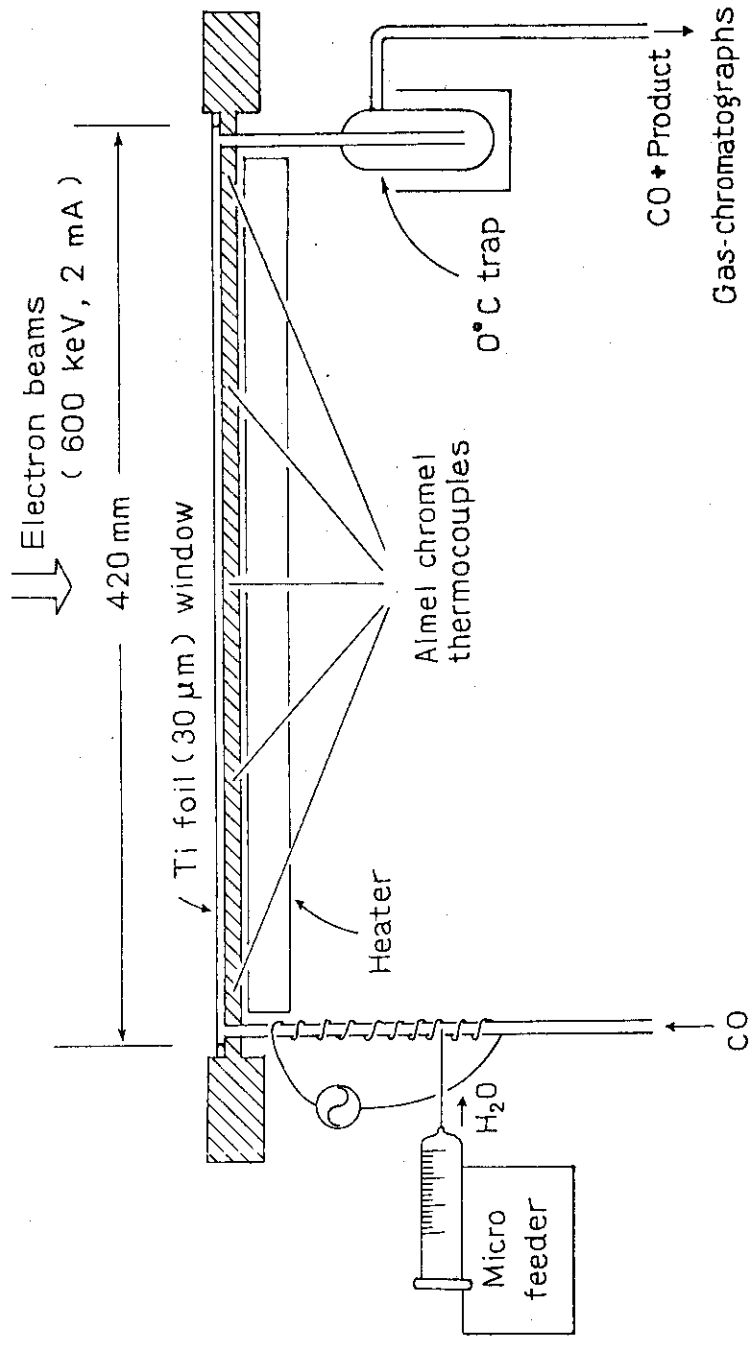

Fig. 1 Schematic of experimental set-up.

electron beam irradiation catalytic activity for the water-gas shift reaction (1) to produce CO_2 and H_2 with small amounts of hydrocarbons. In the present study, analysis was carried out of the products by irradiation of gas mixtures of CO and H_2O both in the absence and presence of silica gel in order to learn the detail of the water-gas shift reaction induced by radiation.

Fig. 1 shows the schematic of experimental set-up. The high temperature flow reactor is made of stainless steel, the inner volume being 420 x 20 x 3 mm^3. CO was fed through a thermal mass flow controller (Ueshima-Brooks) and mixed with H_2O gas which was introduced to the stainless steel tubing through a micro feeder (Furue Sci.) followed by being evaporated by a preheater. The gas mixture of CO and H_2O was irradiated with electron beams of 600 keV and 2 mA either in the presence or absence of silica gel. The temperature of the reactor was controlled by an electric heater attached to the bottom of the reactor. The gas emerging from the reactor was passed through a cold trap to collect unreacted H_2O, and then analyzed by three gaschromatographs in series.

No matter when silica gel was present or not, irradiation of CO and H_2O gas mixture produced CO_2 and H_2 dominantly and low molecular weight hydrocarbons with small amounts of oxygenated compounds such as methanol and acetaldehyde. Table 1 shows the concentrations of the dominant products and hydrocarbons produced from the reaction in the absence of silica gel, i.e., in the homogeneous state and in the presence of silica gel. In the homegeneous reaction, the concentration ratio of CO_2 and H_2 approaches to unity at higher temperatures, suggesting the occurrence of the water-gas shift reaction (1) by electron beams. The presence of silica gel results in increase of the concentration of each product by more than one order of magnitude. The concentration of CO_2 produced over silica gel is greater than 10 times the steady-state value of CO_2 produced when CO alone was irradiated in the presence of silica gel and the concentration of H_2 is greater than 100 times the value of H_2 by irradiation of H_2O-Ar gas mixture over silica gel (see Table 2). It seems worth mentioning that irradiation of H_2O

Table 1 Concentration of Products by Irradiation of 1 : 1 CO-H_2O Gas Mixture

Solid catalyst	———			Silica Gel			
Temperature (°C)	357	400	452	340	363	429	513
Concentration (μmole/ml)							
CO_2	0.510	0.491	0.561	9.81	9.59	8.94	8.23
H_2	0.193	0.261	0.395	6.87	6.89	6.51	6.30
CH_4	0.010	0.013	0.014	0.326	0.300	0.196	0.040
C_2H_4	0.000	0.000	0.000	0.001	0.001	0.000	0.000
C_2H_6	0.002	0.002	0.002	0.037	0.028	0.015	0.004
C_3H_8	0.001	0.001	0.001	0.011	0.011	0.006	0.001

Irradiation: 600 keV, 2 mA.

Flow rate : CO 50 ml/min, H_2O 50 ml/min.

gas produced H_2 and O_2 in the mole ratio of approximately 2 : 1 as shown in Table 2, but O_2 was not detected in the reaction of CO-H_2O gas mixture under any reaction conditions studied. From these facts it may be concluded that the formation of CO_2 and H_2 from CO-H_2O mixture over silica gel is ascribed to the water-gas shift reaction (1).

As can be seen from Table 1, the concentrations of CO_2 and H_2 tend to decrease slightly with the increase of temperature, whereas the concentrations of hydrocarbons decrease drastically at higher temperatures. Similar results were obtained for 70 : 30 CO-H_2O mixture (Table 3) and 24 : 76 mixture (Table 4). The most probable pathway by which hydrocarbon is produced from CO-H_2O mixture would be the one involving the water gas shift reaction (1) followed by the reaction to produce methane (2) and higher hydrocarbons as shown in Scheme I:

Scheme I

$$CO + H_2O \rightarrow CO_2 + H_2 \quad (1)$$

$$3H_2 + CO \rightarrow CH_4 + H_2O \quad (2)$$

The fact that the reaction (2) becomes thermodynamically unfavorable at high temperature is consistent with the observed decrease in the concentrations of hydrocarbons with the

Table 2 Concentration of Products by Irradiation of H_2O-Ar Gas Mixture over Silica Gel

Temperature (°C)	385	404	489	558
Concentration (μmole/ml)				
H_2	0.069	0.066	0.041	0.028
O_2	0.030	0.027	0.017	0.008^8

Irradiation: 600 keV, 2 mA.
Flow rates : H_2O 50 ml/min, Ar 50 ml/min.

Table 3 Concentration of Products by Irradiation of 70/30 CO-H_2O Gas Mixture over Silica Gel

Temperature (°C)	340	363	429	513
Concentration (μmole/ml)				
CO_2	7.64	6.76	6.51	6.08
H_2	4.71	4.13	4.57	4.53
CH_4	0.389	0.390	0.184	0.048
C_2H_4	0.000^5	0.000^8	0.000^9	0.000^4
C_2H_6	0.034	0.035	0.013	0.005
C_3H_8	0.008	0.011	0.005	0.001
CO conversion (%)	19.9	17.7	16.5	15.0

Irradiation: 600 keV, 2 mA.

Table 4 Concentration of Products by Irradiation of 24/76 CO-H_2O Gas Mixture over Silica Gel

Temperature (°C)	340	363	429	513
Concentration (μmole/ml)				
CO_2	15.2	14.7	12.3	11.1
H_2	15.1	14.7	11.0	10.1
CH_4	0.118	0.112	0.024	0.006
C_2H_4	0.000	0.000	0.000	0.000
C_2H_6	0.001	0.001	0.000^4	0.000^2
C_3H_8	0.000^1	0.000^2	0.000	0.000
CO conversion (%)	37.5	36.2	30.1	27.2

Irradiation: 600 keV, 2 mA.

Table 5 Concentration of Products by Irradiation of Aqueous Solution of Formaldehyde over Silica Gel

Temperature (°C)	367	404
CO_2	1.45	0.88
H_2	4.79	4.48
CH_4	0.74	0.85
C_2H_4	0.006	0.024
C_2H_6	0.124	0.193
C_3H_8	0.043	0.079

Irradiation was carried out with electron beams of 600 keV and 2 mA.

Table 6 Concentration of Products by Irradiation of HCOOH-Ar Mixture* over Silica Gel

Temperature (°C)	359	384	466	555
Concentration (μmole/ml)				
CO_2	9.79	9.77	8.57	8.47
H_2	7.21	7.73	6.65	7.07
CH_4	0.310	0.223	0.091	0.033
C_2H_4	0.001	0.001	0.000	0.000
C_2H_6	0.032	0.019	0.007	0.003
C_3H_8	0.011	0.007	0.002	0.000

* Flow rates: HCOOH 73 ml/min, Ar 50 ml/min.

increase of temperature. The possibility involving disproportionation of CO to produce carbon (C_s) and CO_2 followed by the reaction of surface carbon with H_2O as in Scheme II may be excluded since it cannot explain the high concentration of H_2 comparable to CO_2 in the present study.

Scheme II

$$4CO \longrightarrow 2C_s + 2CO_2 \quad (3)$$

$$2H_2O + 2C_s \longrightarrow CH_4 + CO_2 \quad (4)$$

In an attempt to study the mechanism of the water-gas shift reaction over silica gel, product analyses were carried out for the radiation induced reaction of aqueous formaldehyde and formic acid over silica gel. These two systems were selected on the basis of our observation[3] of formyl radical in addition to CO_2^- and OH radicals in the electron spin resonance spectra of CO and H_2O adsorbed on silica gel after γ-irradiation at low temperature. Table 5 shows the products obtained from aqueous formaldehyde. Although the products are identical with those for the water-gas shift reaction, the concentration of H_2 is greater than that of CO_2, in contrast to the result for the water-gas shift reaction. On the other hand, irradiation of formic acid gave the products (Table 6), not only the concentrations but also their temperature dependence being in good agreement with those for the water-gas shift reaction. This result strongly indicates that the water-gas shift reaction induced by electron beam irradiation over silica gel proceeds involving formic acid or its ion as the reaction intermediates. Further study on the mechanism is under way using AES/SIMS surface analysis technique.

(S. Nagai and Y. Shimizu)

1) D. C. Grenoble and M. M. Estadt, J. Catal., 67, 90 (1981).
2) S. Nagai and Y. Shimizu, JAERI-M 9856, 28 (1981).
3) S. Nagai and Y. Shimizu, JAERI-M 82-192, 42 (1982).

5. Electron and Ar^+ Ion Impact Effects on Silica Gel as Studied by AES and SIMS

Previous studies on the radiation chemical reactions of $CO-H_2$[1] mixture, CH_4[2] and $CO-H_2O$ mixture[3] in the presence of various solid catalysts revealed that some insulators such as silica gel and alumina exhibit catalytic activity for the reactions under electron beam irradiation. Although such activity of insulators has been ascribed to transfer of radiation energy from insulators to the gases adsorbed on their surfaces, the mechanism of energy transfer is far from understanding at present. In order to shed some light on the mechanism, studies have been initiated of fundamental processes which take place at gas/solid interfaces when energetic electrons or ions impinge on the surfaces of solids, especially insulators, covered with gases, using a combined surface analysis system of Auger Electron Spectroscopy (AES) and Secondary Ion Mass Spectrometry (SIMS). The processes to be studied include structural change of solid surfaces, state conversion of adsorbed molecules and desorption of gases from surface. Of these, desorption of gases from surface by electron and ion impact has been most extensively studied to date in connection with plasma-material interactions. Searches for the literature on electron and ion impact desorption[4], however, indicate that most of the studies have been confined to the surfaces of metals and semiconductors and quite a few studies have been made on insulator surfaces. Described below are the preliminary results obtained for silica gel concerning the electron impact-induced change of the surface structure and the secondary ion emission from the surface.

Experiments were carried out in an ultrahigh vacuum system (AES-350S, Nichiden Anelva) consisting of Auger spectrometer and secondary ion mass spectrometer. The stainless steel vacuum chamber is connected to a turbomolecular pump (450 l/sec, Leiboldt-Heraeus) and an auxiliary rotary pump (Alcatel) which provide a base pressure as low as 2×10^{-9} Torr. The Auger spectrometer consists basically of a cylindrical mirror

analyser, electron gun (0 ∿ 5 keV) and ion gun (3 keV). The secondary ion mass spectrometer is composed of a quadrupole mass spectrometer (AGA 360) equipped with an energy filter and ion gun (0 ∿ 5 keV).

Silica gel (Mallinckrodt, 100 mesh) was pressed to pellets of 0.1 ∿ 0.3 mm in thickness. The specimen was placed on a sample holder equipped with an ohmic heater. The temperature was measured with a CA thermocouple in contact with the surface of the specimen. The primary beam currents employed in this study were ∿9 μA for electrons and ∿0.4 μA for Ar^+ ions. The beam diameter of both primary electrons and Ar^+ ions during SIMS measurement was 3 mm as measured by a blue cellophane dosimeter (Tokyo Cellophane).

Figure 1 shows the change of Auger spectra of silica gel

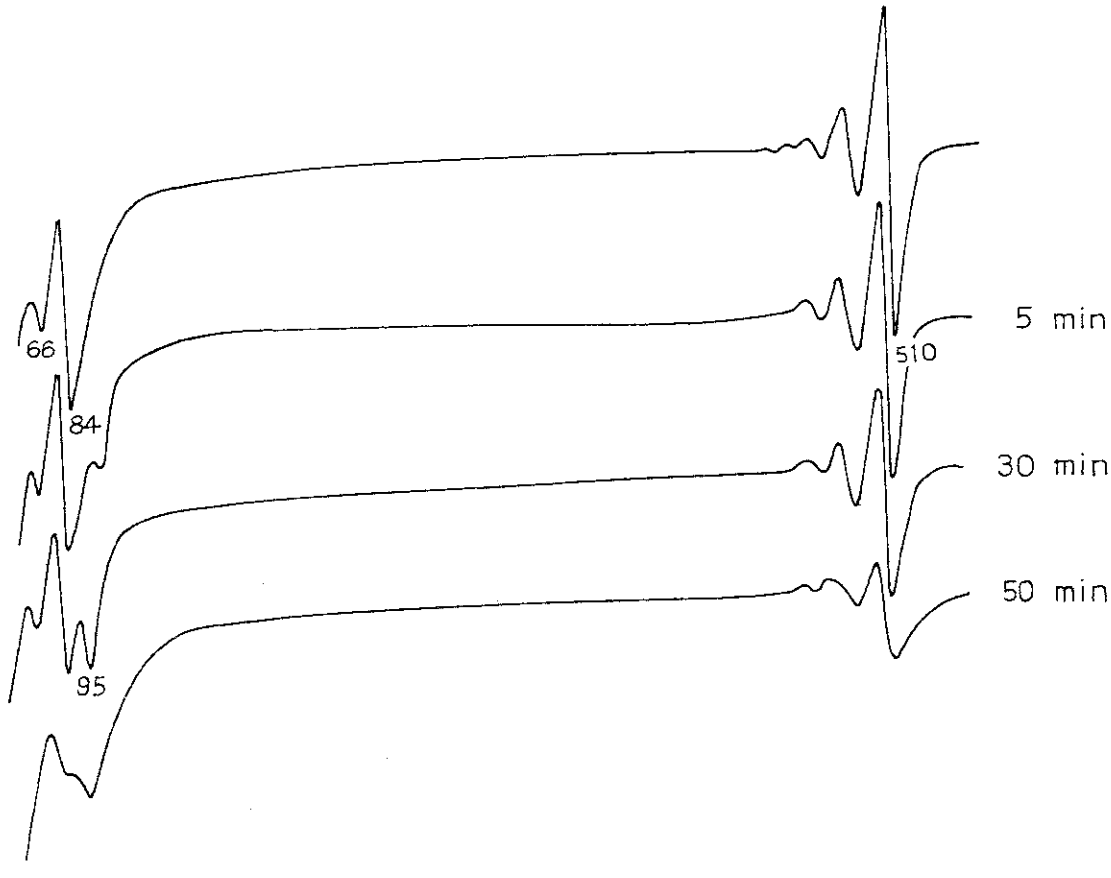

Fig. 1 Variation of Auger spectrum of silica gel during electron irradiation.

with time of impact with electrons (E = 1.5 keV). The peaks at 66 and 84 eV are due to Si_{LVV} transitions and the peak at 510 eV due to O_{KLL} transition. With the impact time, the intensities of these peaks decrease gradually and a new peak at 95 eV due to Si_{LVV} from elemental silicon appears and increases in intensity. The new peak at 95 eV is stable only at ultrahigh vacuum. A prolonged impact results in the distortion of the Auger spectrum (Fig. 1e), owing to the charging up of the sample. Fig. 2 shows the variation of the peak heights of Si(84), Si(95) and O(510) lines with time. These results are in good agreement with those reported for silicon single crystals and vitreous silica[5] and indicate that electron impact on silica gel induces scission of Si-O bonds followed by reduction of the surfaces.

Figure 3 compares the secondary ion mass spectra of silica gel by simultaneous impact of Ar^+ ions and electrons and by Ar^+ ion impact. The secondary ions from silica gel, Si^+, SiO^+, $SiOH^+$, Si_2O^+, and Si_2OH^+, which are the minor components by Ar^+ ion impact, are produced dominantly by the simultaneous impact. It appears that incident electrons neutralize the positive charge induced by Ar^+ ions on the surface to help the sputtering of silica gel by Ar^+ ions. The following results on the desorption of water from silica gel were obtained with the simultaneous impact of 4 keV Ar^+ ions and 1.5 keV electrons.

Dehydration of silica gel at 200°C in the vacuum chamber of the analysis system proved to show little effect on the mass spectrum of the secondary ions from silica gel except two hydrogenated ions, $SiOH^+$ and Si_2OH^+. The intensities of these two ions decreased markedly after dehydration of silica gel as shown in Fig. 4. Figure 5 shows the ion currents of the secondary ions from silica gel before and after dehydration as a function of impact time. It can be seen from Fig. 5b that the ion currents of all ions from silica gel after dehydration showed little change with time. On the other hand, the ion currents of the two ions $SiOH^+$ and Si_2OH^+ from silica gel before dehydration (Fig. 5a) gradually decrease with time to approach the values obtained from silica gel after dehydration,

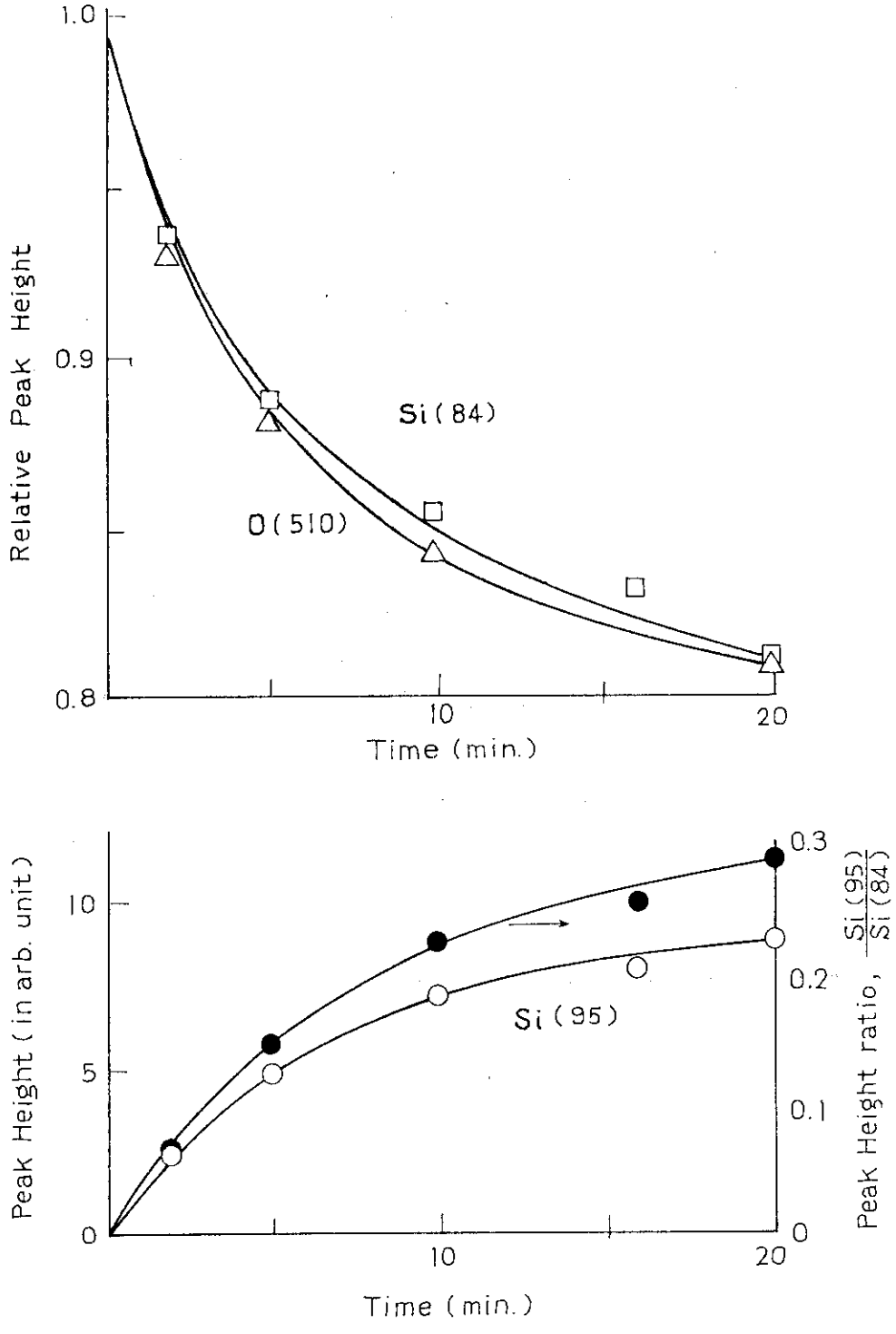

Fig. 2 Variation of Auger peak heights during electron irradiation of silica gel.

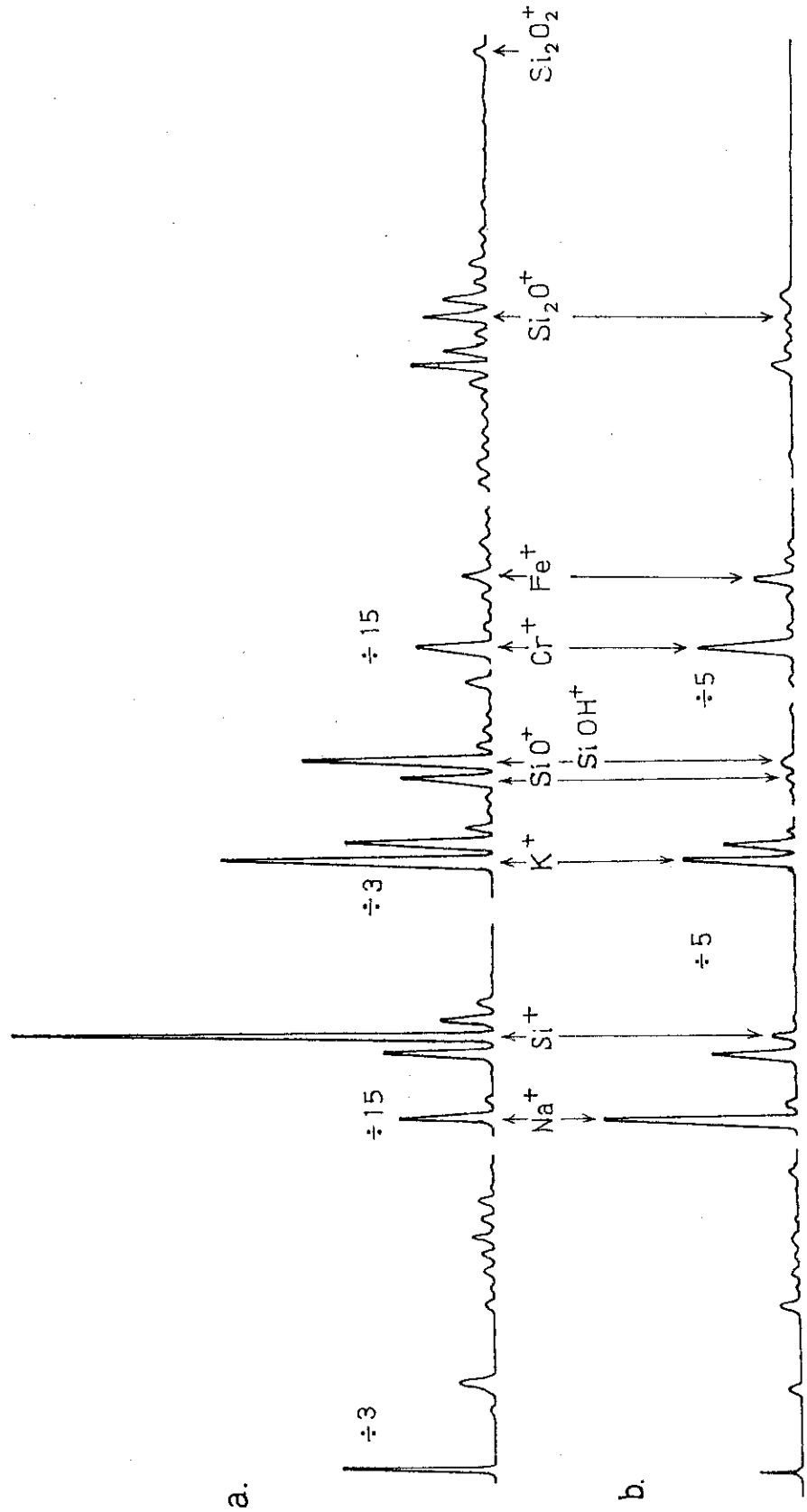

Fig. 3 SIMS spectra of silica gel by Ar^+ + e impact (a) and Ar^+ impact (b).

whereas the ion currents of the other three ions showed no decrease. These findings indicate that the formation of $SiOH^+$ and Si_2OH^+ are closely related to the presence of water adsorbed on silica gel.

On assuming that secondary ion current is proportional to the coverage of adsorbed molecules on solid surfaces, the time dependence of the secondary ion current is shown by eq. (1)[6]:

$$i^+/i_0^+ = \exp\{-(JQ/\varepsilon)t\} \qquad (1)$$

where i_0^+ is the initial value of ion current i^+, J and ε are the current density and charge of primary ions, respectively, and Q is

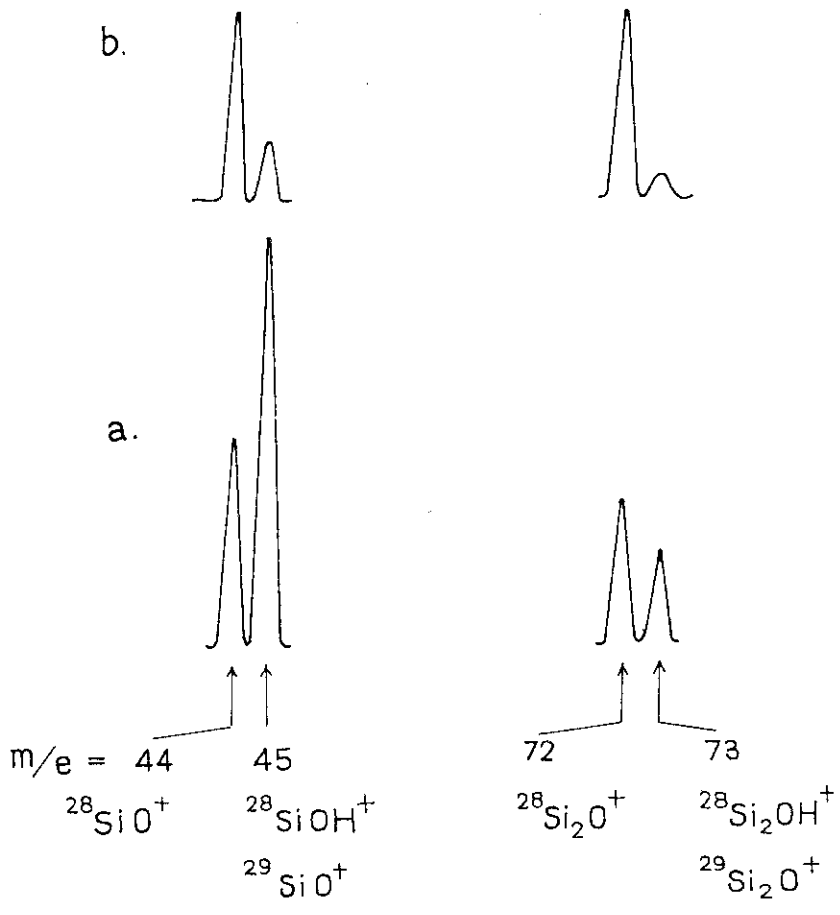

Fig. 4 A part of SIMS spectra of silica gel before (a) and after dehydration (b).

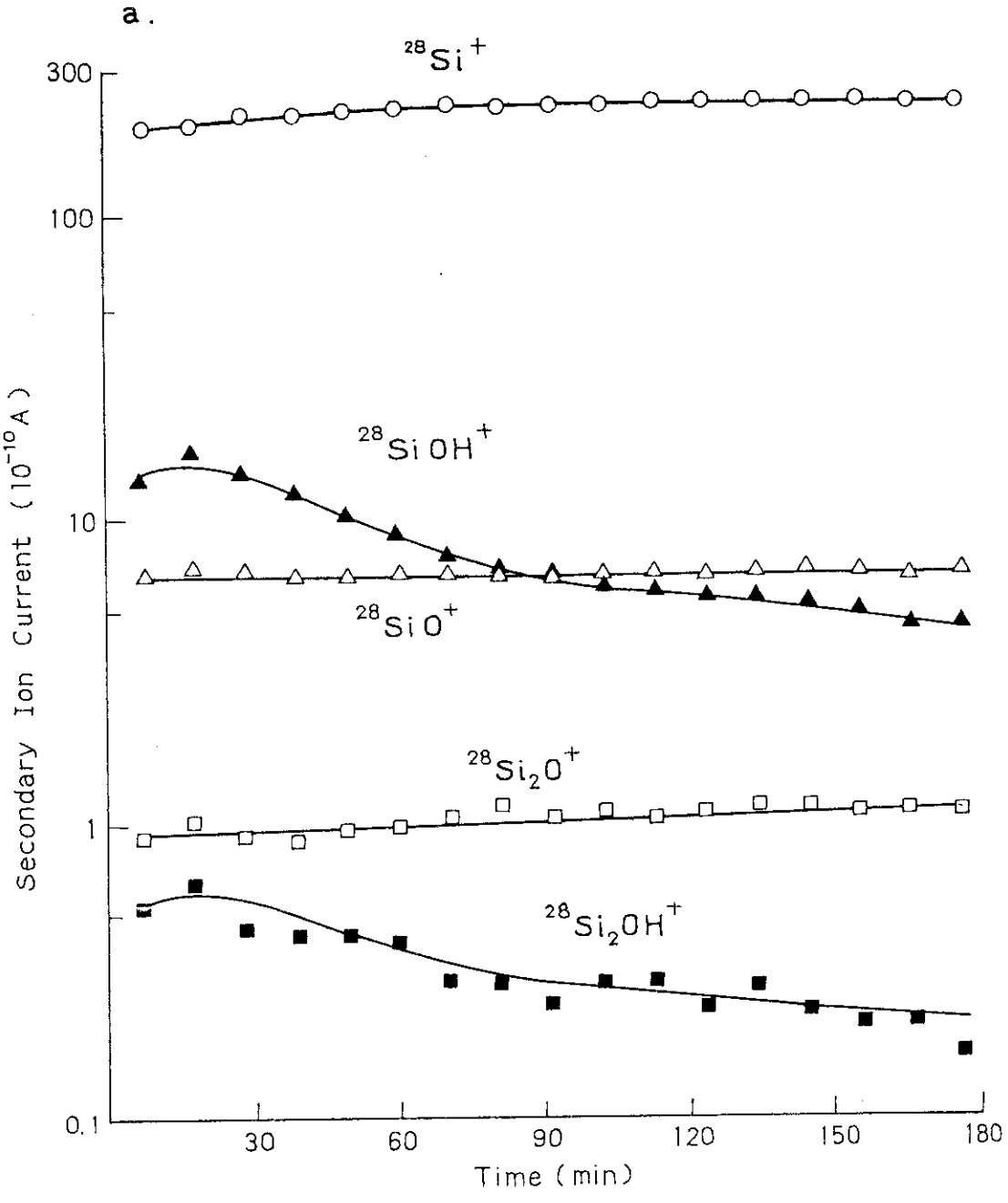

Fig. 5 Secondary ion current vs. sputtering time for silica gel before (a) and after (b) dehydration.

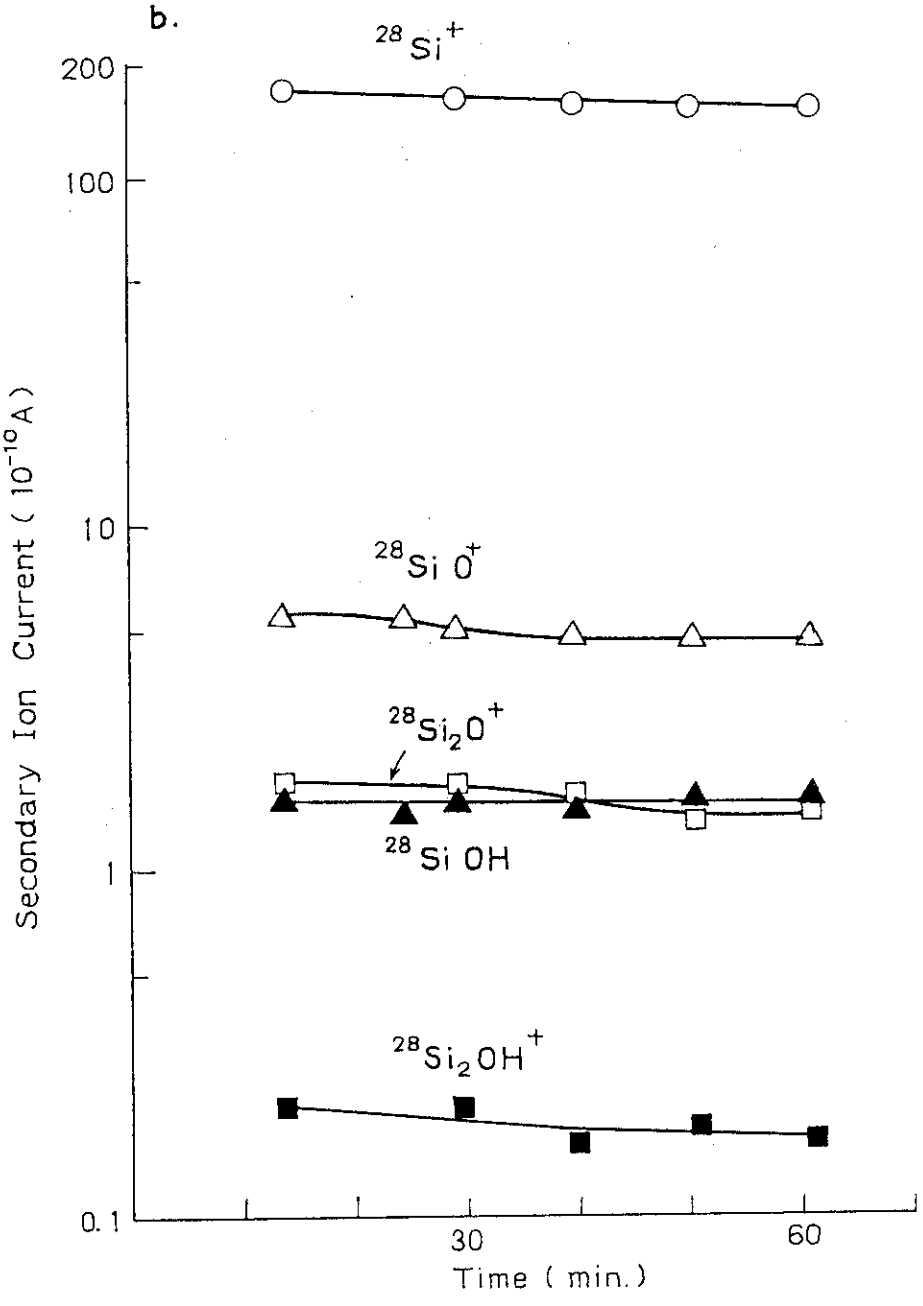
b.
$^{28}Si^+$
200
100
10
1
0.1
$^{28}Si\,O^+$
$^{28}Si_2O^+$
$^{28}Si\,OH$
$^{28}Si_2OH^+$
Secondary Ion Current (10^{-10} A)
30
60
Time (min.)

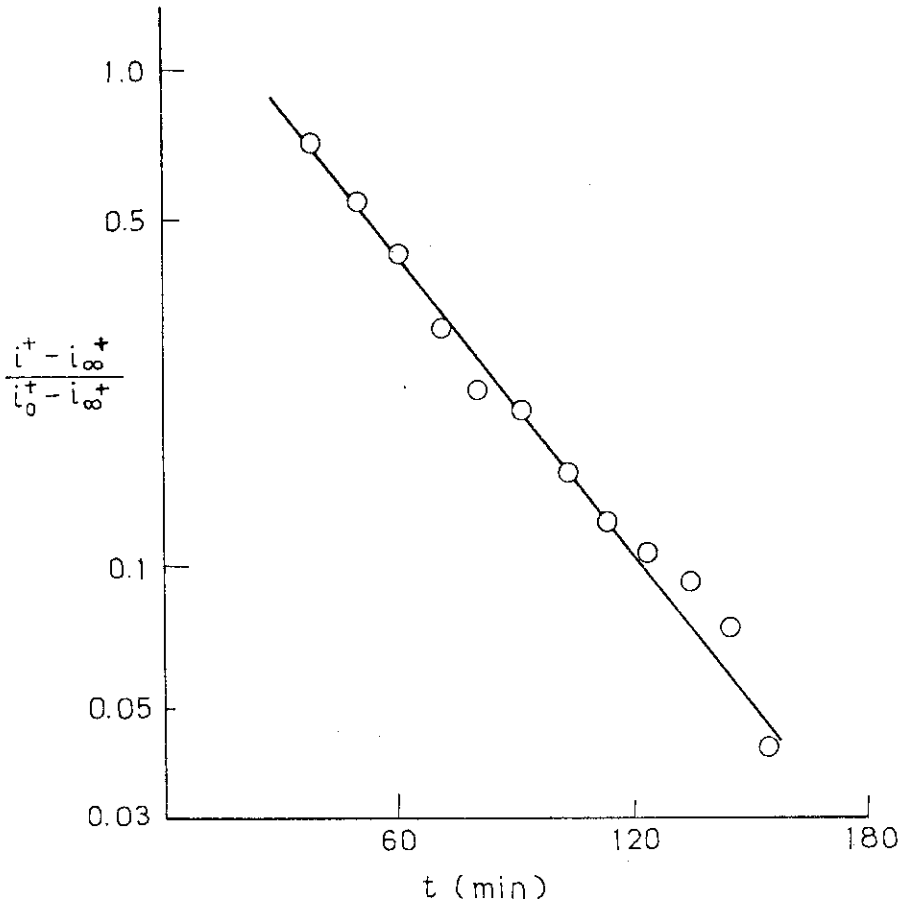

Fig. 6 Plots of the ion currents of $SiOH^+$ observed from silica gel before dehydration according to eq. (2).

the desorption cross section of the molecules on the surface. By denoting the final value of the ion current of $SiOH^+$ or Si_2OH^+ observed from silica gel before dehydration as i_∞^+, the variation of the ion current (i^+) is shown by eq. (2).

$$(i^+ - i_\infty^+)/(i_0^+ - i_\infty^+) = \exp\{-(JQ/\varepsilon)t\} \qquad (2)$$

Plots of the ion currents of $SiOH^+$ from silica gel before dehydration according to eq. (2) provide a straight line as shown in Fig. 6. From the slope together with the known parameters, J and ε, the desorption cross section of water

from silica gel is estimated to be 1.4×10^{-17} cm^2. By taking into account that desorption cross sections reported for various gas/metal and semiconductor combinations lie in the range of $10^{-13} \sim 10^{-19}$ cm^2, the value obtained here seems to be reasonable.

(S. Nagai and Y. Shimizu)

1) S. Nagai, H. Arai, and M. Hatada, Radiat. Phys. Chem., 16, 175 (1980); 17, 807 (1981); JAERI-M 9856, 22 (1981).
2) Y. Shimizu, S. Nagai, and M. Hatada, JAERI-M 9856, 72 (1981); 82-192, 29, 36 (1982); J. Chem. Soc. Faraday Trans 1, 79, 1973 (1983).
3) S. Nagai and Y. Shimizu, This Report; Proc. 7th Itern. Congr. Radiat. Res., A2-22 (1983), Amsterdam.
4) S. Nagai, JAERI-M 9775, 59 (1981).
5) B. Carrière and B. Lang, Surf. Sci., 64, 209 (1977).
6) E. Taglauer, W. Heiland, and J. Onsgaard, Nucl. Instr. Meth., 168, 571 (1980).

6. Angular Dose Distribution of "Bremsstrahlung" from an Electron Accelerator of Rectifying Transformer Type

In an attempt to obtain fundamental data necessary for shielding against "bremsstrahlung" or for X-ray irradiation, the measurement of angular dose distribution has been made on bremsstrahlung generated when an iron target was irradiated with 0.6 MeV electron beam from an accelerator of the rectifying transformer type and the values were compared with those calculated by Monte Calro method using the ETRAN code.

In order to determine the geometrical arrangement of the experimental set up which minimizes the effect of backscattering of the X-rays from the concrete floor, the albedo value (X-ray backscattering ratio) was measured using an Si solid state dosimeter for square area of 2 m x 2 m around the target and

using National thermoluminescent dosimeter (TLD) for whole area in the irradiation room.

Figure 1 shows the experimental set up for the dose measurements. The target made of stainless steel (SUS 304) was fixed 3 cm below the irradiation window of the accelerator, and electron irradiation was carried out at 0.6 MeV and 1 mA.

The experimental set up for the measurement of albedo values is shown in Fig. 2 where the electrons travel downward to the target. The dose rate was measured for different distances (x cm) between the dosimeter and the floor, while the distance (y cm) between the dosimeter and the target was kept constant (y = 30). The results are shown in Fig. 3. It is apparent from the figure that the value obtained for x = 0 (the dosimeter is on the floor) is higher by 25% than that obtained for x = 30, and is independent of x for x > 30. This result seems reasonable from the reported albedo values[1] against concrete obtained using ^{60}Co (average 1.25 MeV) and ^{192}Ir (average 0.4 MeV) gamma ray sources.

On the basis of above results, the target was fixed at 1.4 m above the floor, allowing the dose distribution measurement up to 1 m away from the target. The dose rate measurements at the positions within the zone indicated by the solid lines in Fig. 1 were carried out using the Si solid state detector which moves x or y direction on a conveyor, and the distribution was directly recorded on a strip chart recorder. The results were further treated with a computer using ARGUS-V4 computer code to display bird-eye view, an example of which is shown in Fig. 4 for the dose distribution 10 cm below the target.

From the three-dimensional dose distribution map, angular distribution curves were obtained. An example shown in Fig. 5 shows the distribution obtained 1 m from the target at the accelerator condition of 0.6 MeV, 1 mA. Open circles in Fig. 5 denote the values[2] calculated using eq. (1)

$$\text{Dose rate (R/hr)} = 5.76 \times 10^{-5} \frac{N}{r^2} \sum_{j=1}^{J} \mu_{en}(\bar{k}_j)\, \bar{k}_j \left(\frac{d^2n}{dk d\Omega}\right)_j \Delta k_j \qquad (1)$$

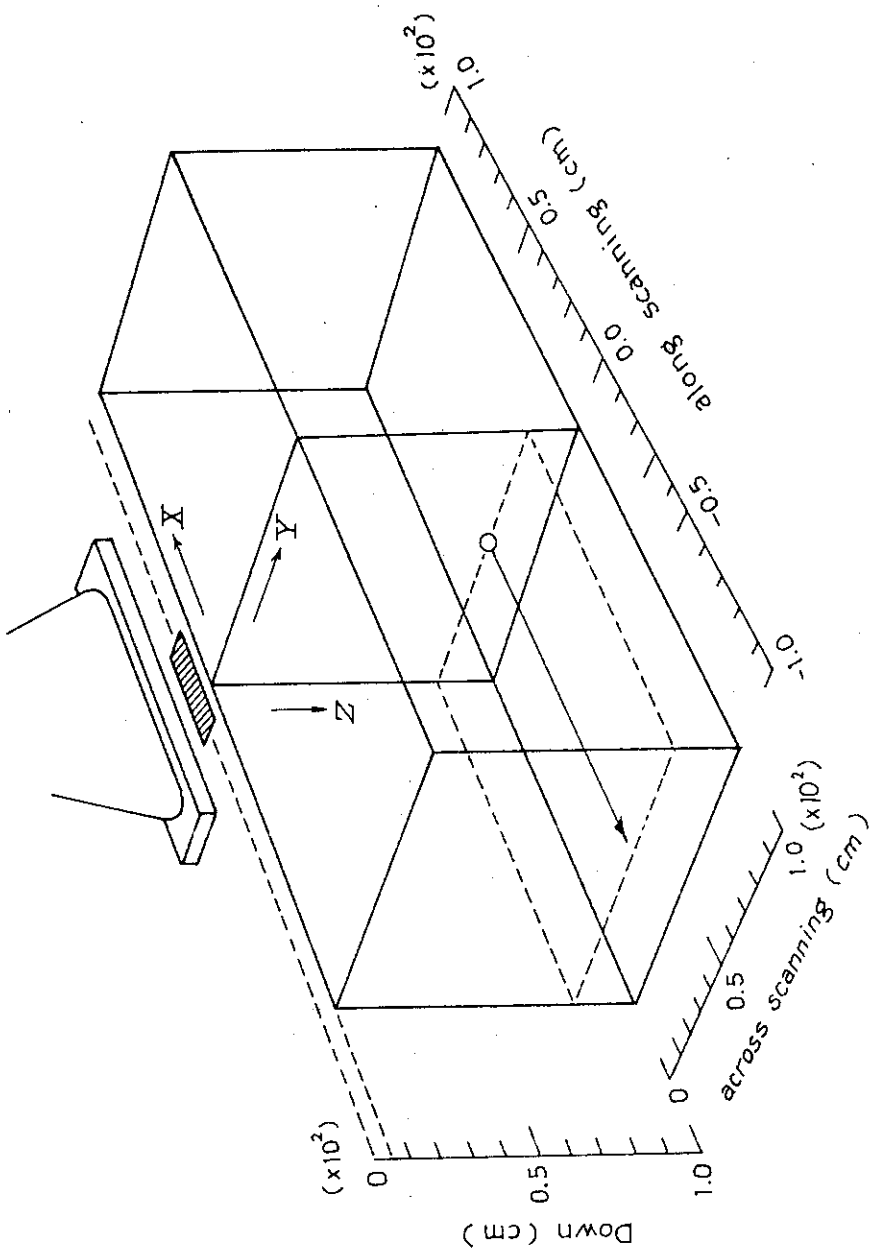

Fig. 1 Coordinate system describing dose measurement zone using Si solid state detector.

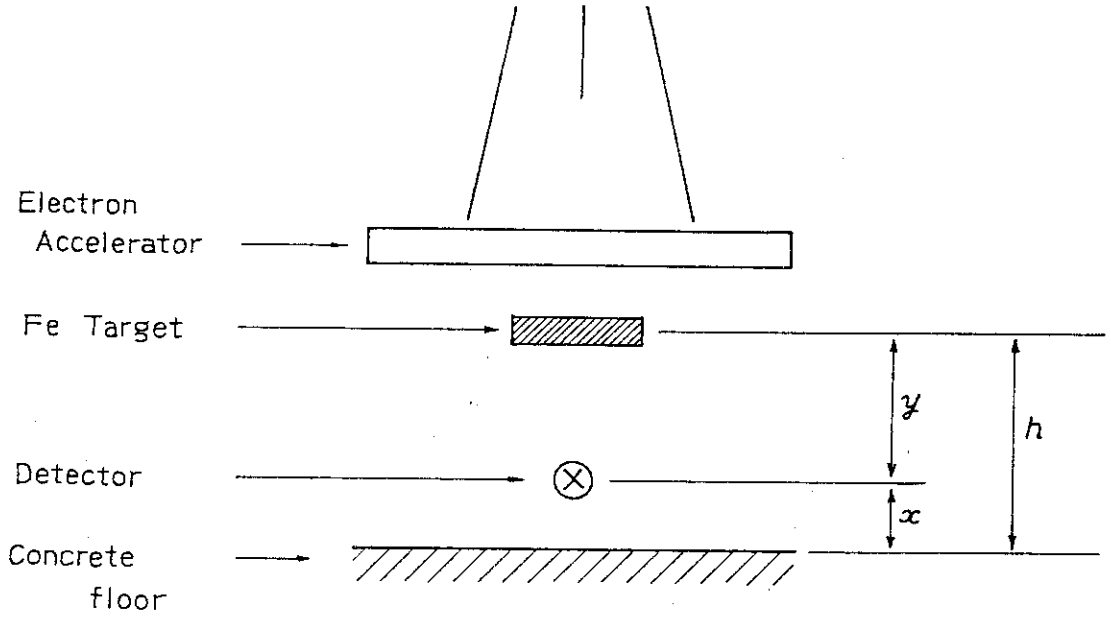

Fig. 2 Geometrical arrangement for albedo measurement.

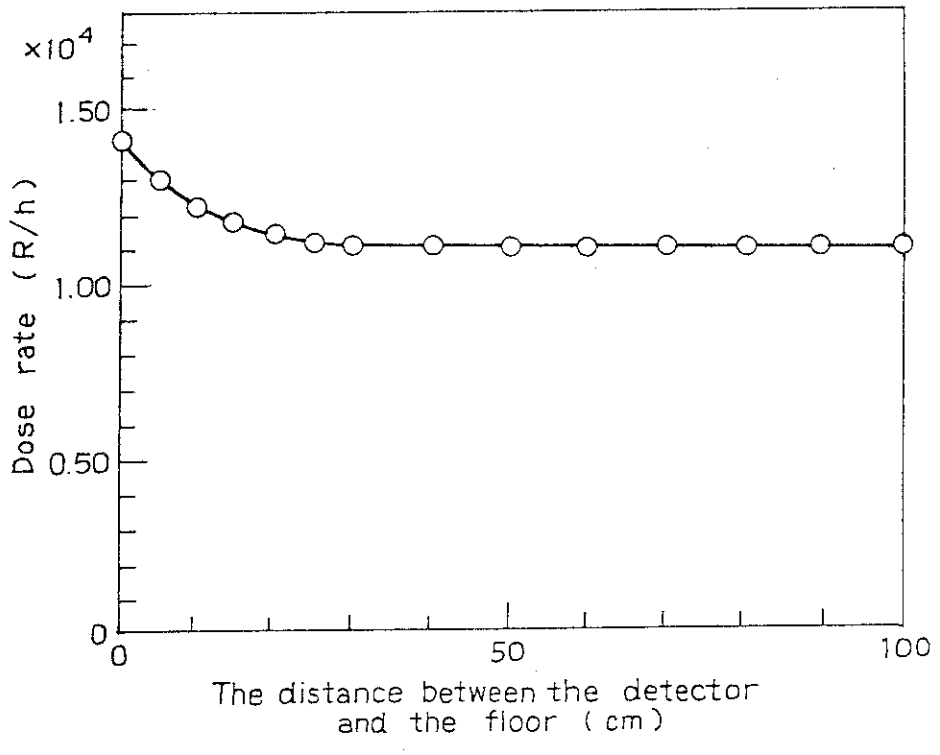

Fig. 3 Dose rate as a function of the distance between the detector and the floor.

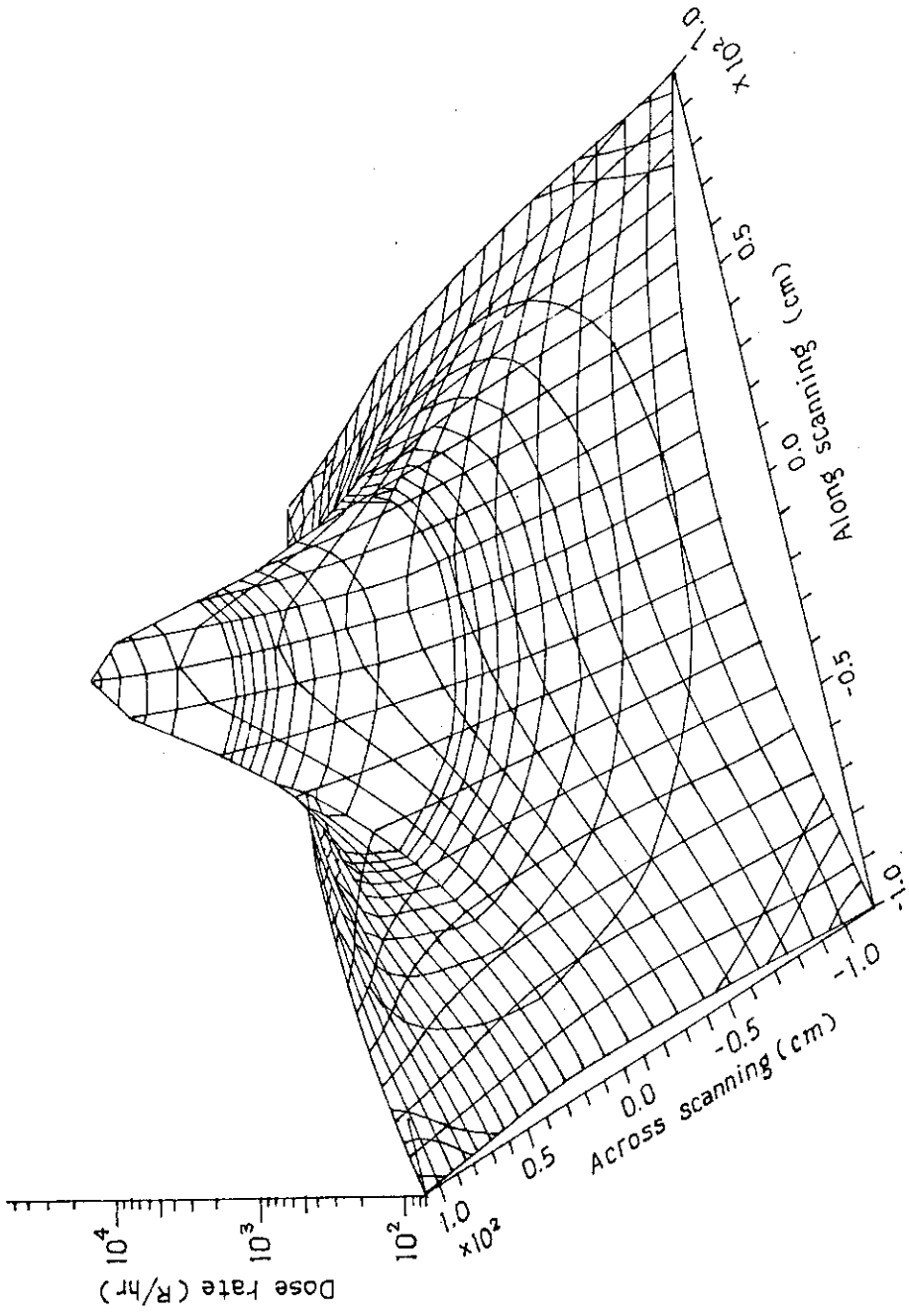

Fig. 4 Bird-eye view showing the dose rate distribution 10 cm below the target. Irradiations were carried out with 0.6 MeV, 1 mA.

where meanings of the symbols are:

$\mu_{en}(\bar{k})$	mass energy absorption coefficient of the absorber for the photon of energy $\bar{k}$ (in cm^2/g)
N	fluence rate of the incident electrons (in electrons/s)
$\bar{k}_j$	average energy of the photons in the j-th energy bin (in MeV)
Δk_j	bin width of the photon energy (in MeV)
$(d^2n/dkd\Omega)_j$	differential photon number at the j-th energy bin and the angle of emission θ (in /MeV·sr·electron) (to be taken from the tables)
r	distance from the point of emission of bremsstrahlung photons to the point P (in cm).

and the flux distribution obtained by Monte Carlo method on ETRAN 15 code[3]. The same geometrical arrangement in the experiment was assumed for the calculation. As shown in Fig. 5, the experimental values agree well with the calculated ones, except for the smaller experimental values for 0° direction due to the self absorption by the cooling water of the target, and the larger experimental values for 60° direction due to scattered X-ray at a mechanical part of the beam shutter, or an ion pump.

The dose rate distributions obtained by TLD method in the irradiation room are shown in Fig. 6 (a), (b) and (c). The TLD elements were set on the floor, walls, or fixed at appropriate intervals on wires in the space above the floor. The irradiation was carried out at 0.6 MeV, 25 mA. The target dimensions fixed on the floor at the center of the room are 2 cm x 16 cm, and the direction of the scanning of the electron beam is south-north.

Figure 6 (a) shows the dose distribution contour map at the floor level. When the target was set at 1 m above the floor, the dose rate 1 m below the target was 3.07×10^4 R/hr

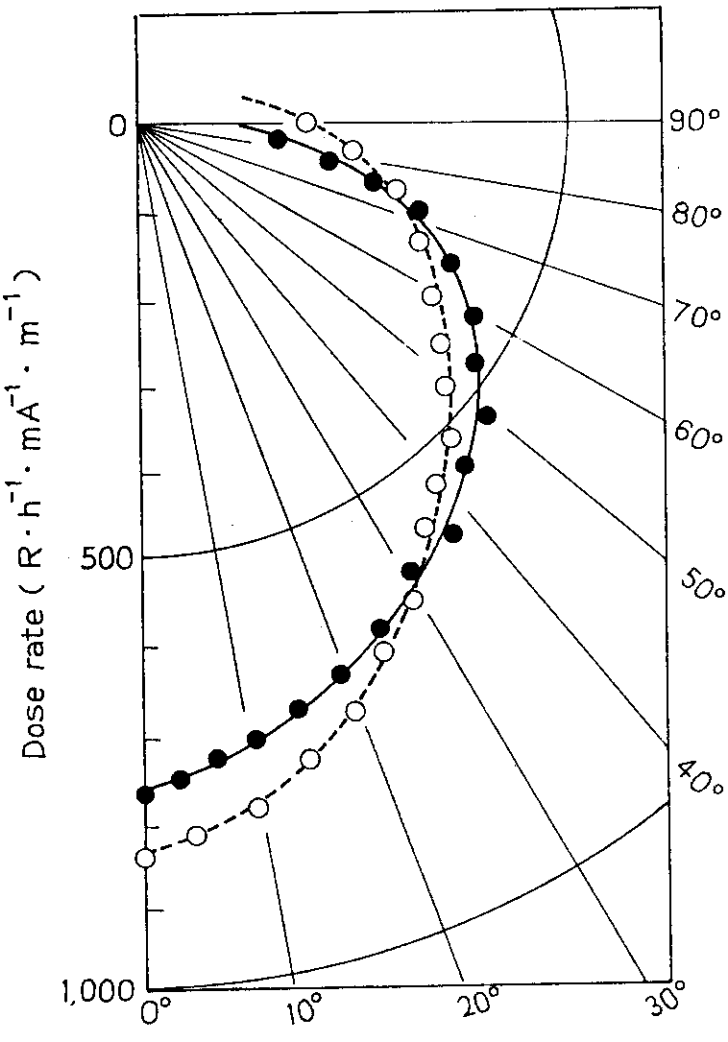

Fig. 5 Angular dose distribution of bremsstrahlung from Fe (SUS 304) target. (●) experimental, (○) calculated by Monte Carlo method. The Irradiation condition: 0.6 MeV, 1 mA.

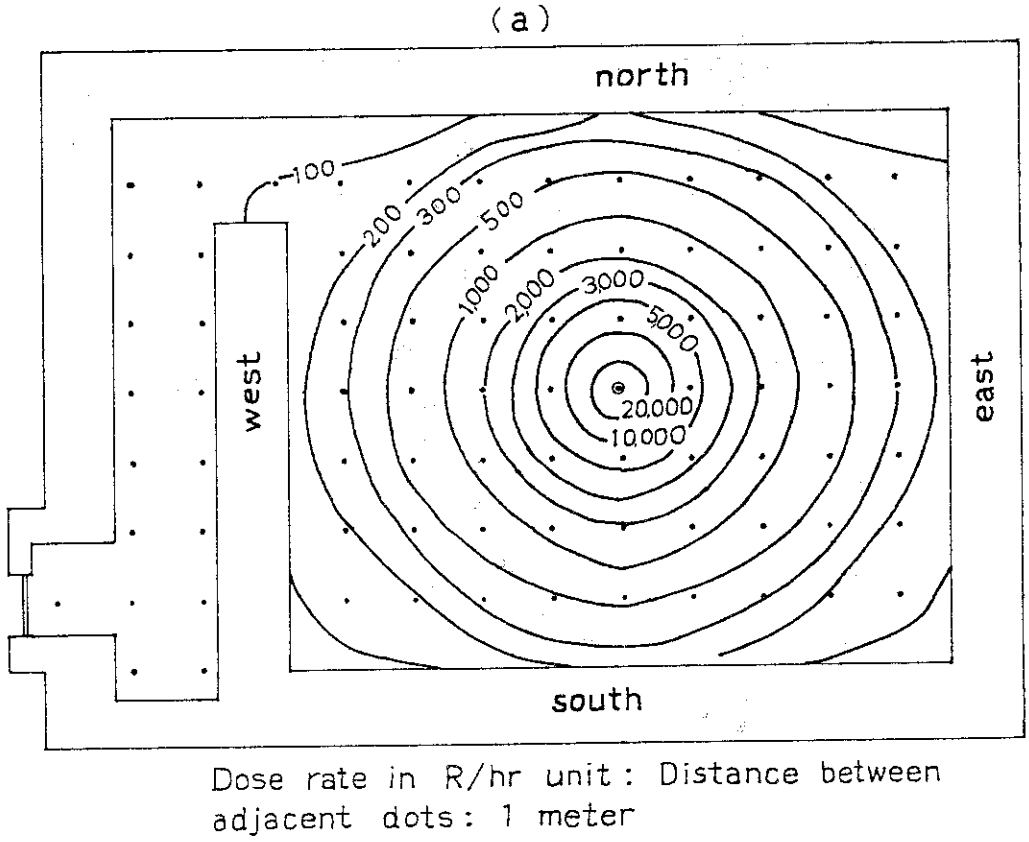

Fig. 6 The dose rate distribution map in the irradiation room. The target position, the center of the room and 1 m above the floor; Irradiation condition: 0.6 MeV, 25 mA. TLD elements were set on the floor (a), 1 m above the floor (b) and 2 m above the floor (c).

(b)

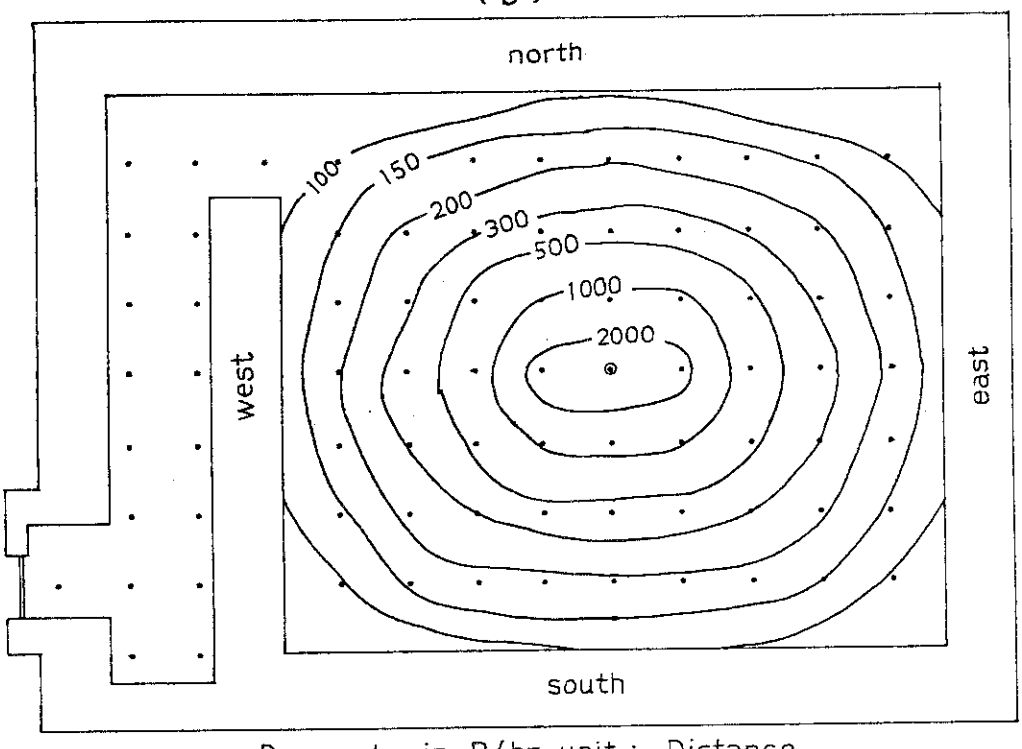

Dose rate in R/hr unit : Distance between adjacent dots : 1 meter

(c)

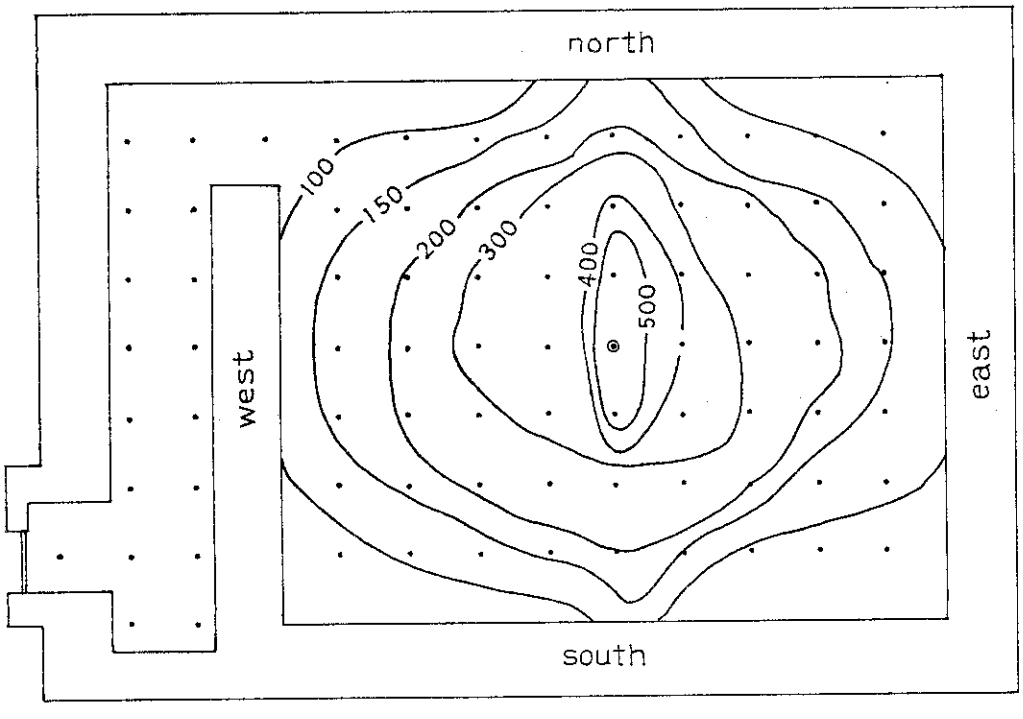

Dose rate in R/hr unit : Distance between adjacent dots : 1 meter

and the circular equi-dose lines appear. The dose distribution map shown in Fig. 6 (b) was obtained at 1 m above the floor where the TLD elements were placed in the plane involving the target.

High dose rate area appeared toward the direction perpendicular to that of electron beam scanning, and equi-dose line appeared as eliptic lines. Fig. 6 (c) shows the dose distribution map obtained at 2 m above the floor, where the contour lines show complex feature indicating strong disturbance involving absorption and scattering of X-rays at the frame of the accelerator, exhaust tubings, ion pump and beam shutter.

(K. Matsuda, T. Takagaki, Y. Nakase, and Y. Nakai)

1) E. T. Clarke, J. F. Batter, Nucl. Sci. Eng., 17, 125 (1963).
2) a) S. Tanaka, et al., JAERI-M 83-019 (1983).
b) S. Tanaka, private communication (1983).
3) M. J. Berger and S. M. Seltzer, Notes on program ETRAN 15, NBS Report 9837 (1968).

7. Cationic Oligomerization of Styrene in the Presence of Chlorobutene

In the previous reports[1,2], cationic oligomerization of butadiene using halogenated hydrocarbons such as benzyl chloride and chlorobutene as chain transfer agent was described. In this study, the radiation-induced oligomerization of styrene (St) with 3-chloro-1-butene (3C1B) has been carried out. Oligomerization was carried out in 50 mole% toluene solution. Solvent and telogen were used after drying with calcium hydride. Irradiation was performed with 1.5 MeV electron beams at 50 μA (2.2×10^5 rad/s), and at 0°C in vacuum. Details of experimental procedures were the same as described before[1].

The relative rate of oligomerization, R_p divided by the initial concentration of styrene [St] is shown in Fig. 1.

The value of $R_p/[St]$ slightly decreases with the addition of small amounts of 3C1B and then increases with increasing [3C1B]/[St] ratio. The value of $R_p/[St]$ at high [3C1B]/[St] ratio is larger than two times that of styrene alone. This indicates that the 3C1B contributes highly to initiation of the oligomerization. Conversion was proportional to irradiation time up to 10% conversion. $R_p/[St]$ was proportional to dose rate of electron beams at [3C1B]/[St] = 0.4. This oligomerization was inhibited by the addition of triethylamine ([TEA]/[St] = 10^{-2}) as a cation scavenger, showing that this reaction proceeds with the cationic mechanism.

In Fig. 2, the $\bar{M}_n$ values of the oligomers obtained decrease rapidly with increasing [3C1B]/[St] ratio and tend to lead to a constant value at high [3C1B]/[St] ratio. The

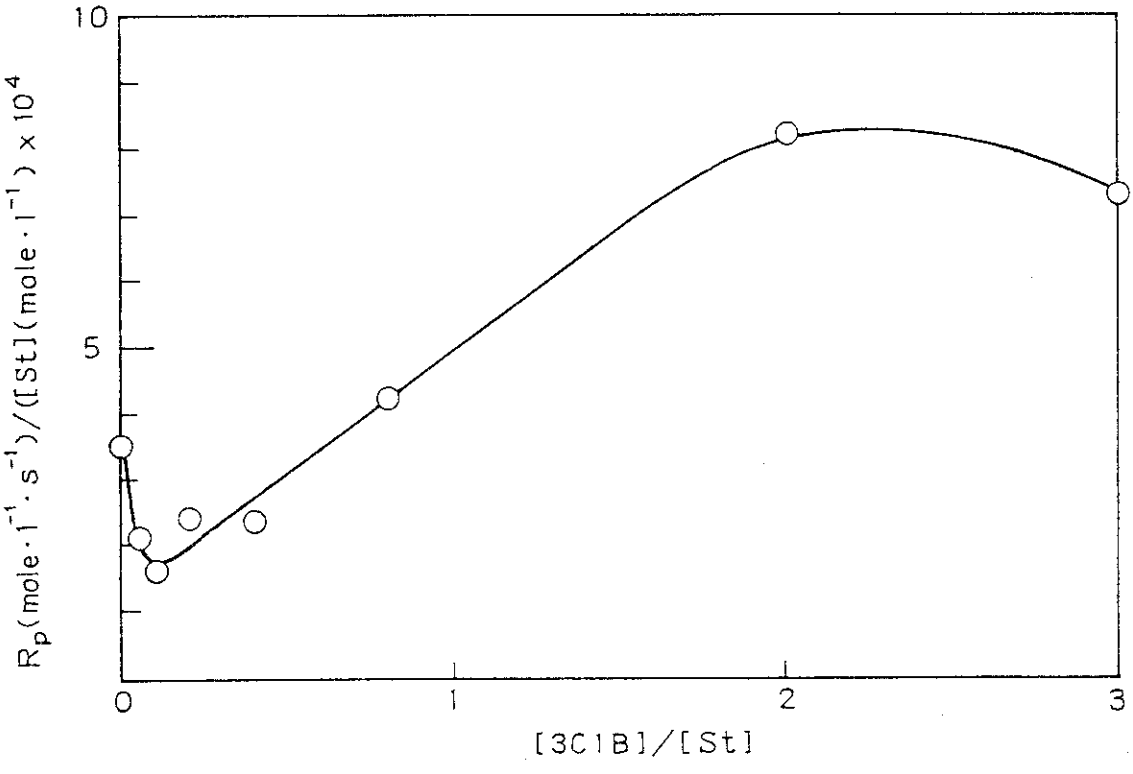

Fig. 1 The relative rate of oligomerization, $R_p/[St]$ as a function of [3C1B]/[St]. Irradiation, 2.2×10^5 rad/s at 0°C.

molecular weight distribution curves of the oligomers are shown in Fig. 3. It is obvious that, with increasing [3C1B]/[St] ratio, the high molecular weight fraction in the products greatly decreases and the oligomer of which $\overline{M}_n$ is about 300 increases. In the range of [3C1B]/[St] $\geq$ 0.8, the product is virtually composed of the oligomer alone. The oligomer obtained was soluble in methanol.

Infrared spectrum of the oligomer prepared is shown in Fig. 4. The oligomer was cast as film onto NaCl plate from carbon disulfide solution. The absorption bands observed at wavenumbers of 3060, 3027, 2924, 2851, 1944, 1871, 1801, 1601, 1583, 1493, 1452, 1373, 1069, 1028, 907, 757, and 699 cm^{-1} are certainly the characteristic bands of polystyrene[3]. The intensities of these bands coincide with those of the bands of polystyrene. It is apparent that the oligomer is composed of

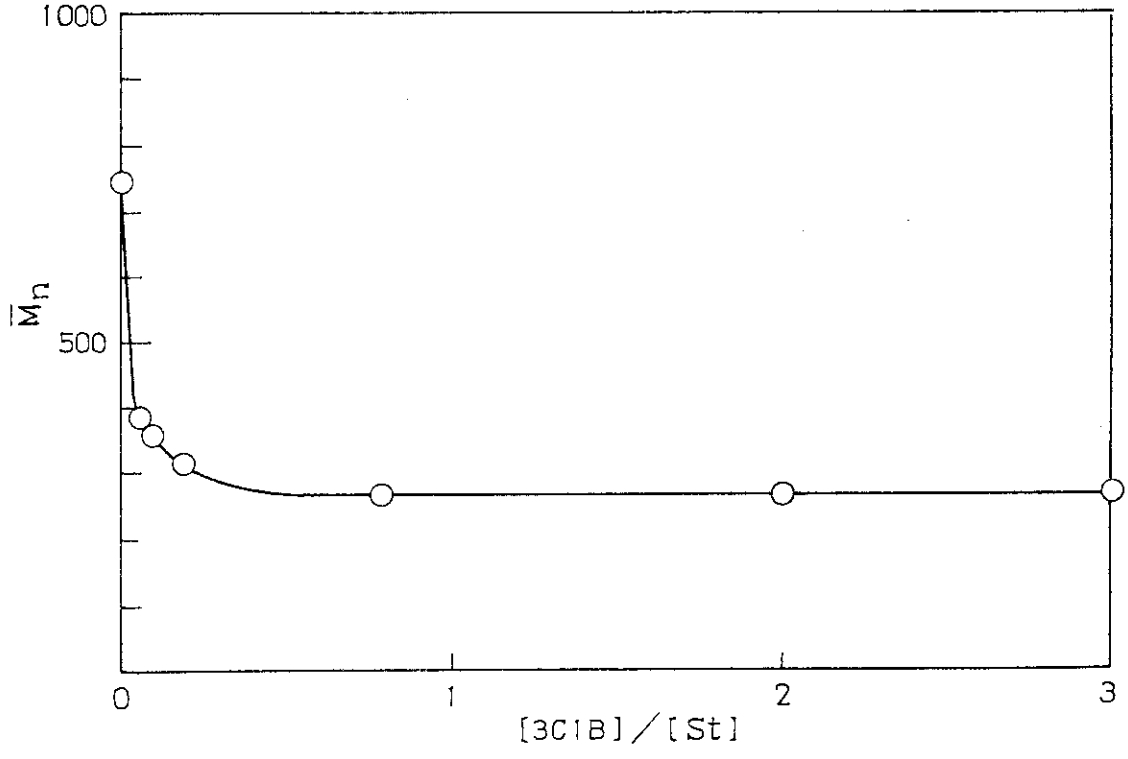

Fig. 2 Number average molecular weights of the oligomers obtained, $\overline{M}_n$ as a function of [3C1B]/[St].

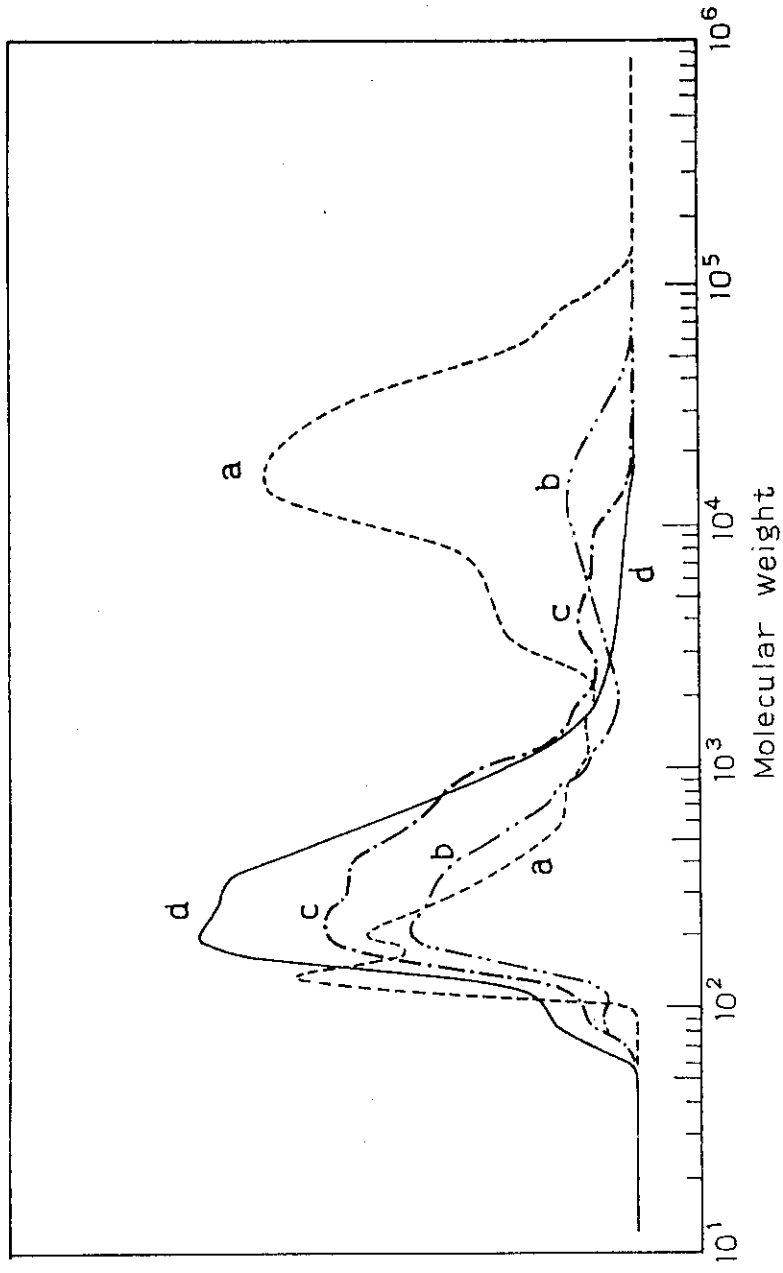

Fig. 3 Molecular weight distribution curves of the oligomers obtained at different [3C1B]/[St]. [3C1B]/[St]: a, 0; b, 0.1; c, 0.2, d, 0.8.

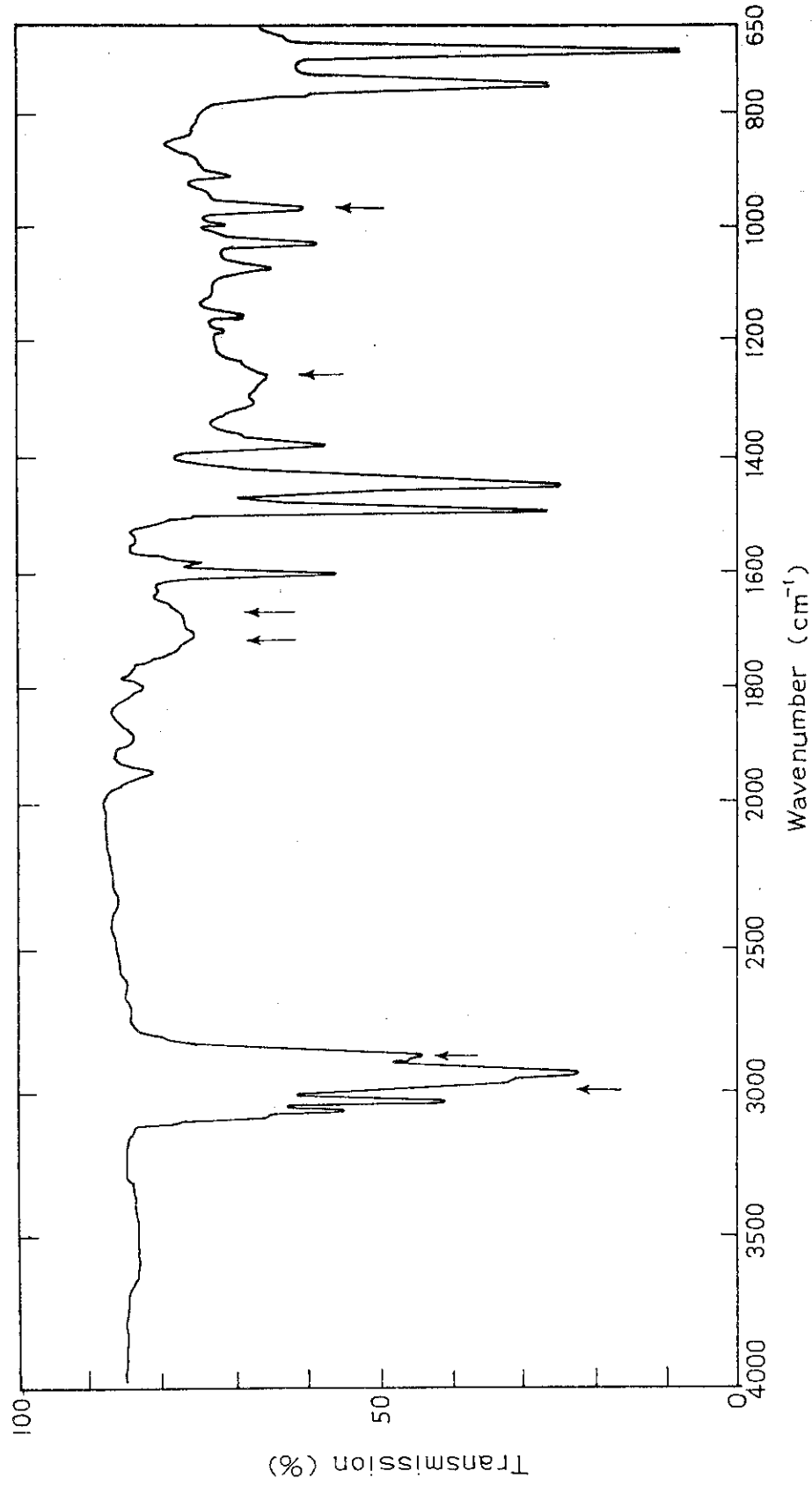

Fig. 4 Infrared spectrum of the oligomer obtained from styrene with 3C1B.

polystyrene chain.

The bands marked with arrows in Fig. 4 were not found in the spectrum of pure polystyrene. The bands at 2960, 2870, 1715, 1675, and 965 cm^{-1} were assigned to ν_{as} CH_3, ν_s CH_3, $\nu C=O$ of ketone, $\nu C=C$ of $\overset{R}{H}\!>\!C=C\!<\!\overset{H}{R}$ (trans), and $\delta C-H$ out-of-plane (trans), respectively. The band at 1258 cm^{-1} could not be assigned. Vinyl structure was not included in the oligomer, since the bands arising from terminal vinyl structure at 1645, 1440, 990, and 910 cm^{-1} were not found. The presence of small amount of ketone appears to indicate the oxidation of C=C bond of the oligomer. It seems that the band of C-Cl bond overlapps with the band of phenyl group (757 cm^{-1}, $\delta C-H$ out-of-plane), because the intensity of the band at 757 cm^{-1} of the oligomer is stronger than that of polystyrene.

Methyl group and trans C=C bond would be the constituents of initiating end group formed in the initiation. Ionization and initiation of the oligomerization are shown in the reactions (1), (2), and (3).

$$CH_2{=}CH(\phi) \xrightarrow{H^+} CH_3{-}\overset{+}{C}H(\phi) \qquad (1)$$

$$CH_3{-}CH(Cl){-}CH{=}CH_2 \longrightarrow CH_3{-}\overset{+}{C}H{\cdots}CH{\cdots}CH_2 + Cl^- \qquad (2)$$

$$CH_3{-}\overset{+}{C}H{\cdots}CH{\cdots}CH_2 + CH_2{=}CH(\phi) \longrightarrow CH_3{-}CH{=}CH{-}CH_2{-}CH_2{-}\overset{+}{C}H(\phi) \qquad (3)$$

It is considered that the structure of carbonium cation[4] produced by irradiation of 3C1B is the one presented in reaction (2). Through the initiation of reaction (3), the initiating end-group with CH_3 and trans C=C bond is formed. Vinyl group contained in 3C1B does not remain in the oligomer.

Elemental analysis of the oligomers was carried out in order to determine the terminating end-group. Table 1 shows the abundance of chlorine, i.e., the ratio of observed chlorine content and calculated chlorine content based on $\bar{M}_n$ of the oligomers. The abundances for the oligomers prepared using

Table 1 Abundances of the Terminal Chlorine Atom Contained in Styrene Oligomers

[3C1B]/[St]	$\bar{M}_n$	Abundance of chlorine
0.2	435	0.871
0.8	359	1.17

Irradiation: 2.2×10^5 rad/s at 0°C.

3C1B were approximately 1, indicating that each molecule of the oligomers contains one chlorine atom. The abundance indicates that the chain transfer occurred frequently in the system. Propagation, chain transfer, and termination of the oligomerization are shown in reactions (4), (5), and (6), respectively. Structure of terminating end-group of the oligomer should be determined by reaction (5).

$$\text{--- } CH_2\text{-}\overset{+}{C}H\text{(}\phi\text{)} + CH_2\text{=}CH\text{(}\phi\text{)} \longrightarrow \text{--- } CH_2\text{-}CH\text{(}\phi\text{)}\text{-}CH_2\text{-}\overset{+}{C}H\text{(}\phi\text{)} \quad (4)$$

$$\text{--- } CH_2\text{-}\overset{+}{C}H\text{(}\phi\text{)} + CH_3\text{-}CH(Cl)\text{-}CH\text{=}CH_2$$

$$\longrightarrow \text{--- } CH_2\text{-}CH(\phi)\text{-}Cl + CH_3\text{-}CH\overset{+}{\cdots}CH\cdots CH_2 \quad (5)$$

$$\text{--- } CH_2\text{-}\overset{+}{C}H\text{(}\phi\text{)} + H_2O$$

$$\longrightarrow \text{--- } CH\text{=}CH\text{(}\phi\text{)} + H_3O^+ \quad (6)$$

From the analyses of the products, it is considered that the oligomer obtained was a telomer composed of the structure of $CH_3\text{-}CH\text{=}CH\text{-}CH_2\text{-}(\text{-}CH_2\text{-}CH(\phi)\text{-})_n\text{-}Cl$.

(M. Nishii, K. Hayashi, and S. Okamura)

1) K. Hayashi and S. Okamura, JAERI-M 9856, 91 (1981).
2) K. Hayashi and S. Okamura, JAERI-M 82-192, 55, 61 (1982).
3) K. Nakanishi, "Sekigaisen Kyushu Supekutoru", Nankodo, Tokyo (1960).
4) T. Asahara and H. Kise, Bull. Chem. Soc. Japan, 39, 2739 (1966).

8. Radiation-Induced Emulsion Polymerization of Styrene at High Dose Rate

The characteristics of radiation-induced emulsion polymerization of styrene (St) was examined by studying the particle size and the molecular weight distribution of the polymer latex produced.

Emulsion polymerization of styrene was performed at room temperature by an electron beam irradiation using sodium lauryl sulfate (SLS) as an emulsifier. Measurements of the particle size were carried out by "Nanosizer" (Coulter Ltd.), and the molecular weight distribution was determined by a gel permeation chromatographic (GPC) method.

Figure 1 shows the GPC curves of polymer latex prepared under such conditions as a constant dose rate and various SLS concentrations, i.e. [SLS]/[St]. Particle sizes are also described in Figure 1 together with the irradiation time when the polymer yield attains about 100%. The particle sizes are smaller at higher [SLS]/[St], and fall in a constant value of 30 ∿ 33 nm (300 ∿ 330 Å) at ranges of [SLS]/[St] ≧ 6.0 wt%.

It has been reported[1] that the GPC curve of polystyrene prepared under the electron beam irradiation is composed of three components. The GPC curves obtained here are separated into three components according to the method mentioned in the previous report[1]. Peak I indicates the curve of oligomers with molecular weight of about 1000, Peak II polymers obtained by radical polymerization, and Peak III by cationic

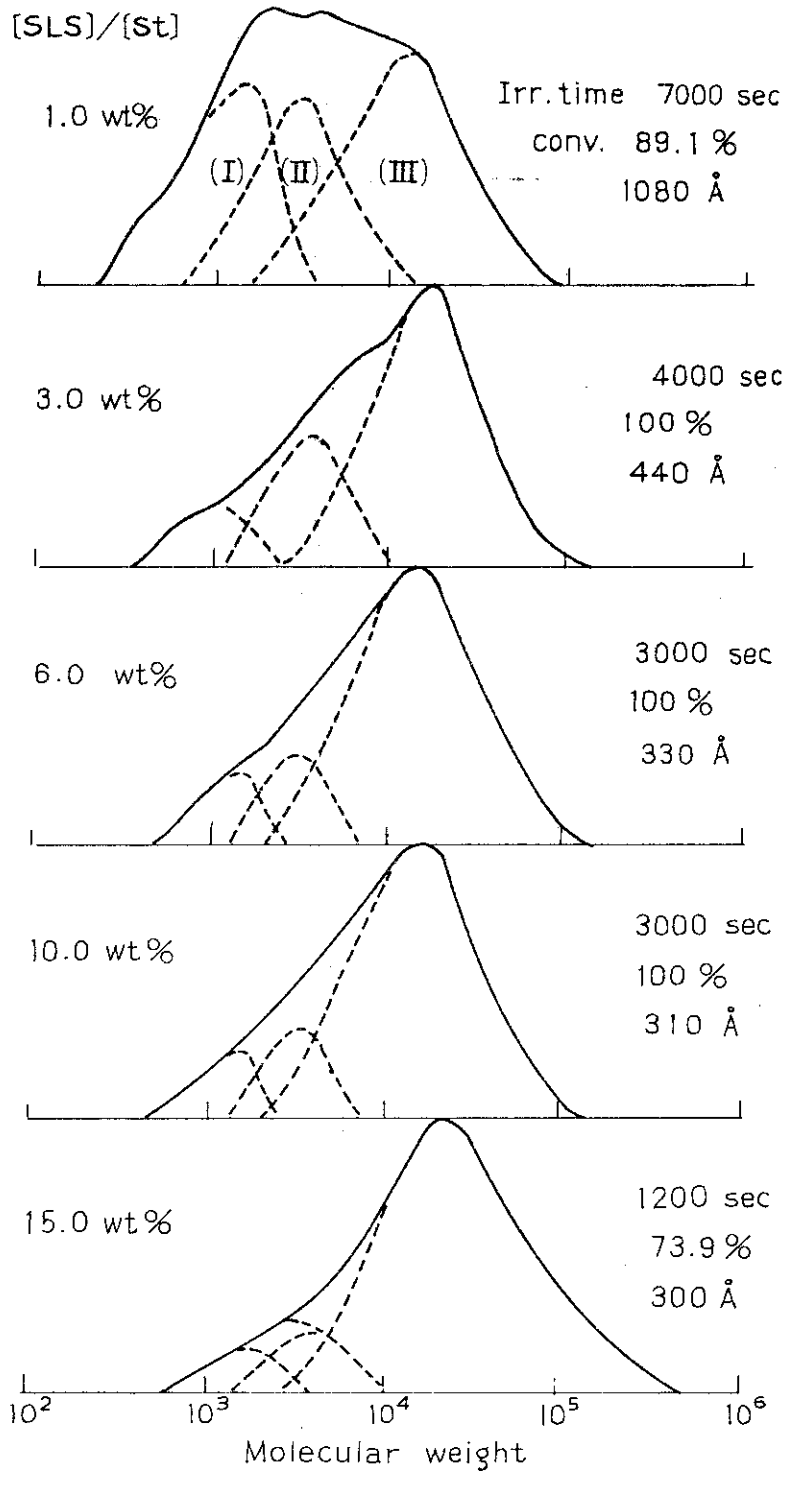

Fig. 1 GPC curves of polystyrene obtained by emulsion polymerization of styrene at various concentrations of emulsifier (SLS).

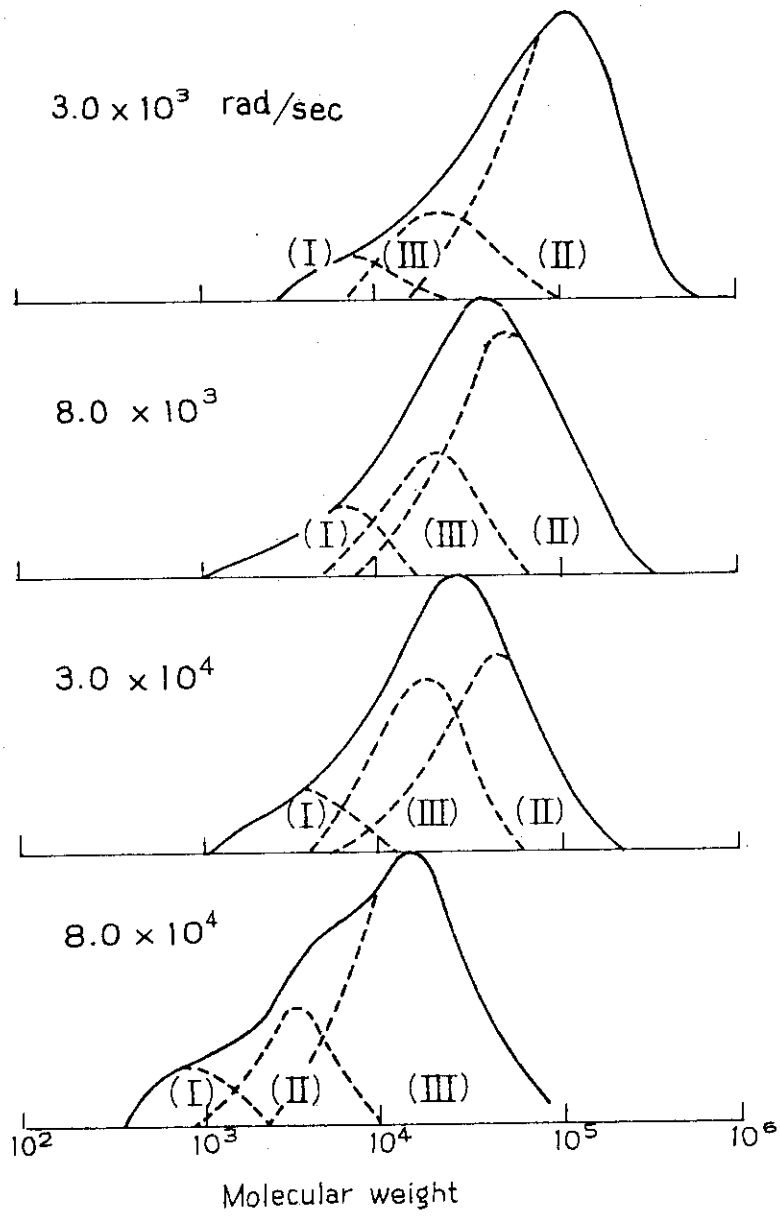

Fig. 2 GPC curves of polystyrene obtained at various dose rates.

polymerization, respectively. The higher the [SLS]/[St], the more the amount of polymer produced by cationic process. On the other hand, the amounts of oligomer and radical polymer decrease at higher [SLS]/[St].

Figure 2 shows the GPC curves of polymers prepared under various dose rates. The dose-rate effect on the molecular weight distribution indicates that radical polymers (Peak II) predominate at a low-dose rate region to give small amounts of oligomer (Peak I) and cationic polymers (Peak III), while at a higher dose rate cationic polymers predominate. The molecular weight distributions of cationic polymers are narrow. Figure 3 shows the number average molecular weight (M_n) of cationic and radical polymers as a function of the dose rate.

M_n of radical polymers decreases with increasing dose rate ($M_n = kD^{-1}$), while M_n of cationic polymers keeps constant ($M_n \simeq$

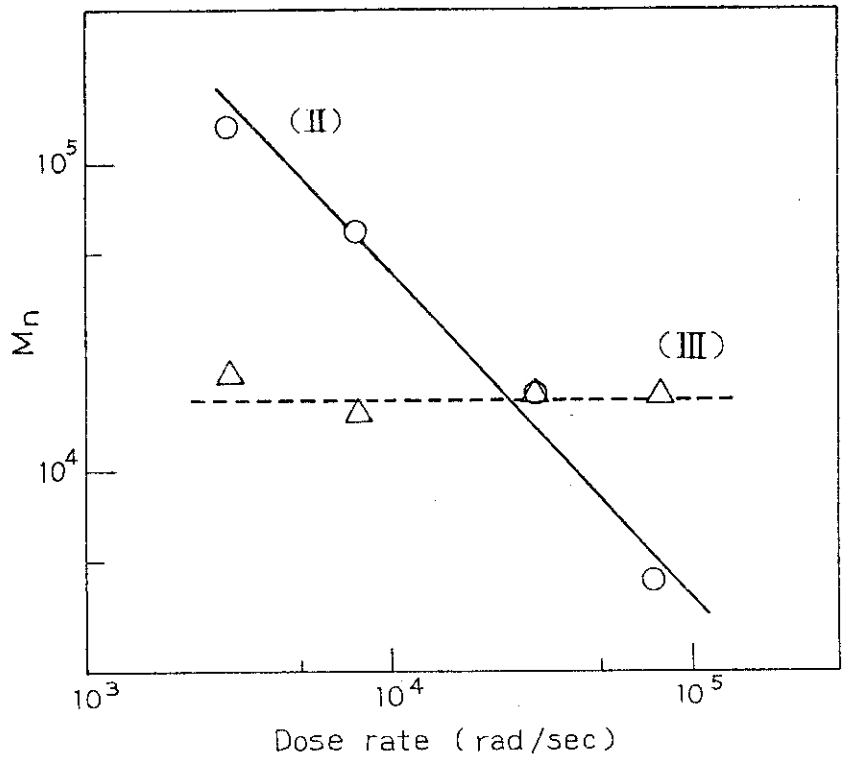

Fig. 3 Molecular weight (M_n) of polystyrene by radical (II) and cationic (III) processes vs. dose rate.

2 x 10^4) at a constant water concentration irrespective of dose rate.

The rate of polymerization (R_p) as function of dose rate is shown in Fig. 4. R_p of cationic polymers (Peak III) increases with increasing dose rate, and the dose rate exponent of R_p in the experimental region is 0.54, but R_p of radical polymers is independent of dose rate. Particle size of polymers keeps constant (ca. 450 Å) at various dose rates.

In the radiation-indiced polymerization of vinyl monomers, the dose rate exponent of R_p varied from 0.6 to 1.0 depending on the emulsion concentration for vinyl acetate[2,3], and about 0.3 for methyl methacrylate[4]. The value of 0.54 for styrene obtained here shall be re-examined with referring to those results.

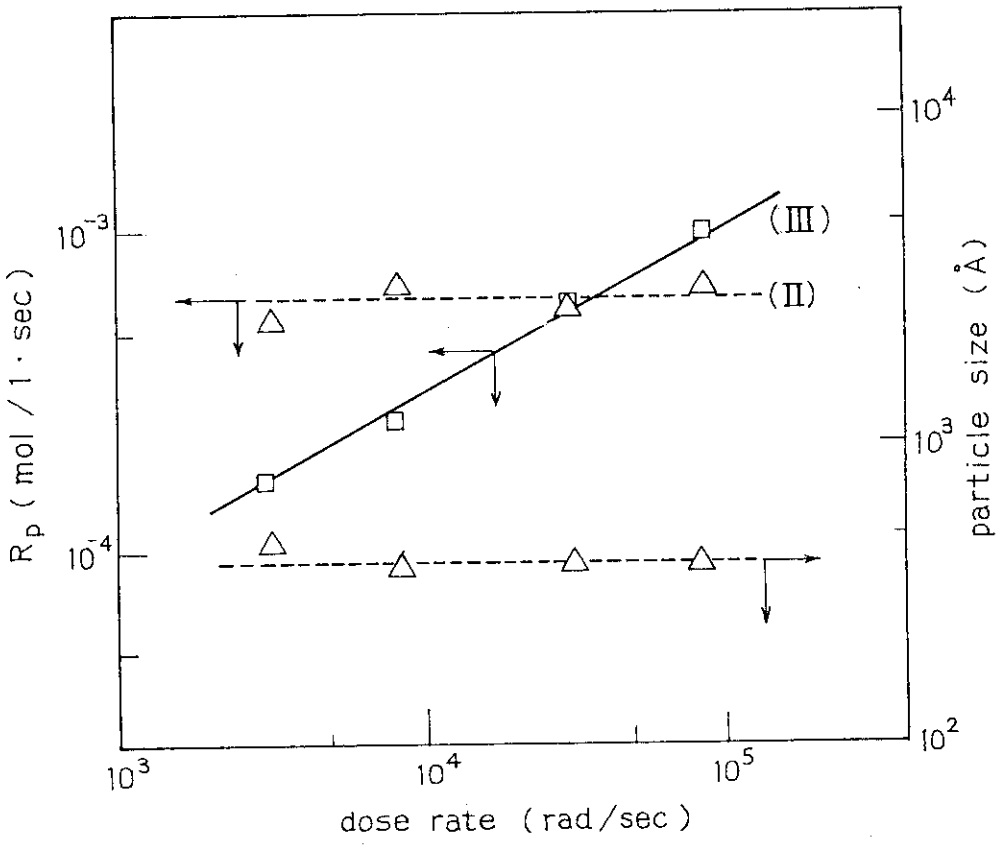

Fig. 4 Rate of emulsion polymerization of styrene and particle size of obtained polymers vs. dose rate.

In conclusion, the characteristics of radiation-induced emulsion polymerization from the viewpoint of molecular weight distribution and particle size are summarized as follows: 1) the particle size of emulsion is smaller than 50 nm (500 Å) at the concentrations of the emulsifier above 3.0 wt%, 2) the molecular weight of polymers obtained by cationic process keeps almost constant with rather narrow distribution, irrespective of dose rate, 3) emulsion polymerization by electron beam irradiation takes place both by the radical and cationic processes, and the higher the dose rate, the more the cationic polymer.

(J. Takezaki and K. Hayashi)

1) J. Takezaki, T. Okada, and I. Sakurada, J. Appl. Polym. Sci., 22, 3311 (1977).
2) V. Stannet, J. A. Gervasi, J. Kearney, and K. Araki, J. Appl. Polym. Sci., 13, 1175 (1969).
3) F. Sunddardi, J. Appl. Polym. Sci., 24, 1031 (1979).
4) Inagaki, K. Yagi, S. Saeki, and S. Okamura, Kobunshi Kagaku, 17, 135 (1960).

9. Surface Grafting of Fluorine-Containing Monomer onto Poly(vinyl chloride) Composite Disc

The purpose of this study is to form thin layer containing fluorine on the surface of poly(vinyl chloride) (PVC) disc by radiation grafting of fluorine-containing monomer.

In the previous report[1], it was shown that the grafting of fluorine-containing monomers proceeded mainly inside the PVC disc. It was also made clear that polymerization inside the disc proceeded thermally and no effect of radiation was perceived.

The PVC disc of the same chemical composition as that used in the previous report (PVC : carbon black = 100 : 20 by weight) but of different batch was employed in the present study. The disc of 1 mm thick and 26 cm in diameter was cut into small

pieces (20 mm x 6 mm) and used in experiments. Fluorine-containing monomers were 2, 2, 3, 3-tetrafluoropropyl methacrylate (F_4C_3MA) and pentafluorostyrene (F_5St) which were used previously[1]. The grafting was carried out using vapor phase radiation-grafting technique. As described in the previous report[1], this technique is superior to an immersion-grafting, since the vapour phase grafting does not deform the surface feature of the disc consisting of many fine pits and shows higher efficiency in monomer utilization.

The grafting was made at room temperature (24°C) and 50°C, and at a dose rate of 5.8×10^4 and 2.9×10^4 rad/h. The grafted surface was examined by X-ray photoelectron spectroscopy using a Shimadzu ESCA 750 electron spectrometer with Mg K_α generated at 80 kV, 30 mA as a radiation source. Surface structure was further examined by optical and electron microscopy. Surface wettability was estimated from the contact angle for aniline by a sessile drop method. Electric conductivity was measured by reading insulating resistance value directly when both surfaces of the sample piece were in contact with electrode plates.

Table 1 shows the surface properties of the F_4C_3MA grafted PVC disc. The contact angle of the grafted disc changed from 30° for the starting ungrafted disc to 54° for radiation-polymerized F_4C_3MA homopolymer film in 1 ∿ 2h of irradiation time. The sample irradiated for a time between 1 and 2h or under other conditions also showed either value for the starting disc or for the F_4C_3MA homopolymer film, and no intermediate values were obtained.

The third column of Table 1 shows the observed values of insulating resistance, which are direct read-off values for whole sample (20 x 6 x 1 mm). The value of 120 MΩ is the upper limit of the instrument. The ungrafted PVC disc has electric resistance as low as 0.01 MΩ which is due to carbon black contained in the disc. The electric resistance of the grafted disc increased abruptly by two orders of magnitude between 5 and 7 hr of irradiation time after gradual initial increase with irradiation time. It is noted that irradiation

Table 1 Surface Properties of Tetrafluoropropyl Methacrylate Graft PVC Disc

Irrad. time (h)	Contact angle (degree)	Electric resistance (MΩ)	Atomic ratio, F/(F+Cl) (%)
Starting PVC	30	0.01	0
1	27	0.07	41
2	55	0.08	71
3	52	0.10	89
5	53	0.50	99
7	54	90.	100
16	54	120.	100

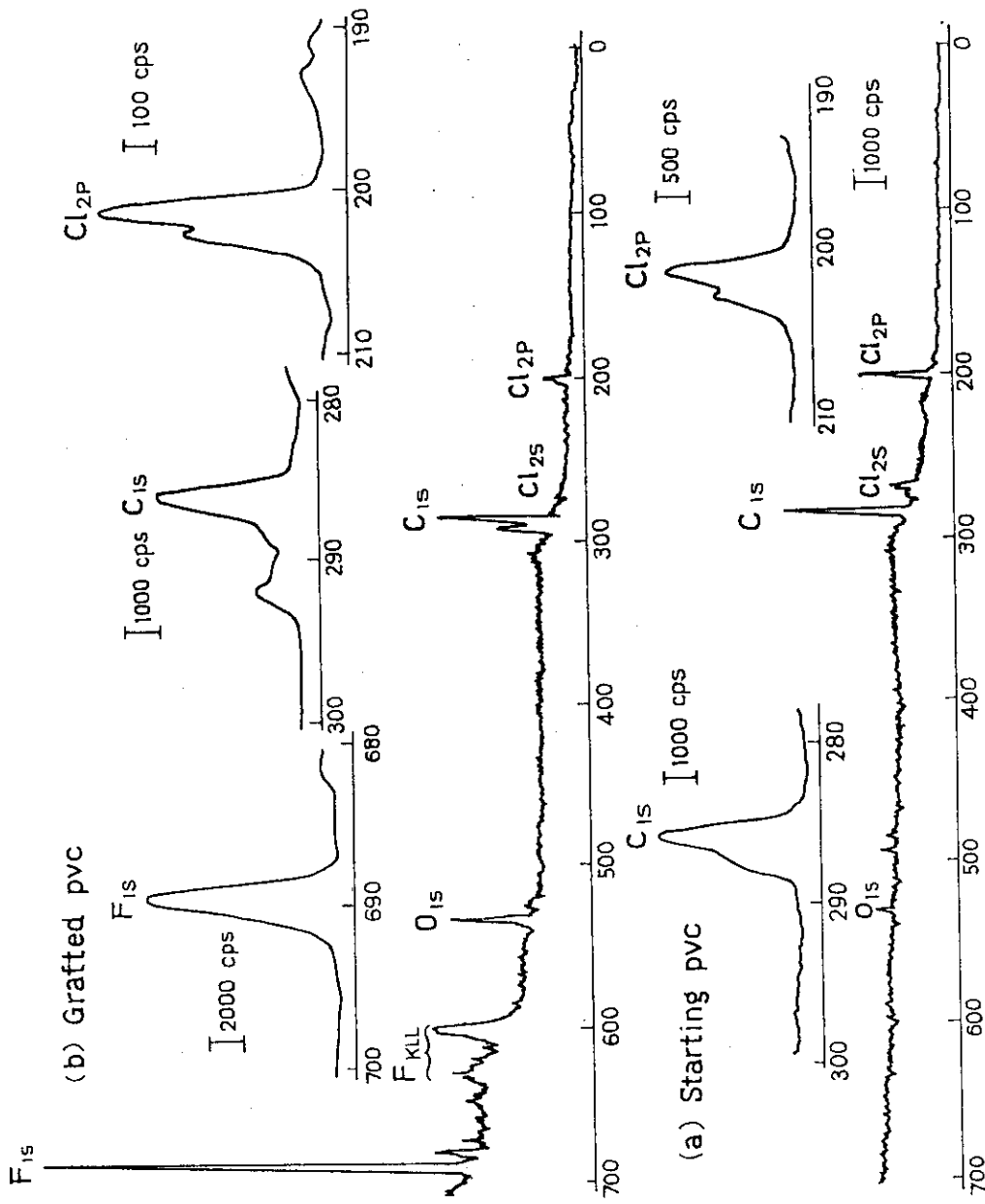

Fig. 1 ESCA spectra for PVC disc and tetrafluoropropyl methacrylate graft PVC disc.

time at which the electric resistance increases sharply is always longer than that at which the contact angle does.

Figure 1 shows the ESCA spectra of the ungrafted (a) and F_4C_3MA grafted (b) PVC disc. The spectrum of ungrafted disc shows strong C_{1s} and Cl_{2p} peaks at ca. 290 and 200 eV, respectively. A peak due to oxygen adsorbed on the surface is also observed in the spectrum. In the spectrum of the F_4C_3MA grafted disc strong peak due to F_{1s} appears at a bond energy of 690 eV in addition to the C_{1s} and Cl_{2p} peaks observed in that of the ungrafted disc. This indicates the presence of fluorine compounds on the surface of the grafted disc. Further, as shown in the enlarged spectrum the C_{1s} peak for the grafted disc has a distinct shoulder which is not found for the ungrafted disc. This also supports the presence of fluorine compounds on the surface since such a splitting is owing to the chemical shift of C_{1s} peak of the carbon atom bonded to fluorine atom.

In order to estimate the amount of the grafted fluorine compound quantitatively, the atomic ratios of F to F + Cl in the surface layer of the grafted disc have been calculated using areas of the peaks due to F_{1s} and Cl_{2p} and their photoionization cross sections. The relation between F/(F+Cl) and irradiation time for the F_4C_3MA grafted disc is listed in the last column of Table 1.

In the initial stage of the grafting, the value of F/(F+Cl) increased rapidly with irradiation time and it approached to 100% as the irradiation continued further, indicating that the fluorine compound started to cover the disc surface rapidly, and then the rate of grafting on the surface decreased gradually at the later stage.

Results of the three experiments indicate that the grafting of the fluorine-containing monomer takes place on the surface with irradiation time, but the time dependence of the change in the surface properties do not agree among the three methods employed. Similar results were obtained when the grafting was carried out at 50°C although the grafting rate at 50°C is larger than that at room temperature. Similar results

were also obtained when F_5St monomer was used instead of F_4C_3MA although the grafting rate is smaller than that obtained in the case of F_4C_3MA.

The optical and electron microscopic observations together with the above results lead to the conclusion that many small islands of fluorine-containing polymer formed on the disc surface at the initial stage of grafting grow gradually to cover the surface almost completely.

One possible reason why the surface grafting occurred successfully on the samples used in the present study may be that the surface properties are slightly different from those used previously.

(K. Kaji and K. Hayashi)

1) K. Kaji and K. Hayashi, JAERI-M 82-192, 88 (1982).

10. Radiation-Induced Formation of Color Center in Poly(methyl methacrylate)

Poly(methyl methacrylate) (PMMA) is conveniently used for radiation dosimetry. The change of the optical density (OD) induced by radiation is related quantitatively to radiation dose up to 5 Mrad (50 kGy)[1], and is considered to be due to the formation of radicals in PMMA from the fact that the decay curve observed for OD agrees well with that for radical concentration[2].

Many investigations carried out on the radiation effects on PMMA reached to the same conclusion that both the main-chain scission and the side-chain scission occur when the polymer is exposed to radiation. This conclusion is based on the experimental results on molecular weight decrease by irradiation in vacuum[3], electron spin resonance spectra assigned to macroradical generated by the main-chain scission and those assigned to methyl and formyl radicals formed by the removal of side-chain group[4], and volatile low molecular weight compounds produced by the removal of ester group from main-chain[5]. Since the ratio of the number of ester groups

removed to that of main-chain scissions by the irradiation in vacuum was reported as 0.82[5] or 0.71[6], the main- and side-chain scissions were considered to occur comparably.

The aim of the present work is to study the relation between the change of OD and that of molecular weight by the irradiation in order to get further information on the origin of radiation-induced OD change in PMMA.

PMMA sample is a transparent plate of 1 mm thick Clarex® (supplied by Nitto Jushi Co., Ltd.), or Radix®, the latter of which is commercially available dosimeter. The irradiation of

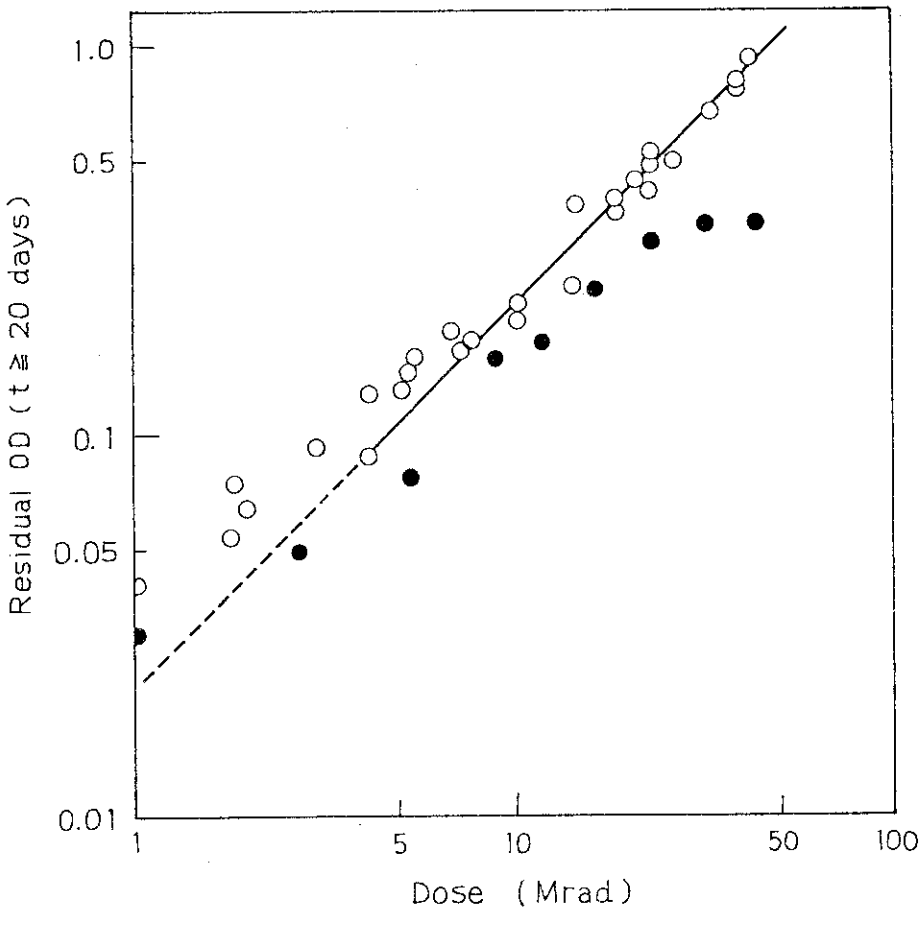

Fig. 1 Relationship between dose and residual optical density obtained for the irradiated poly(methyl methacrylate) after storage in dark in air for more than 20 days: (o, 31°C; ●, -196°C).

the film was carried out using ^{60}Co γ-ray source either at room temperature (31°C) or at liquid nitrogen temperature (-196°C). The OD was measured at room temperature at the wavelength of 314 nm which is recommended for dosimetry purpose. Molecular weights of the irradiated samples were determined by a gel permeation chromatographic method using tetrahydrofuran as solvent.

When the irradiated film was stored in dark in air at room temperature, the OD of the film decreased exponentially with time and then reached a constant value which is referred to as residual OD according to Chadwick[7]. The residual OD obtained after storage for more than 20 days is plotted as a function of dose in logarithmic scales in Fig. 1, where it is evident that

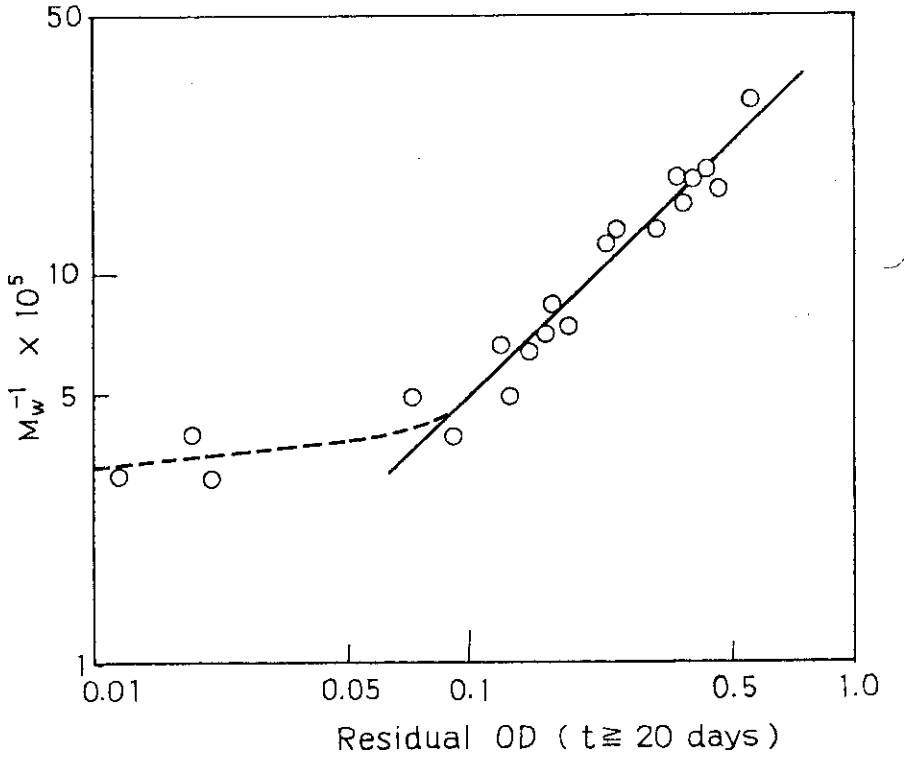

Fig. 2 Reciprocal molecular weights of the irradiated poly(methyl methacrylate). Residual optical density was obtained for the sample stored in dark in air for more than 20 days.

linear relation is found to exist between log OD and log dose and that the irradiations at the two temperatures give similar results.

Figure 2 shows the relation between the residual OD and the reciprocal of the molecular weight (M_W). The points lie on a straight line of a slope of unity in the OD range above 0.1, indicating that the OD is proportional to the number of polymer chain ends, and therefore, that the OD change is mainly resulted from the bond scission occurred at main-chain. On the other hand, however, the reciprocal of the molecular weight is almost independent of OD in the OD range below 0.1, suggesting that the OD change is not resulted from the bond scission at the main-chain, but from that at the side-chain. Since the dose required for giving OD of 0.1 to the film is determined as 5 Mrad from the plot shown in Fig. 1, the result mentioned above leads to the conclusion that the bond scission predominates at the side-chain below 5 Mrad, but above this dose, bond scission mainly occurs at the main-chain followed by side-chain splitting.

(Y. Nakase)

1) "Practical Methods for Processing Level Radiation Dosimetry", ed. Research Committee on Processing Level Radiation Dosimetry, Irradation Development Association, 1978.
2) "The Radiation Chemistry of Macromolecules", Vol. II, ed. M. Dole, Academic Press, N.Y., 1973.
3) A. R. Shultz, P. I. Roth, and J. M. Berge, J. Polym. Sci. A, 1, 1651 (1963).
4) D. Campbell, J. Polym. Sci. D, 4, 91 (1970).
5) A. Todd, J. Polym. Sci., 42, 223 (1960).
6) J. F. Kircher, F. A. Sliemer, R. A. Markle, W. B. Gager, and R. I. Leininger, J. Phys. Chem., 69, 189 (1965).
7) K. H. Chadwick, Radiat. Res., 4, 282 (1970).

III. LIST OF PUBLICATIONS

[1] Published Papers

1. H. Arai, S. Nagai, and M. Hatada, "Synthesis of Organic Acids by Electron Beam Irradiation of CO/CH_4 Mixture", Z. Phys. Chem. N. F., 131, 47 (1982).

2. H. Arai, S. Nagai, K. Matsuda, and M. Hatada, "The Electron Beam Radiolysis of CH_4/N_2O Mixtures", Z. Phys. Chem. N. F., 131, 57 (1982).

3. H. Arai, S. Nagai, and M. Hatada, "The Electron Beam Radiolysis of CH_4/CO_2 Mixtures", Z. Phys. Chem. N. F., 131, 69 (1982).

4. S. Sugimoto, "The γ-Ray Induced Chemical Reactions of CO/H_2 Mixture", Int. J. Appl. Rad. Isot., 34, 599 (1983).

5. Y. Nakase and N. Akasaka, "Preparation of Metal Ion Exchange Resin by Radiation-Induced Graft Polymerization", JAERI-M 82-059 (1982).

6. Y. Nakase, I. Kuriyama, T. Takahashi, and S. Isshiki, "Radiation-Induced Conductivity in Polymeric Insulating Materials Degraded under Specified Condition", IEEE Trans. Electr. Insul., EI-17, 306 (1982).

7. Y. Nakase and I. Kuriyama, "Radiation Resistance of Ethylene-Propylene-Ethylidene Norbornene Terpolymer Cured by Peroxide", Rept. Prog. Polym. Phys. Japan, 25, 3052 (1982).

8. Y. Nakase, I. Kuriyama, T. Takahashi, and S. Isshiki, "Studies on Radiation-Induced Current in Polymeric Insulating Materials and Their Fine Structure", J. Mater. Sci., 17, 3052 (1982).

9. K. Hayashi, "Processing of G.P.C. Data to Obtain Molecular Weight Distributions of Polymers", Rept. Prog. Polym. Phys. Japan, 25, 5 (1982).

10. K. Hayashi and T. Kijima, "GPC Data Processing System", JAERI-M 82-212 (1982).

11. K. Hayashi, T. Kijima, S. Okamura, S. Egusa, and K. Maku-uchi, "Formation of Fine Particle Emulsion by High-Dose-Rate Polymerization", J. Polym. Sci., Polym. Letter Ed., 20, 643 (1982).

Reviews and Patent Applications

12. K. Kaji, "Future Progress in Radiation Polymer Chemistry", Kobunshi, 31, 33 (1982).

13. Y. Nakase, K. Hayashi, and T. Yagi, "Preparation of Metal Ion Absorbing Resins", Japan Kokai, 57-150247.

14. K. Hayashi and S. Okamura, "Preparation of Fine Emulsion Particles", Japan Kokai, 57-66025.

15. K. Kaji, "Radiation-Induced Grafting onto Polyethylene to Impart Heat-Resistance and Flame-Retardance", Kogyo Zairyo, 31, 98 (1983).

[2] Oral Presentations

1. Y. Shimizu, S. Nagai, and M. Hatada, "Radiation Chemical Reaction of Methane in the Presence of Molecular Sieves", The 25th Discussion Meeting on Radiation Chemistry (Sendai), Sep. 29, 1982.

2. S. Sugimoto and M. Hatada, "The γ-Ray-Induced Reaction of Mathane at Elevated Pressures — Effect of Temperature and Pressure", The 25th Discussion Meeting on Radiation Chemistry (Sendai), Sep. 29, 1982.

3. S. Nagai, Y. Shimazu, and K. Matsuda, "Studies of Water Gas Shift Reaction Induced by Electron Beam Irradiation", The 25th Discussion Meeting on Radiation Chemistry (Sendai), Sep. 29, 1982.

4. Y. Nakase and I. Kuriyama, "Effect of Crosslinking on Radiation Resistance of Ethylene-Propylene Rubbers", The 31st Discussion Meeting on Polymer Science (Nagoya), Oct. 20, 1982.

5. K. Hayashi, T. Ohnishi, T. Kijima, and S. Okamura, "Radiation-Induced Telomerization of Butadiene and Bromine Containing Hydrocarbons", The 31st Annual Meeting of Polymer Society of Japan (Tokyo), May 30, 1982.

6. K. Hayashi, T. Kijima, and S. Okamura, "Emulsion Polymerization of Styrene by High Dose Rate Electron Beams", The 2nd Discussion Meeting on Polymer Microsphers (Fukui), Nov. 11, 1982.

IV. EXTERNAL RELATIONS

The laboratory welcomed the visit by Mr. M. T. Razzak, Mr. M. Said, IAEA trainees from Indonesia and Malaysia, on May 14, 1982.

A local meeting of the working group on "Plasma-Material Interactions" under the Atomic and Molecular Data Committee of JAERI was held in the laboratory on June 10, 1982. Discussion was made on the data needs and problems of the plasma-material interaction, and on the schedule of activity of the working group in the fiscal year.

Dr. K. A. Edvardsson of the Studsvik Science Research Laboratory delivered a lecture on "Radiation Effects on DNA Molecules" on June 17, 1982.

We welcomed trainees from industrial companies for one week training course on pure and applied radiation chemistry from 21st through 29th, October, 1982.

Professor E. P. Goldberg of Florida State University delivered a lecture on "Metal-Polymer Composites" on November 9, 1982.

Dr. Kuriyama was a guest speaker at the Osaka Liaison Committee for Promotion of Advanced Technology on "Radiation Application to Chemical Industry", in November 1982.

Some studies in this laboratory was conducted under the cooperative agreement with Prof. R. Kitamaru of Chemical Research Institute, Kyoto University and with Prof. R. Tsuji of Department of Nuclear Science of Kinki University.

V. LIST OF SCIENTISTS

(Mar. 31, 1983)

[1] Staff Members

Isamu KURIYAMA	Dr., polymer physicist, Director
Seizo OKAMURA	Professor emeritus, Kyoto University
Motoyoshi HATADA	Dr., physical chemist
Kanae HAYASHI*	Dr., polymer chemist
Yoshiaki NAKASE	Dr., polymer chemist
Siro NAGAI	Dr., physical chemist
Shun'ichi SUGIMOTO	Physical chemist
Koji MATSUDA	Radiation physicist
Jun'ichi TAKEZAKI	Physical chemist
Masanobu NISHII	Dr., polymer chemist
Torao TAKAGAKI	Radiation physicist
Kanako KAJI	Dr., polymer chemist
Yuichi SHIMIZU	Physical chemist

* Died on February 16, 1983.